Searches for electroweak neutralino and chargino production in channels with Higgs, *Z*, and *W* bosons in *pp* collisions at 8 TeV

V. Khachatryan *et al.*[*]

(CMS Collaboration)

Searches for supersymmetry (SUSY) are presented based on the electroweak pair production of neutralinos and charginos, leading to decay channels with Higgs, *Z*, and *W* bosons and undetected lightest SUSY particles (LSPs). The data sample corresponds to an integrated luminosity of about 19.5 fb^{-1} of proton-proton collisions at a center-of-mass energy of 8 TeV collected in 2012 with the CMS detector at the LHC. The main emphasis is neutralino pair production in which each neutralino decays either to a Higgs boson (*h*) and an LSP or to a *Z* boson and an LSP, leading to *hh*, *hZ*, and *ZZ* states with missing transverse energy (E_T^{miss}). A second aspect is chargino-neutralino pair production, leading to *hW* states with E_T^{miss}. The decays of a Higgs boson to a bottom-quark pair, to a photon pair, and to final states with leptons are considered in conjunction with hadronic and leptonic decay modes of the *Z* and *W* bosons. No evidence is found for supersymmetric particles, and 95% confidence level upper limits are evaluated for the respective pair production cross sections and for neutralino and chargino mass values.

I. INTRODUCTION

Supersymmetry (SUSY) [1–8], one of the most widely considered extensions of the standard model (SM) of particle physics, stabilizes the Higgs boson mass at the electroweak energy scale, may predict unification of the strong, weak, and electromagnetic forces, and might provide a dark matter candidate. Supersymmetry postulates that each SM particle is paired with a SUSY partner from which it differs in spin by one-half unit, with otherwise identical quantum numbers. For example, squarks, gluinos, and winos are the SUSY partners of quarks, gluons, and *W* bosons, respectively. Supersymmetric models contain extended Higgs sectors [8,9], with higgsinos the SUSY partners of Higgs bosons. Neutralinos $\tilde{\chi}^0$ (charginos $\tilde{\chi}^{\pm}$) arise from the mixture of neutral (charged) higgsinos with the SUSY partners of neutral (charged) electroweak vector bosons.

In this paper, we consider R-parity-conserving models [10]. In R-parity-conserving models, SUSY particles are created in pairs. Each member of the pair initiates a decay chain that terminates with a stable lightest SUSY particle (LSP) and SM particles. If the LSP interacts only via the weak force, as in the case of a dark matter candidate, the LSP escapes detection, potentially yielding large values of missing momentum and energy.

Extensive searches for SUSY particles have been performed at the CERN LHC, but so far the searches have not uncovered evidence for their existence [11–22]. The recent discovery [23–25] of the Higgs boson, with a mass of about 125 GeV, opens new possibilities for SUSY searches. In the SUSY context, we refer to the 125 GeV boson as "*h* " [26], the lightest neutral *CP*-even state of an extended Higgs sector. The *h* boson is expected to have the properties of the SM Higgs boson if all other Higgs bosons are much heavier [27]. Neutralinos and charginos are predicted to decay to an *h* or vector (*V* = *Z*, *W*) boson over large regions of SUSY parameter space [28–34]. Pair production of neutralinos and/or charginos can thus lead to *hh*, *hV*, and *VV*$^{(\prime)}$ states. Requiring the presence of one or more *h* bosons provides a novel means to search for these channels. Furthermore, the observation of a Higgs boson in a SUSY-like process would provide evidence that SUSY particles couple to the Higgs field, a necessary condition for SUSY to stabilize the Higgs boson mass. This evidence can not be provided by search channels without the Higgs boson.

In this paper, searches are presented for electroweak pair production of neutralinos and charginos that decay to the *hh*, *hZ*, and *hW* states. Related SUSY searches sensitive to the corresponding *ZZ* state are presented in Refs. [35,36]. We assume the Higgs boson *h* to have SM properties. The data sample, corresponding to an integrated luminosity of around 19.5 fb^{-1} of proton-proton collisions at $\sqrt{s}$ = 8 TeV, was collected with the CMS detector at the LHC. For most of the searches, a large value of missing energy transverse to the direction of the proton beam axis (E_T^{miss}) is required.

The *hh*, *hZ*, and *ZZ* topologies arise in a number of SUSY scenarios. As a specific example, we consider an R-parity-conserving gauge-mediated SUSY-breaking (GMSB) model [28,34] in which the two lightest neutralinos $\tilde{\chi}_1^0$ and $\tilde{\chi}_2^0$, and the lightest chargino $\tilde{\chi}_1^{\pm}$, are higgsinos.

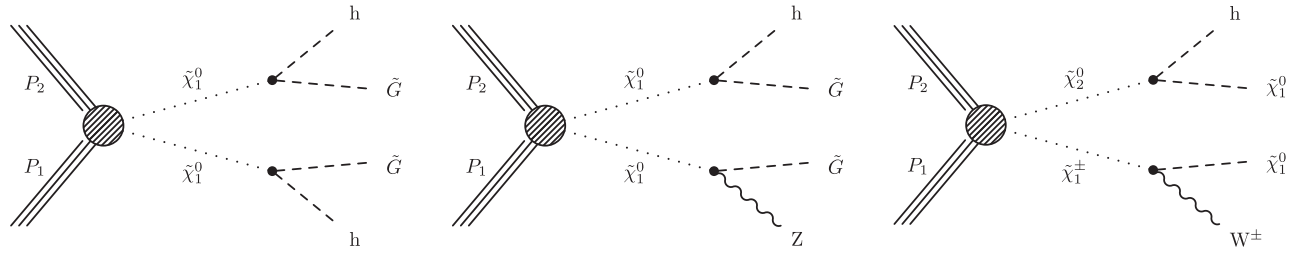[*] Full author list given at the end of the article.

FIG. 1. Event diagrams for the SUSY scenarios considered in this analysis. (Left) and (center) hh and hZ production in a GMSB model [28,34], where h is the Higgs boson, $\tilde{\chi}_1^0$ is the lightest neutralino NLSP, and $\tilde{G}$ is the nearly massless gravitino LSP. The $\tilde{\chi}_1^0\tilde{\chi}_1^0$ state is created through $\tilde{\chi}_1^0\tilde{\chi}_2^0$, $\tilde{\chi}_1^0\tilde{\chi}_1^\pm$, $\tilde{\chi}_2^0\tilde{\chi}_1^\pm$, and $\tilde{\chi}_1^\pm\tilde{\chi}_1^\mp$ production followed by the decay of the $\tilde{\chi}_2^0$ and $\tilde{\chi}_1^\pm$ states to the $\tilde{\chi}_1^0$ and undetected SM particles, with $\tilde{\chi}_2^0$ and $\tilde{\chi}_1^\pm$ the second-lightest neutralino and the lightest chargino, respectively. (Right) hW production through chargino-neutralino $\tilde{\chi}_1^\pm\tilde{\chi}_2^0$ pair creation, with $\tilde{\chi}_1^0$ a massive neutralino LSP.

In this model, the $\tilde{\chi}_1^0$, $\tilde{\chi}_2^0$, and $\tilde{\chi}_1^\pm$ are approximately mass degenerate, with $\tilde{\chi}_1^0$ the lightest of the three states. The LSP is a gravitino $\tilde{G}$ [37], the SUSY partner of a graviton. The $\tilde{\chi}_2^0$ and $\tilde{\chi}_1^\pm$ higgsinos decay to the $\tilde{\chi}_1^0$ state plus low-p_T SM particles, where p_T represents momentum transverse to the beam axis. The $\tilde{\chi}_1^0$ higgsino, which is the next-to-lightest SUSY particle (NLSP), undergoes a two-body decay to either an h boson and $\tilde{G}$ or to a Z boson and $\tilde{G}$, where $\tilde{G}$ is nearly massless, stable, and weakly interacting. The pair production of any of the combinations $\tilde{\chi}_1^0\tilde{\chi}_2^0$, $\tilde{\chi}_1^0\tilde{\chi}_1^\pm$, $\tilde{\chi}_2^0\tilde{\chi}_1^\pm$, or $\tilde{\chi}_1^\pm\tilde{\chi}_1^\mp$ is allowed [28], enhancing the effective cross section for the $\tilde{\chi}_1^0\tilde{\chi}_1^0$ di-higgsino state and thus for hh and hZ production [Fig. 1 (left) and (center)]. The production of ZZ combinations is also possible. The final state includes two LSP particles $\tilde{G}$, leading to E_T^{miss}. Note that $\tilde{\chi}_2^0\tilde{\chi}_2^0$ and direct $\tilde{\chi}_1^0\tilde{\chi}_1^0$ production are not allowed in the pure higgsino limit, as is considered here.

For the hh combination, we consider the $h(\to b\bar{b})h(\to b\bar{b})$, $h(\to \gamma\gamma)h(\to b\bar{b})$, and $h(\to \gamma\gamma)h(\to ZZ/WW/\tau\tau)$ decay channels, with $b\bar{b}$ a bottom quark-antiquark pair and where the ZZ, WW, and $\tau\tau$ states decay to yield at least one electron or muon. For the hZ combination, we consider the $h(\to \gamma\gamma)Z(\to 2\,\text{jets})$, $h(\to \gamma\gamma)Z(\to ee/\mu\mu/\tau\tau)$, and $h(\to b\bar{b})Z(\to ee/\mu\mu)$ channels, where the $\tau\tau$ pair yields at least one electron or muon. We combine the results of the current study with those presented for complementary Higgs and Z boson decay modes in Refs. [35,36] to derive overall limits on electroweak GMSB hh, hZ, and ZZ production.

As a second specific example of a SUSY scenario with Higgs bosons, we consider the R-parity-conserving chargino-neutralino $\tilde{\chi}_1^\pm\tilde{\chi}_2^0$ electroweak pair production process shown in Fig. 1 (right), in which the $\tilde{\chi}_1^\pm$ chargino is winolike and the $\tilde{\chi}_1^0$ neutralino is a massive, stable, weakly interacting binolike LSP, where a bino is the SUSY partner of the B gauge boson. This scenario represents the SUSY process with the largest electroweak cross section [38]. It leads to the hW topology, with E_T^{miss} present because of the two LSP particles. The decay channels considered are $h(\to \gamma\gamma)W(\to 2\,\text{jets})$ and $h(\to \gamma\gamma)W(\to \ell\nu)$, with ℓ an electron, muon, or leptonically decaying τ lepton. We

combine these results with those based on complementary decay modes of this same scenario [36] to derive overall limits.

The principal backgrounds arise from the production of a top quark-antiquark ($t\bar{t}$) pair, a W boson, Z boson, or photon in association with jets ($W + \text{jets}$, $Z + \text{jets}$, and $\gamma + \text{jets}$), and multiple jets through the strong interaction (QCD multijet). Other backgrounds are due to events with a single top quark and events with rare processes such as $t\bar{t}V$ or SM Higgs boson production. The QCD multijet category as defined here excludes events in the other categories. For events with a top quark or W boson, significant E_T^{miss} can arise if a W boson decays leptonically, producing a neutrino, while for events with a Z boson, the decay of the Z boson to two neutrinos can yield significant E_T^{miss}. For $\gamma + \text{jets}$ events, $Z + \text{jets}$ events with $Z \to \ell^+\ell^-$ ($\ell = e, \mu$), and events with all-hadronic final states, such as QCD multijet events, significant E_T^{miss} can arise if the event contains a charm or bottom quark that undergoes semi-leptonic decay, but the principal source of E_T^{miss} is the mismeasurement of jet p_T ("spurious" E_T^{miss}).

This paper is organized as follows. In Secs. II, III, and IV, we discuss the detector and trigger, the event reconstruction, and the event simulation. Section V presents a search for hh SUSY events in which both Higgs bosons decay to a $b\bar{b}$ pair. Section VI presents searches for hh, hZ, and hW SUSY events in which one Higgs boson decays to a pair of photons. A search for hZ SUSY events with a Higgs boson that decays to a $b\bar{b}$ pair and a Z boson that decays to an e^+e^- or $\mu^+\mu^-$ pair is presented in Sec. VII. In Sec. VIII, we briefly discuss the studies of Refs. [35,36] as they pertain to the SUSY scenarios considered here. The interpretation of the results is presented in Sec. X and a summary in Sec. XI.

II. DETECTOR AND TRIGGER

A detailed description of the CMS detector is given elsewhere [39]. A superconducting solenoid of 6 m internal diameter provides an axial magnetic field of 3.8 T. Within the field volume are a silicon pixel and strip tracker, a

crystal electromagnetic calorimeter, and a brass-and-scintillator hadron calorimeter. Muon detectors based on gas ionization chambers are embedded in a steel flux-return yoke located outside the solenoid. The CMS coordinate system is defined with the origin at the center of the detector and with the z axis along the direction of the counterclockwise beam. The transverse plane is perpendicular to the beam axis, with ϕ the azimuthal angle (measured in radians), θ the polar angle, and $\eta = -\ln[\tan(\theta/2)]$ the pseudorapidity. The tracking system covers the region $|\eta| < 2.5$, the muon detector $|\eta| < 2.4$, and the calorimeters $|\eta| < 3.0$. Steel-and-quartz-fiber forward calorimeters cover $3 < |\eta| < 5$. The detector is nearly hermetic, permitting accurate measurements of energy balance in the transverse plane.

The trigger is based on the identification of events with one or more jets, bottom-quark jets (b jets), photons, or charged leptons. The main trigger used for the $hh \to b\bar{b}b\bar{b}$ analysis (Sec. V) requires the presence of at least two jets with $p_T > 30$ GeV, including at least one tagged b jet, and $E_T^{\mathrm{miss}} > 80$ GeV. For the diphoton studies (Sec. VI), there must be at least one photon with $p_T > 36$ GeV and another with $p_T > 22$ GeV. The study utilizing $Z \to \ell^+\ell^-$ events (Sec. VII) requires at least one electron or muon with $p_T > 17$ GeV and another with $p_T > 8$ GeV. Corrections are applied to the selection efficiencies to account for trigger inefficiencies.

III. EVENT RECONSTRUCTION

The particle-flow (PF) method [40,41] is used to reconstruct and identify charged and neutral hadrons, electrons (with associated bremsstrahlung photons), muons, and photons, using an optimized combination of information from CMS subdetectors. The reconstruction of photons for the $h \to \gamma\gamma$–based searches is discussed in Sec. VI. Hadronically decaying τ leptons (τ_h) are reconstructed using PF objects (we use the "hadron-plus-strips" τ-lepton reconstruction algorithm [42] with loose identification requirements). The event primary vertex, taken to be the reconstructed vertex with the largest sum of charged-track p_T^2 values, is required to contain at least four charged tracks and to lie within 24 cm of the origin in the direction along the beam axis and 2 cm in the perpendicular direction. Charged hadrons from extraneous pp interactions within the same or a nearby bunch crossing ("pileup") are removed [43]. The PF objects serve as input for jet reconstruction, based on the anti-k_T algorithm [44,45], with a distance parameter of 0.5. Jets are required to satisfy basic quality criteria (jet ID [46]), which eliminate, for example, spurious events caused by calorimeter noise. Contributions to an individual jet's p_T from pileup interactions are subtracted [47]. Finally, jet energy corrections are applied as a function of p_T and η to account for residual effects of nonuniform detector response [48].

The missing transverse energy E_T^{miss} is defined as the modulus of the vector sum of the transverse momenta of all PF objects. The E_T^{miss} vector is the negative of that same vector sum. We also make use of the E_T^{miss} significance variable $\mathcal{S}_{\mathrm{MET}}$ [49], which represents a χ^2 difference between the observed result for E_T^{miss} and the $E_T^{\mathrm{miss}} = 0$ hypothesis. The $\mathcal{S}_{\mathrm{MET}}$ variable provides an event-by-event assessment of the consistency of the observed E_T^{miss} with zero, given the measured content of the event and the known measurement resolutions. Because it accounts for finite jet resolution on an event-by-event basis, $\mathcal{S}_{\mathrm{MET}}$ provides better discrimination between signal and background events than does E_T^{miss}, for background events with spurious E_T^{miss}.

The identification of b jets is performed using the combined secondary vertex (CSV) algorithm [50,51], which computes a discriminating variable for each jet based on displaced secondary vertices, tracks with large impact parameters, and kinematic variables, such as jet mass. Three operating points are defined, denoted "loose," "medium," and "tight." These three working points yield average signal efficiencies for b jets (misidentification probabilities for light-parton jets) of approximately 83% (10%), 70% (1.5%), and 55% (0.1%), respectively, for jets with $p_T > 60$ GeV [51].

We also make use of isolated electrons and muons, either vetoing events with such leptons in order to reduce background from SM $t\bar{t}$ and electroweak boson production (Secs. V, VI A, and VI B), or selecting these events because they correspond to the targeted signal process (Secs. VI C and VII). Isolated electron and muon identification is based on the variable R_{iso}, which is the scalar sum of the p_T values of charged hadrons, neutral hadrons, and photons within a cone of radius $R_{\mathrm{cone}} \equiv \sqrt{(\Delta\phi)^2 + (\Delta\eta)^2}$ around the lepton direction, corrected for the contributions of pileup interactions, divided by the lepton p_T value itself. For the analyses presented here, $R_{\mathrm{cone}} = 0.3$ (0.4) for electrons (muons), unless stated otherwise.

IV. EVENT SIMULATION

Monte Carlo (MC) simulations of signal and background processes are used to optimize selection criteria, validate analysis performance, determine signal efficiencies, and evaluate some backgrounds and systematic uncertainties.

Standard model background events are simulated with the MADGRAPH 5.1.3.30 [52], POWHEG 301 [53–55], and PYTHIA 6.4.26 [56] generators. The $t\bar{t}$ events (generated with MADGRAPH) incorporate up to three additional partons, including b quarks, at the matrix element level. The $t\bar{t} + b\bar{b}$ events account for contributions from gluon splitting. The SM processes are normalized to cross section calculations valid to next-to-leading order (NLO) or next-to-next-to-leading order [57–63], depending on availability, and otherwise to leading order. For the simulation of SM

events, the GEANT4 [64] package is used to model the detector and detector response.

Signal events are simulated with the MADGRAPH 5.1.5.4 generator, with a Higgs boson mass of 126 GeV [65]. Up to two partons from initial-state radiation (ISR) are allowed. To reduce computational requirements, the detector and detector response for signal events are modeled with the CMS fast simulation program [66], with the exception of the signal events for the $hh \to b\bar{b}b\bar{b}$ study (Sec. V), for which GEANT4 modeling is used. For the quantities based on the fast simulation, the differences with respect to the GEANT-based results are found to be small ($\lesssim 5\%$). Corrections are applied, as appropriate, to account for the differences. The signal event rates are normalized to the NLO plus next-to-leading-logarithmic (NLO + NLL) cross sections [38,67,68] for the GMSB hh, hZ, and ZZ channels, and to the NLO cross sections [38,69] for the electroweak hW channel. For the GMSB scenarios [Fig. 1 (left) and (center)], the $\tilde{\chi}_1^0$, $\tilde{\chi}_2^0$, and $\tilde{\chi}_1^\pm$ particles are taken to be mass-degenerate pure higgsino states, such that any SM particles arising from the decays of the $\tilde{\chi}_2^0$ and $\tilde{\chi}_1^\pm$ states to the $\tilde{\chi}_1^0$ state are too soft to be detected. Signal MC samples are generated for a range of higgsino mass values $m_{\tilde{\chi}_1^0}$, taking the LSP (gravitino $\tilde{G}$) mass to be 1 GeV (i.e., effectively zero). The decays of the $\tilde{\chi}_1^0$ higgsinos are described with a pure phase-space matrix element. For the electroweak hW scenario [Fig. 1 (right)], we make the simplifying assumption $m_{\tilde{\chi}_2^0} = m_{\tilde{\chi}_1^\pm}$ [36] and generate event samples for a range of $\tilde{\chi}_2^0$ and LSP ($\tilde{\chi}_1^0$) mass values, with the decays of the $\tilde{\chi}_1^\pm$ chargino and $\tilde{\chi}_2^0$ neutralino described using the BRIDGE v2.24 program [70]. Note that we often consider small LSP masses in this study, viz., $m_{\tilde{G}} = 1$ GeV for the GMSB scenario, and, in some cases, $m_{\tilde{\chi}_1^0} = 1$ GeV for the electroweak hW scenario [see Figs. 11, 12, 22 (bottom), and 23, below]. These scenarios are not excluded by limits [71] on Z boson decays to undetected particles for the cases considered here, in which the LSP is either a gravitino or a binolike neutralino [72].

All MC samples incorporate the CTEQ6L1 or CTEQ6M [73,74] parton distribution functions, with PYTHIA used for parton showering and hadronization. The MC events are corrected to account for pileup interactions, such that they describe the distribution of reconstructed vertices observed in data. The simulations are further adjusted so that the b-jet tagging and misidentification efficiencies match those determined from control samples in the data. The b-jet tagging efficiency correction factor depends slightly on the jet p_T and η values and has a typical value of 0.99, 0.95, and 0.93 for the loose, medium, and tight CSV operating points [50]. Additional corrections are applied so that the jet energy resolution in signal samples corresponds to the observed results. A further correction, implemented as described in Appendix B of Ref. [18], accounts for mismodeling of ISR in signal events.

V. SEARCH IN THE $hh \to b\bar{b}b\bar{b}$ CHANNEL

With a branching fraction of about 0.56 [75], $h \to b\bar{b}$ decays represent the most likely decay mode of the Higgs boson. The $h(\to b\bar{b})h(\to b\bar{b})$ final state thus provides a sensitive search channel for SUSY hh production. For this channel, the principal visible objects are the four b jets. Additional jets may arise from ISR, final-state radiation, or pileup interactions. For this search, jets (including b jets) must satisfy $p_T > 20$ GeV and $|\eta| < 2.4$. In addition, we require the following:

(i) exactly four or five jets, where $p_T > 50$ GeV for the two highest p_T jets;

(ii) E_T^{miss} significance $\mathcal{S}_{\text{MET}} > 30$;

(iii) no identified, isolated electron or muon candidate with $p_T > 10$ GeV; electron candidates are restricted to $|\eta| < 2.5$ and muon candidates to $|\eta| < 2.4$; the isolation requirements are $R_{\text{iso}} < 0.15$ for electrons and $R_{\text{iso}} < 0.20$ for muons;

(iv) no τ_h candidate with $p_T > 20$ GeV and $|\eta| < 2.4$;

(v) no isolated charged particle with $p_T > 10$ GeV and $|\eta| < 2.4$, where the isolation condition is based on the scalar sum $R_{\text{iso}}^{\text{ch}}$ of charged-particle p_T values in a cone of radius $R_{\text{cone}} = 0.3$ around the charged-particle direction, excluding the charged particle itself, divided by the charged-particle p_T value; we require $R_{\text{iso}}^{\text{ch}} < 0.10$;

(vi) $\Delta\phi_{\text{min}} > 0.5$ for events with $30 < \mathcal{S}_{\text{MET}} < 50$ and $\Delta\phi_{\text{min}} > 0.3$ for $\mathcal{S}_{\text{MET}} > 50$, where $\Delta\phi_{\text{min}}$ is the smallest difference in ϕ between the E_T^{miss} vector and any jet in the event; for the $\Delta\phi_{\text{min}}$ calculation we use less restrictive criteria for jets compared with the standard criteria: $|\eta| < 5.0$, no rejection of jets from pileup interactions, and no jet ID requirements, with all other conditions unchanged.

The isolated charged-particle requirement rejects events with a τ_h decay to a single charged track as well as events with an isolated electron or muon in cases where the lepton is not identified. The $\Delta\phi_{\text{min}}$ restriction eliminates QCD multijet and all-hadronic $t\bar{t}$ events, whose contribution is expected to be large at small values of $\mathcal{S}_{\text{MET}}$. The use of less-restrictive jet requirements for the $\Delta\phi_{\text{min}}$ calculation yields more efficient rejection of these backgrounds.

Three mutually exclusive samples of events with tagged b jets are defined:

(i) 2b sample: Events in this sample must contain exactly two tight b jets and no medium b jets;

(ii) 3b sample: Events in this sample must contain two jets that are tight b jets, a third jet that is either a tight or a medium b jet, and no other tight, medium, or loose b jet;

(iii) 4b sample: Events in this sample must contain two jets that are tight b jets, a third jet that is either a tight or medium b jet, and a fourth jet that is either a tight, medium, or loose b jet.
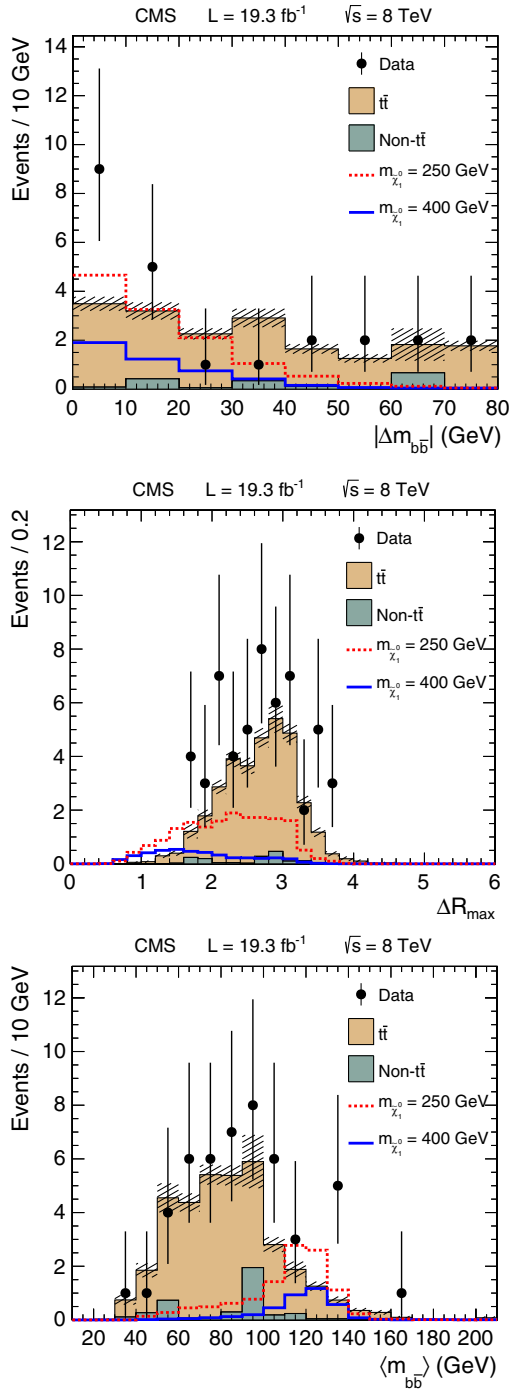
FIG. 2 (color online). Distributions of events in the 4b sample of the $hh \to b\bar{b}b\bar{b}$ analysis, after all signal region requirements are applied except for that on the displayed variable, in comparison with simulations of background and signal events: (top) $|\Delta m_{b\bar{b}}|$, (middle) $\Delta R_{\max}$, and (bottom) $\langle m_{b\bar{b}} \rangle$. For the signal events, results are shown for higgsino ($\tilde{\chi}_1^0$) mass values of 250 and 400 GeV, with an LSP (gravitino) mass of 1 GeV. The background distributions are stacked while the signal distributions are not. The hatched bands indicate the statistical uncertainty of the total SM simulated prediction.

The sample most sensitive to signal events is the 4b sample. The 3b sample is included to improve the signal efficiency. The 2b sample is depleted in signal events and is used to help evaluate the background, as described below. The dominant background arises from $t\bar{t}$ events in which one top quark decays hadronically while the other decays to a state with a lepton ℓ through $t \to b\ell\nu$, where the lepton is not identified and the neutrino provides a source of genuine E_T^{miss}.

To reconstruct the two Higgs boson candidates in an event, we choose the four most b-like jets based on the value of the CSV discriminating variable. These four jets can be grouped in three unique ways to form a pair of Higgs boson candidates. Of the three possibilities, we choose the one with the smallest difference $|\Delta m_{b\bar{b}}| \equiv |m_{b\bar{b},1} - m_{b\bar{b},2}|$ between the two candidate masses, where $m_{b\bar{b}}$ is the invariant mass of two tagged b jets. We calculate the distance $\Delta R \equiv \sqrt{(\Delta\phi)^2 + (\Delta\eta)^2}$ between the two jets for each $h \to b\bar{b}$ candidate. We call the larger of these two values $\Delta R_{\max}$. In signal events, the two b jets from the decay of a Higgs boson generally have similar directions since the Higgs boson is not normally produced at rest. Thus the two ΔR values tend to be small, making $\Delta R_{\max}$ small. In contrast, for the dominant background, from the class of $t\bar{t}$ events described above, three jets tend to lie in the same hemisphere, while the fourth jet lies in the opposite hemisphere, making $\Delta R_{\max}$ relatively large.

A signal region (SIG) is defined using the variables $|\Delta m_{b\bar{b}}|$, $\Delta R_{\max}$, and the average of the two Higgs boson candidate mass values $\langle m_{b\bar{b}} \rangle \equiv (m_{b\bar{b},1} + m_{b\bar{b},2})/2$. We require
  (i) $|\Delta m_{b\bar{b}}| < 20$ GeV;
  (ii) $\Delta R_{\max} < 2.2$;
  (iii) $100 < \langle m_{b\bar{b}} \rangle < 140$ GeV.
These requirements are determined through an optimization procedure that takes into consideration both the higgsino discovery potential and the ability to set stringent limits in the case of nonobservation. Distributions of these variables for events in the 4b event sample are shown in Fig. 2.

A sideband region (SB) is defined by applying the SIG-region criteria except using the area outside the following rectangle in the $|\Delta m_{b\bar{b}}|$-$\langle m_{b\bar{b}} \rangle$ plane:
  (i) $|\Delta m_{b\bar{b}}| < 30$ GeV;
  (ii) $90 < \langle m_{b\bar{b}} \rangle < 150$ GeV.
Schematic representations of the SIG and SB regions are shown in Fig. 3 (upper left).

To illustrate the basic principle of the background determination method, consider the 4b and 2b samples. We can define four observables, denoted A, B, C, and D:
  (i) A: number of background events in the 4b-SIG region;
  (ii) B: number of background events in the 4b-SB region;
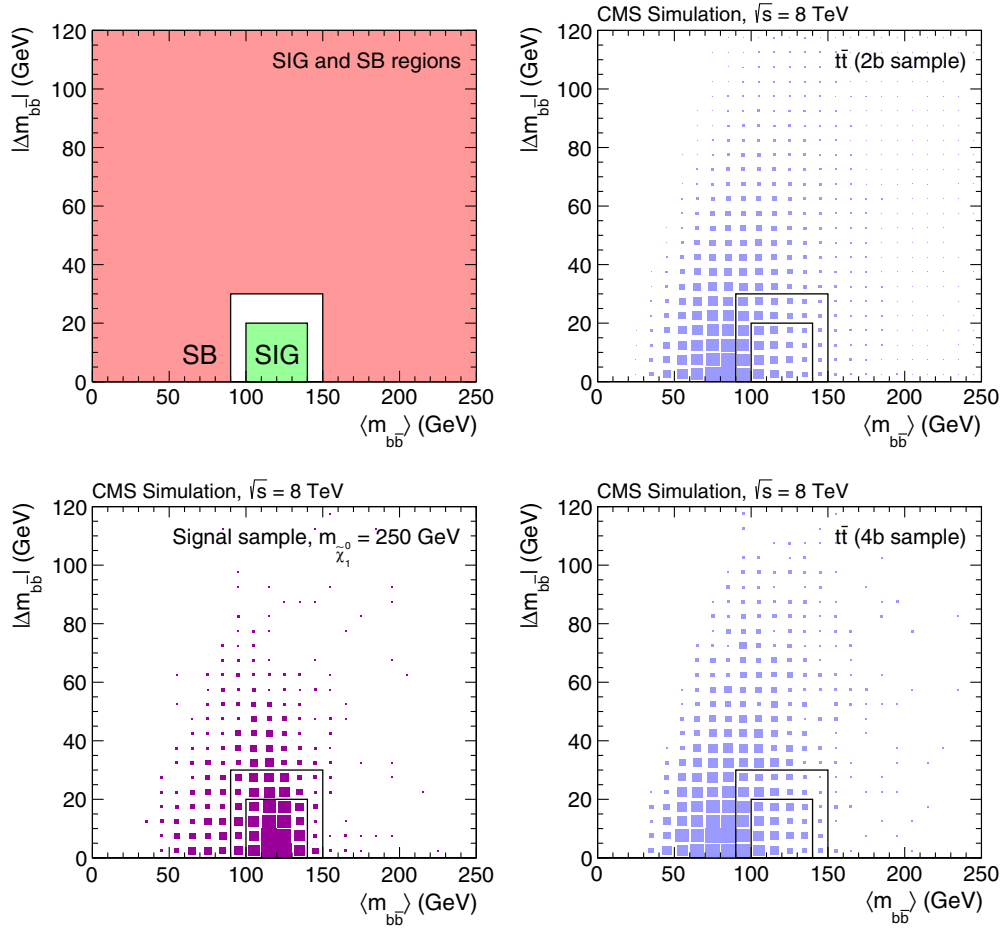 (iii) C: number of background events in the 2b-SIG region;

FIG. 3 (color online). (Top left) Illustration of the signal (SIG) and sideband (SB) regions in the $|\Delta m_{b\bar{b}}|$ versus $\langle m_{b\bar{b}} \rangle$ plane of the $hh \to b\bar{b}b\bar{b}$ analysis. (Top right and bottom right) Distributions of simulated $t\bar{t}$ events in the 2*b* and 4*b* samples. (Bottom left) Distribution of simulated signal events in the 4*b* sample for a higgsino ($\tilde{\chi}_1^0$) mass of 250 GeV and an LSP (gravitino) mass of 1 GeV. The plots employ an arbitrary integrated luminosity. The size of a box is proportional to the relative number of events.

(iv) D: number of background events in the 2*b*-SB region.

We assume that the ratio of the number of background events in the SIG region to that in the SB region, denoted as the SIG/SB ratio, is the same for the 2*b* and 4*b* samples. This assumption is supported by (for example) the similarity between the 2*b* and 4*b* results shown in the top-right and bottom-right plots of Fig. 3. We further assume that the 2*b*-SIG and all SB regions are dominated by background. The prediction for the number of background events in the 4*b*-SIG region is then given by the algebraic expression A = BC/D. The same result applies replacing the 4*b* sample by the 3*b* sample in the above discussion.

In practice, we examine the data in four bins of $\mathcal{S}_{\mathrm{MET}}$, which are indicated in Table I. The background yields in the four $\mathcal{S}_{\mathrm{MET}}$ bins of the 2*b*-SIG, 3*b*-SIG, and 4*b*-SIG regions are determined simultaneously in a likelihood fit, with the SIG/SB ratios for the background in all three *b*-jet samples constrained to a common value (determined in the fit) for each $\mathcal{S}_{\mathrm{MET}}$ bin separately. Figure 4 shows the predictions of

the SM simulation for the SIG/SB ratios, in the four bins of $\mathcal{S}_{\mathrm{MET}}$, for the three *b*-jet samples (for purposes of comparison, the data are also shown). It is seen that for each individual bin of $\mathcal{S}_{\mathrm{MET}}$, the SIG/SB ratio of SM events is predicted to be about the same for all three *b*-jet samples, i.e., within $\mathcal{S}_{\mathrm{MET}}$ bin 1, the 2*b*, 3*b*, and 4*b* results are all about the same, within $\mathcal{S}_{\mathrm{MET}}$ bin 2 they are all about the same, etc., supporting the key assumption of the method. Figure 4 includes the results determined from the likelihood fit for the SIG/SB ratio in each bin, assuming the SUSY signal yield to be zero. Note that in setting limits (Sec. X), the contributions of signal events to both the signal and sideband regions are taken into account, and thus, e.g., the level of signal contribution to the SB regions does not affect the results.

The four bins of $\mathcal{S}_{\mathrm{MET}}$ correspond roughly to $E_{\mathrm{T}}^{\mathrm{miss}}$ ranges of 106–133 GeV, 133–190 GeV, 190–250 GeV, and > 250 GeV, respectively, as determined from a sample of events selected with loosened criteria. For this result, the edges of the $E_{\mathrm{T}}^{\mathrm{miss}}$ ranges are adjusted so that the number of

TABLE I.　Observed numbers of events and corresponding SM background estimates in bins of E_T^{miss} significance $\mathcal{S}_{MET}$ for the $hh \to b\bar{b}b\bar{b}$ analysis. For the SM background estimate, the first uncertainty is statistical and the second systematic. Numerical results for example signal scenarios, are given in Tables VIII and IX of the Appendix.

$\mathcal{S}_{MET}$ bin	$\mathcal{S}_{MET}$ range	SM background (3b-SIG)	Data (3b-SIG)	SM background (4b-SIG)	Data (4b-SIG)
1	30–50	$6.7^{+1.4+1.0}_{-1.1-0.7}$	4	$2.9^{+0.8+0.5}_{-0.6-0.4}$	4
2	50–100	$11.6^{+1.9+0.9}_{-1.6-0.7}$	15	$4.9^{+1.1+1.4}_{-0.9-0.9}$	7
3	100–150	$2.44^{+0.84+0.56}_{-0.64-0.35}$	1	$0.59^{+0.39+0.09}_{-0.26-0.09}$	3
4	>150	$1.50^{+0.82+0.64}_{-0.54-0.32}$	0	$0.40^{+0.39+0.26}_{-0.22-0.10}$	0

selected $t\bar{t}$ MC events is about the same within the respective E_T^{miss} and $\mathcal{S}_{MET}$ bins. The loosened selection criteria, specifically no requirement on $\Delta\phi_{min}$ and a requirement of least two tight b jets with no other b-jet restrictions, permit more QCD multijet events to enter the sample, allowing the relative merits of the E_T^{miss} and $\mathcal{S}_{MET}$ variables to be tested. The results are illustrated in Fig. 5. The $\mathcal{S}_{MET}$ variable is seen to provide better rejection of background events with spurious E_T^{miss} than does E_T^{miss}, as mentioned in Sec. III.

To evaluate the systematic uncertainty of the background estimate, we consider two terms, determined from simulation, which are treated as separate nuisance parameters in the likelihood fit. The first term is determined for each bin of $\mathcal{S}_{MET}$ in the 4b (3b) sample. It is given by the difference from unity of the double ratio R, where R is the SIG/SB ratio of 4b (3b) events divided by the SIG/SB ratio of 2b events ("nonclosure result"), or else by the statistical uncertainty of R, whichever is larger. The size of this uncertainty varies between 14% and 40%, with a typical value of 25%. The second term accounts for potential

differences between the SIG/SB ratio of $t\bar{t}$ and QCD multijet events as well as for the possibility that the fraction of $t\bar{t}$ and QCD multijet events differs between the 2b, 3b, and 4b samples. Based on studies with a QCD multijet data control sample, the fraction of background events due to QCD multijet events is conservatively estimated to be less than 20%. We reevaluate the background assuming that the fraction of QCD multijets varies by the full 20% between the 2b and 4b samples and find the nonclosure to be 7%, which we define as the associated uncertainty.

The observed numbers of events in the 3b-SIG and 4b-SIG regions are shown in Fig. 6 as a function of $\mathcal{S}_{MET}$, in comparison with the SM background predictions from the likelihood fit and the predictions of two signal scenarios. Numerical values are given in Table I.
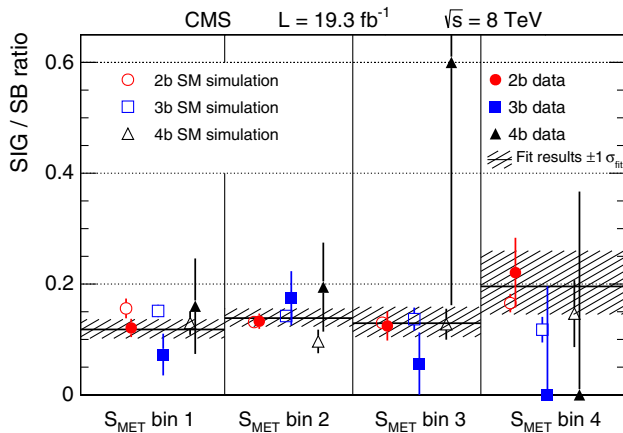

FIG. 4 (color online).　Ratio of the number of events in the signal (SIG) region to that in the sideband (SB) region as a function of $\mathcal{S}_{MET}$ bin (see Table I), for the 2b, 3b, and 4b event samples of the $hh \to b\bar{b}b\bar{b}$ analysis. The simulated results account for the various expected SM processes. The results of a likelihood fit to data, in which the SIG/SB ratio is determined separately for each bin, are also shown.
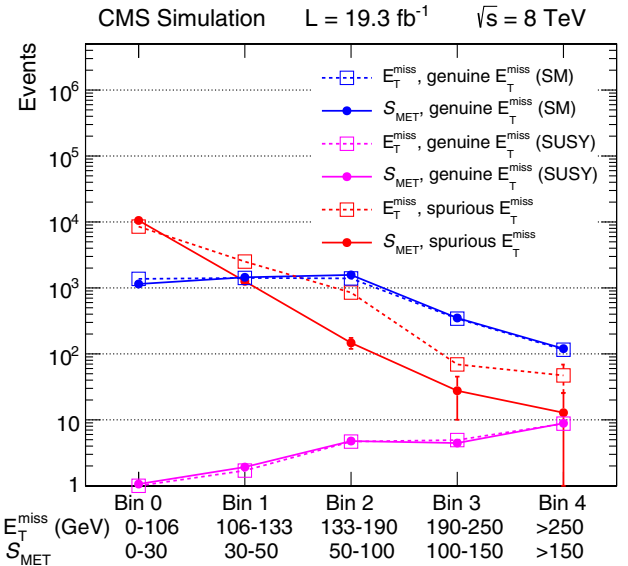

FIG. 5 (color online).　Distribution of simulated $t\bar{t}$ ["genuine E_T^{miss} (SM)"], signal ["genuine E_T^{miss} (SUSY)"], and QCD multijet ("spurious E_T^{miss}") events using loosened selection criteria (see text) in bins of $\mathcal{S}_{MET}$ and E_T^{miss}. The uncertainties are statistical. The bin edges for E_T^{miss} have been adjusted so that the number of $t\bar{t}$ events in each bin is about the same as for the corresponding $\mathcal{S}_{MET}$ bin. The signal events correspond to the higgsino pair production scenario of Fig. 1 (left) with a higgsino ($\tilde{\chi}_1^0$) mass of 250 GeV and an LSP (gravitino) mass of 1 GeV.
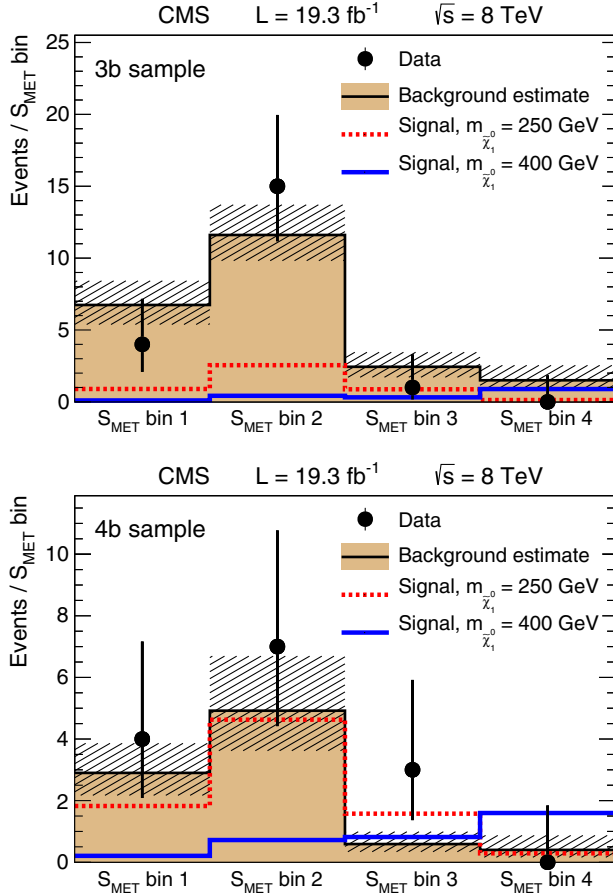
FIG. 6 (color online).   Observed numbers of events as a function of E_T^{miss} significance ($\mathcal{S}_{MET}$) bin for the $hh \to b\bar{b}b\bar{b}$ analysis, in comparison with the SM background estimate from the likelihood fit, for the (top) $3b$-SIG and (bottom) $4b$-SIG regions. The hatched bands show the total uncertainty of the background prediction, with statistical and systematic terms combined. The expected (unstacked) results for signal events, with higgsino ($\tilde{\chi}_1^0$) mass values of 250 and 400 GeV and an LSP (gravitino) mass of 1 GeV, are also shown.

VI. SEARCH IN THE *hh, hZ,* AND *hW* CHANNELS WITH ONE $h \to \gamma\gamma$ DECAY

We next describe searches for hh, hZ, and hW states in channels with one Higgs boson that decays to photons. While the $h \to \gamma\gamma$ branching fraction is small [75], the expected diphoton invariant-mass signal peak is narrow, allowing the SM background to be reduced. For hh production, we search in channels in which the second Higgs boson decays to $b\bar{b}$, WW, ZZ, or $\tau\tau$, where, in the case of these last three modes, at least one electron or muon is required to be present in the final state. For the hZ and hW combinations, we search in the channels in which the Z or W boson decays either to two light-flavor jets or leptonically, where the leptonic decays yield at least one electron or muon.

Photon candidates are reconstructed from "superclusters" of energy deposited in the electromagnetic calorimeter [76,77], with energies determined using a multivariate regression technique [24,77]. To reduce contamination from electrons misidentified as photons, photon candidates are rejected if they register hit patterns in the pixel detector that are consistent with a track. The photon candidates are required to satisfy loose identification criteria based primarily on their shower shape and isolation [78]. Signal events tend to produce decay products in the central region of the detector, because of the large masses of the produced SUSY particles. Therefore, photon candidates are restricted to $|\eta| < 1.44$.

Events must contain at least one photon candidate with $p_T > 40$ GeV and another with $p_T > 25$ GeV. The $h \to \gamma\gamma$ boson candidate is formed from the two highest p_T photons in the event. The resulting diphoton invariant mass $m_{\gamma\gamma}$ is required to appear in the Higgs boson mass region defined by $120 < m_{\gamma\gamma} < 131$ GeV.

For the searches described in this section, jets must have $p_T > 30$ GeV and $|\eta| < 2.4$. Tagged b jets are defined using the CSV-medium criteria.

A. $hh \to \gamma\gamma b\bar{b}$

For the search in the $h(\to \gamma\gamma)h(\to b\bar{b})$ channel, we require

  (i) exactly two tagged b jets, which together form the $h \to b\bar{b}$ candidate;

 (ii) the invariant mass $m_{b\bar{b}}$ of the two tagged b jets to lie in the Higgs boson mass region defined by $95 < m_{b\bar{b}} < 155$ GeV;

(iii) no identified, isolated electron or muon candidate, where the lepton identification criteria are $p_T > 15$ GeV and $|\eta| < 2.4$, with the isolation requirements $R_{iso} < 0.15$ for electrons and $R_{iso} < 0.12$ for muons.

The distribution of $m_{\gamma\gamma}$ for the selected events is shown in Fig. 7. The principal background arises from events in which a neutral hadron is misidentified as a photon.

The SM background, with the exception of the generally small contribution from SM Higgs boson production, is evaluated using $m_{\gamma\gamma}$ data sidebands defined by $103 \le m_{\gamma\gamma} \le 118$ GeV and $133 \le m_{\gamma\gamma} \le 163$ GeV. We construct the quantity S_T^h, which is the scalar sum of the p_T values of the two Higgs boson candidates. The distribution of S_T^h is measured separately in each of the two sidebands. Each sideband distribution is then normalized to correspond to the expected number of background events in the signal region. To determine the latter, we perform a likelihood fit of a power-law function to the $m_{\gamma\gamma}$ distribution between 103 and 163 GeV, excluding the $118 < m_{\gamma\gamma} < 133$ GeV region around the Higgs boson mass. The result of this fit is shown by the solid (blue) curve in Fig. 7. The scaled distributions of S_T^h from the two sidebands are found to be consistent with each other and are averaged. This average is taken to
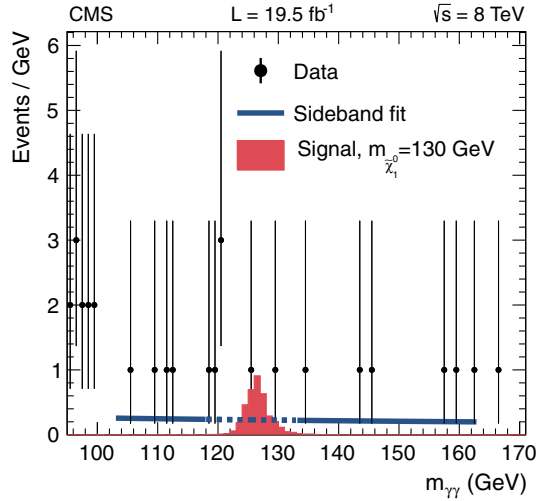
FIG. 7 (color online).   Distribution of diphoton invariant mass $m_{\gamma\gamma}$ after all selection criteria are applied except for that on $m_{\gamma\gamma}$, for the $h(\to\gamma\gamma)h(\to b\bar{b})$ search. The result of a fit to a power-law function using data in the sideband regions (see text) is indicated by the solid line. The dotted line shows an interpolation of the fitted function into the Higgs boson mass region excluded from the fit. The expected results for signal events, with a higgsino ($\tilde{\chi}_1^0$) mass value of 130 GeV and an LSP (gravitino) mass of 1 GeV, are also shown.

be the estimate of the SM background (other than that from SM Higgs boson production), with half the difference assigned as a systematic uncertainty.

To account for the background from SM Higgs boson production, which peaks in the $m_{\gamma\gamma}$ signal region and is not accounted for with the above procedure, we use simulated events. A systematic uncertainty of 30% is assigned to this result, which accounts both for the uncertainty of the SM Higgs boson cross section [75] and for potential misrepresentation of the data by the simulation in the tails of kinematic variables like S_T^h.

To illustrate the difference in the distribution of S_T^h between signal and background events, Fig. 8 (top) shows the distribution of S_T^h for a sample of events selected in the same manner as the nominal sample except with loose CSV requirements for the b-jet tagging, for improved statistical precision. The distributions for two signal scenarios, and for the SM background determined as described above, are also shown. It is seen that S_T^h tends to be larger for signal events than for background events, providing discrimination between the two.

The corresponding results for the nominal selection criteria are shown in Fig. 8 (bottom), with numerical values given in Table II.

B. hZ and $hW \to \gamma\gamma + 2$ jets

For the hZ and hW channels with $h \to \gamma\gamma$ and either $W \to 2$ jets or $Z \to 2$ jets, the vector boson candidate is formed from two jets that yield a dijet mass m_{jj} consistent
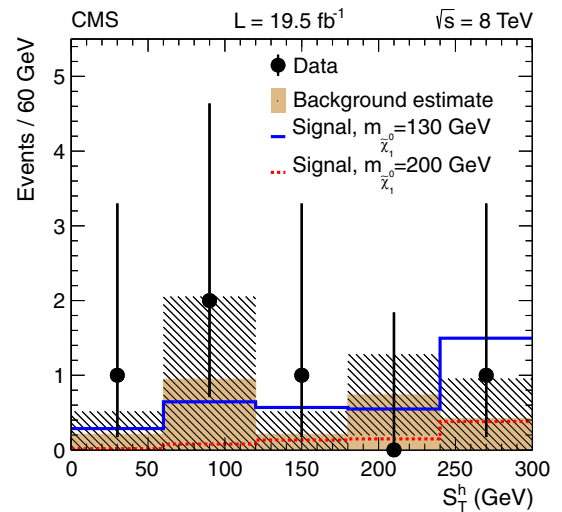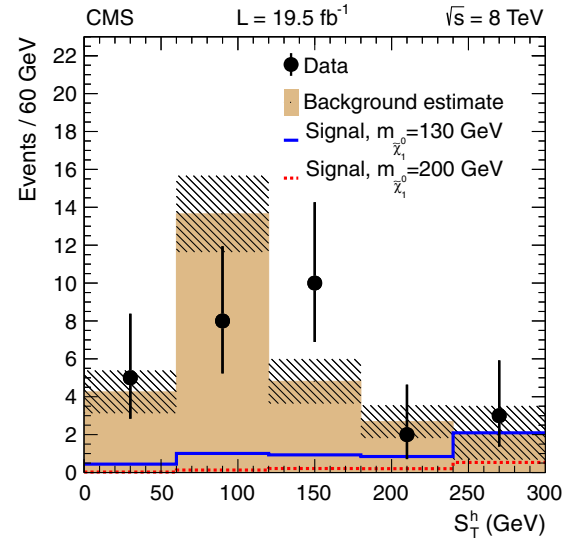

FIG. 8 (color online).   Observed numbers of events as a function of the scalar sum of p_T values of the two Higgs boson candidates, S_T^h, for the $hh \to \gamma\gamma b\bar{b}$ analysis, in comparison with the SM background estimate, (top) for a control sample with loose tagging requirements for b jets, and (bottom) for the nominal selection. The hatched bands show the total uncertainty of the background prediction, with statistical and systematic terms combined. The (unstacked) results for signal events, with higgsino ($\tilde{\chi}_1^0$) mass values of 130 and 200 GeV and an LSP (gravitino) mass of 1 GeV, are also shown.

with that of a W or Z boson, $70 < m_{jj} < 110$ GeV. Multiple candidates per event are allowed. The fraction of events with multiple candidates is 16%. The average number of candidates per event is 1.2. Events with isolated electrons and muons are rejected, using the criteria of Sec. VI A. To avoid overlap with the sample discussed in Sec. VI A, events are rejected if a loose-tagged b jet combined with a medium-tagged b jet yields an invariant mass in the range $95 < m_{b\bar{b}} < 155$ GeV. The distribution of $m_{\gamma\gamma}$ for the selected events is shown in Fig. 9 (top).

TABLE II. Observed numbers of events and corresponding SM background estimates, in bins of Higgs-boson-candidate variable S_T^h (see text), for the $hh \to \gamma\gamma b\bar{b}$ analysis. The uncertainties shown for the SM background estimates are the combined statistical and systematic terms, while those shown for signal events are statistical. The expected yields for signal events, with a higgsino mass value of 130 GeV and an LSP (gravitino) mass of 1 GeV, are also shown.

S_T^h bin (GeV)	SM background	Data	hh events, $m_{\tilde{\chi}_1^0} = 130$ GeV
0–60	$0.21^{+0.28}_{-0.21}$	1	0.28 ± 0.03
60–120	$0.95^{+0.99}_{-0.95}$	2	0.63 ± 0.04
120–180	$0.21^{+0.29}_{-0.21}$	1	0.55 ± 0.04
180–240	0.74 ± 0.38	0	0.53 ± 0.04
> 240	$0.42^{+0.49}_{-0.42}$	1	1.46 ± 0.06

The SM background estimate is obtained using the procedure described in Sec. VI A except using the E_T^{miss} variable rather than the S_T^h variable, viz., from the average of the scaled E_T^{miss} distributions derived from the two $m_{\gamma\gamma}$ sidebands, summed with the prediction from simulated SM Higgs boson events. The solid (blue) curve in Fig. 9 (top) shows the result of the power-law fit to the $m_{\gamma\gamma}$ sideband regions. The scaled E_T^{miss} distributions from the two sidebands are found to be consistent with each other within their uncertainties.

The measured distribution of E_T^{miss} for the selected events is shown in Fig. 9 (bottom) in comparison with the SM background estimate and with the predictions from two signal scenarios. Numerical values are given in Table III.

C. hh, hZ, and $hW \to \gamma\gamma$ + leptons

We next consider hh, hZ, and hW combinations in which a Higgs boson decays into a pair of photons, while the other boson (h, Z, or W) decays to a final state with at least one lepton (electron or muon). For the hh channel this signature encompasses events in which the second Higgs boson decays to $h \to ZZ$, WW, or $\tau\tau$, followed by the leptonic decay of at least one Z, W, or τ particle, including the case where one Z boson decays to charged leptons and the other to neutrinos.

The lepton identification criteria are the same as those presented in Sec. VI A with the additional requirement that the ΔR separation between an electron or muon candidate and each of the two photon candidates exceed 0.3. To reduce the background in which an electron is misidentified as a photon, events are eliminated if the invariant mass formed from an electron candidate and one of the two $h \to \gamma\gamma$ photon candidates lies in the Z boson mass region $86 < m_{e\gamma} < 96$ GeV. Electron candidates are rejected if they appear within $1.44 < |\eta| < 1.57$, which represents a transition region between the barrel and endcap electromagnetic calorimeters [39], where the reconstruction
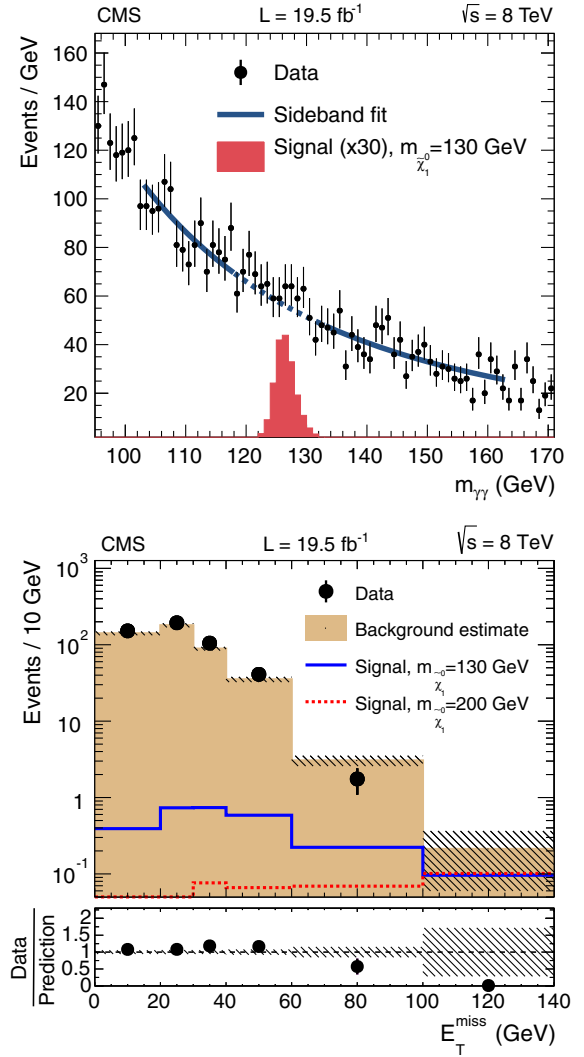

FIG. 9 (color online). Results for the hZ and hW analysis in the $\gamma\gamma + 2$ jets final state after all selection criteria are applied except for that on the displayed variable. (Top) Distribution of diphoton invariant mass $m_{\gamma\gamma}$. The result of a fit to a power-law function using data in the sideband regions (see text) is indicated by the solid line. The dotted line shows an interpolation of the fitted function into the Higgs boson mass region excluded from the fit. The expected result for hZ signal events with a higgsino ($\tilde{\chi}_1^0$) mass of 130 GeV and an LSP (gravitino) mass of 1 GeV, multiplied by a factor of 30 for better visibility, is also shown. (Bottom) Observed numbers of events as a function of E_T^{miss} in comparison with the SM background estimate. The hatched bands show the total uncertainty of the background prediction, with statistical and systematic terms combined. The expected (unstacked) results for hZ signal events, with the indicated values of the higgsino ($\tilde{\chi}_1^0$) mass and an LSP (gravitino) mass of 1 GeV, are also shown.

efficiency is difficult to model. To prevent overlap with the other searches, events are allowed to contain at most one medium-tagged b jet.

We select a sample with at least one muon and an orthogonal sample with no muons but at least one electron. We refer to these samples as the muon and electron

TABLE III.   Observed numbers of events and corresponding SM background estimates, in bins of missing transverse energy E_T^{miss}, for the $hV \to \gamma\gamma + 2$ jets analysis, where V represents a W or Z boson. The uncertainties shown for the SM background estimates are the combined statistical and systematic terms, while those shown for signal events are statistical. The expected yields for hZ signal events, with a higgsino mass value of 130 GeV and an LSP (gravitino) mass of 1 GeV, are also shown.

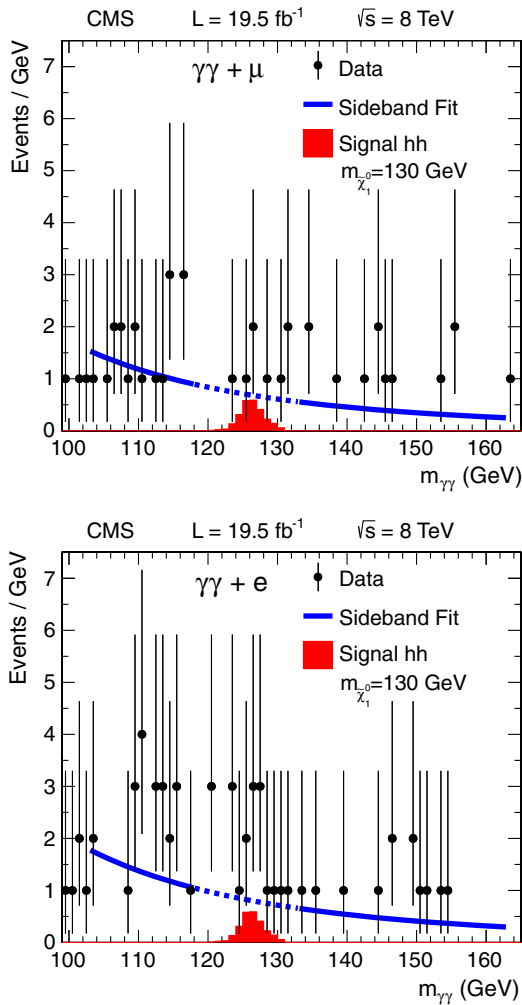| E_T^{miss} (GeV)	SM background	Data	hZ events, $m_{\tilde{\chi}_1^0} = 130$ GeV
0–20	288 ± 15	305	0.76 ± 0.03
20–30	183 ± 10	195	0.71 ± 0.03
30–40	91.1 ± 4.7	105	0.72 ± 0.03
40–60	72.0 ± 5.0	82	1.14 ± 0.04
60–100	12.5 ± 1.9	7	0.87 ± 0.03
> 100	0.96 ± 0.61	0	0.37 ± 0.02

FIG. 10 (color online).   Distribution of the diphoton invariant mass $m_{\gamma\gamma}$ after all selection criteria are applied except for that on $m_{\gamma\gamma}$, for the hh, hZ, and $hW \to \gamma\gamma +$ leptons analysis, for the (top) muon and (bottom) electron samples. The result of a fit to a power-law function using data in the sideband regions (see text) is indicated by the solid line. The dotted line shows an interpolation of the fitted function into the Higgs boson mass region excluded from the fit. The expected results for hh events, with a higgsino ($\tilde{\chi}_1^0$) mass value of 130 GeV and an LSP (gravitino) mass of 1 GeV, are also shown.

samples, respectively. About 93% of the events in each sample contain only a single electron or muon, and there are no events for which the sum of electron and muon candidates exceeds 2 (only two events have one electron and one muon). The $m_{\gamma\gamma}$ distributions for the two samples are shown in Fig. 10.

The SM background is evaluated in the same manner as described in Sec. VI A except using the transverse mass variable $M_T \equiv \sqrt{2E_T^{miss} p_T^\ell [1 - \cos(\Delta\phi_{\ell,E_T^{miss}})]}$ in place of the S_T^h variable, where p_T^ℓ is the transverse momentum of the highest p_T lepton, with $\Delta\phi_{\ell,E_T^{miss}}$ the difference in azimuthal angle between the p_T^ℓ and E_T^{miss} vectors. For SM background events with W bosons, the M_T distribution exhibits an endpoint near the W boson mass. In contrast, for signal events, the value of M_T can be much larger. As an alternative, we tested use of the E_T^{miss} distribution to evaluate the SM background and found the M_T distribution to be slightly more sensitive.

The SM background estimate is thus given by the average of the scaled M_T distributions from the two $m_{\gamma\gamma}$ sidebands, summed with the contribution from simulated SM Higgs boson events. The solid (blue) curves in Fig. 10 show the results of the power-law fits to the $m_{\gamma\gamma}$ sideband regions. For the electron channel [Fig. 10 (bottom)], a cluster of events is visible at $m_{\gamma\gamma} \approx 112$ GeV. We verified that the prediction for the number of background events is stable within about one standard deviation of the statistical uncertainty for alternative definitions of the sideband regions, such as $110 < m_{\gamma\gamma} < 118$ GeV for the lower sideband rather than $103 < m_{\gamma\gamma} < 118$ GeV.

The M_T distributions of the selected events are presented in Fig. 11. Numerical values are given in Table IV. The background estimates and predictions from several signal scenarios are also shown. Results for the alternative method to evaluate the SM background, based on the E_T^{miss} distribution rather than the M_T distribution, are shown in Fig. 12. For the muon channel, the data exhibit a small deficit with respect to the SM background estimate. For the electron channel, there is an excess of 2.1 standard
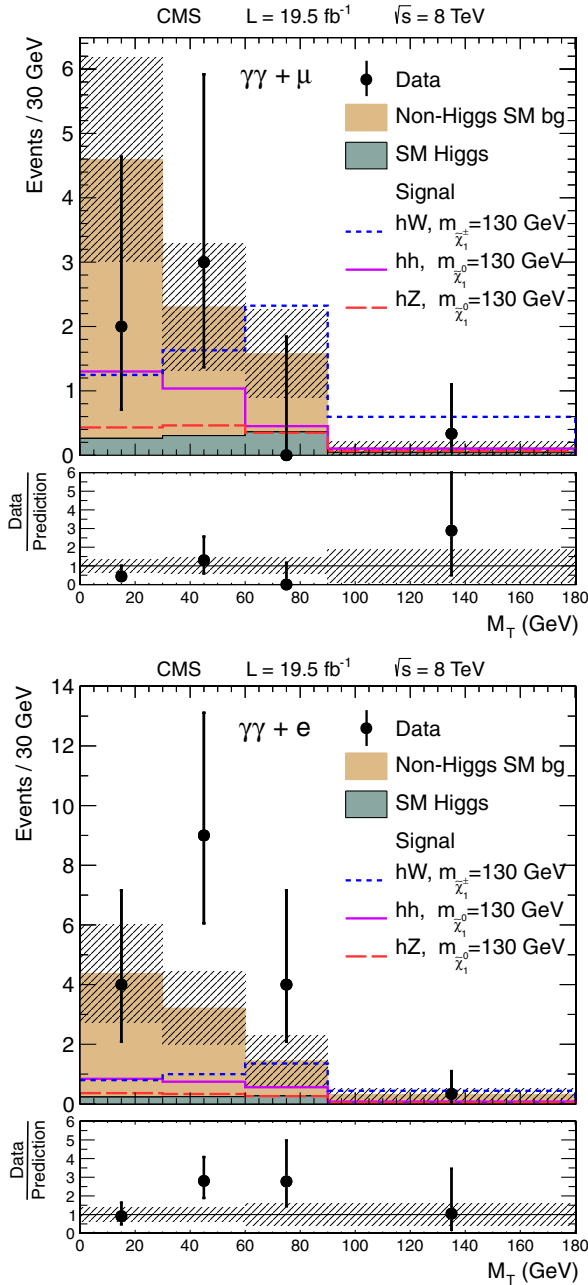
FIG. 11 (color online).   Observed numbers of events as a function of transverse mass M_T for the hh, hZ, and $hW \rightarrow \gamma\gamma +$ leptons analysis, in comparison with the (stacked) SM background estimates, for the (top) muon and (bottom) electron samples. The hatched bands show the total uncertainty of the background prediction, with statistical and systematic terms combined. The (unstacked) results for various signal scenarios are also shown. For the hh and hZ scenarios, the higgsino ($\tilde{\chi}_1^0$) mass is 130 GeV and the LSP (gravitino) mass is 1 GeV. For the hW scenario, $m_{\tilde{\chi}_2^0} = m_{\tilde{\chi}_1^\pm} = 130$ GeV and $m_{\tilde{\chi}_1^0} = 1$ GeV [see Fig. 1 (right)].

FIG. 12 (color online).   Observed numbers of events as a function of E_T^{miss} for the hh, hZ, and $hW \rightarrow \gamma\gamma +$ leptons analysis in comparison with the (stacked) SM background estimates, for the (top) muon and (bottom) electron samples. The hatched bands show the total uncertainty of the background prediction, with statistical and systematic terms combined. The (unstacked) results for various signal scenarios are also shown. For the hh and hZ scenarios, the higgsino ($\tilde{\chi}_1^0$) mass is 130 GeV and the LSP (gravitino) mass is 1 GeV. For the hW scenario, $m_{\tilde{\chi}_2^0} = m_{\tilde{\chi}_1^\pm} = 130$ GeV and $m_{\tilde{\chi}_1^0} = 1$ GeV.

deviations. Note that this result does not account for the so-called look-elsewhere effect [79]. The excess of data events in the electron channel above the SM background prediction clusters at low values $E_T^{\mathrm{miss}} \lesssim 30$ GeV, as seen in
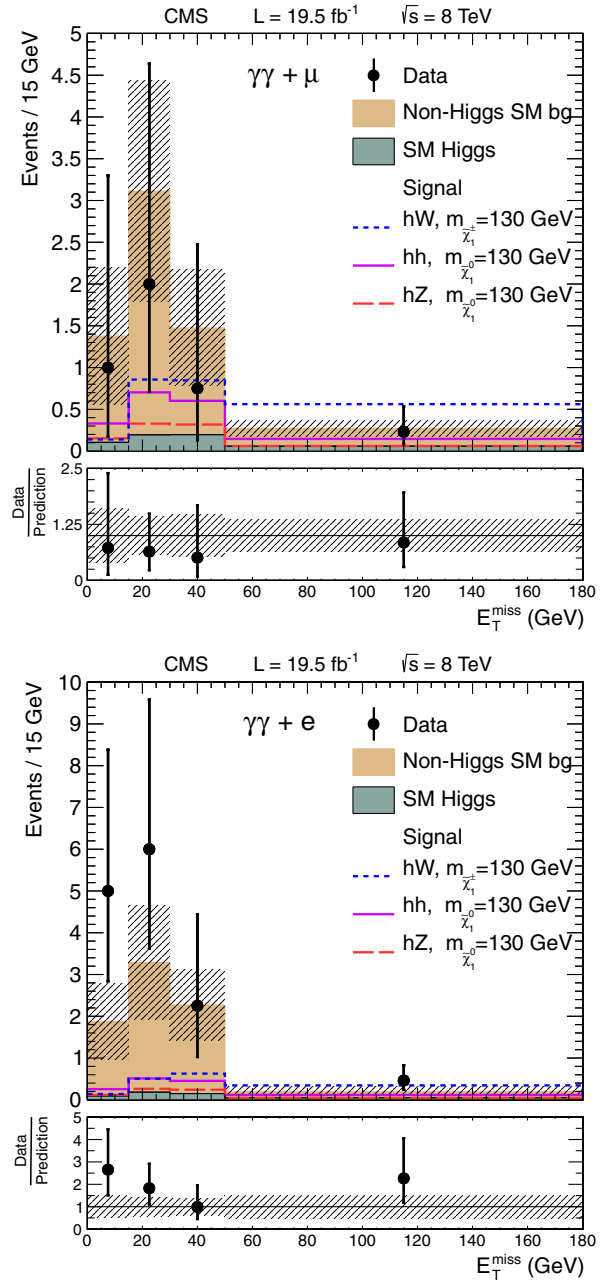
Fig. 12 (bottom). Summing the electron and muon channels, we obtain 24 observed events compared to 18.9 ± 3.1 expected SM events, corresponding to an excess of 1.3 standard deviations. To investigate the excess in the

TABLE IV. Observed numbers of events and corresponding SM background estimates, in bins of transverse mass M_{T}, for the hh, hZ, and $hW \to \gamma\gamma$ + leptons analysis. The uncertainties shown for the SM background estimates are the combined statistical and systematic terms, while those shown for signal events are statistical. The column labeled "hW events" shows the expected number of events from the chargino-neutralino pair-production process of Fig. 1 (right), taking $m_{\tilde{\chi}_2^0} = m_{\tilde{\chi}_1^\pm} = 130$ GeV and $m_{\tilde{\chi}_1^0} = 1$ GeV.

	Muon sample			Electron sample		
M_{T} (GeV)	SM background	Data	hW events	SM background	Data	hW events
0–30	4.6 ± 1.6	2	1.2 ± 0.1	4.4 ± 1.7	4	0.80 ± 0.06
30–60	2.31 ± 0.99	3	1.5 ± 0.1	3.2 ± 1.2	9	1.0 ± 0.1
60–90	1.59 ± 0.68	0	2.1 ± 0.1	1.44 ± 0.85	4	1.4 ± 0.1
>90	0.35 ± 0.30	1	1.6 ± 0.1	0.96 ± 0.58	1	1.3 ± 0.1

electron channel, we varied the functional form used to fit the sideband data (an exponential function was used rather than a power-law function), modified the definitions of the sideband and signal regions, as mentioned above, and altered the photon identification criteria. All variations yielded consistent results, with an excess in the electron channel of about 2 standard deviations. An ensemble of MC pseudoexperiments was used to verify that the background evaluation procedure is unbiased. Since the excess in the electron channel is neither large nor signal-like, and since there is not a corresponding excess in the muon channel, we consider the excess seen in Fig. 11 (bottom) to be consistent with a statistical fluctuation. Note that if we apply looser or tighter photon selection criteria relative to the nominal criteria, the significance of the excess decreases in a way that is consistent with its explanation as a statistical fluctuation.

VII. SEARCH IN THE hZ CHANNEL WITH $h \to b\bar{b}$ AND $Z \to \ell^+\ell^-$

We now describe the search in the SUSY hZ channel with $h \to b\bar{b}$ and $Z \to \ell^+\ell^-$ ($\ell = e, \mu$). Electron and muon candidates are required to satisfy $p_{\mathrm{T}} > 20$ GeV, $|\eta| < 2.4$, and $R_{\mathrm{iso}} < 0.15$. For the R_{iso} variable, a cone size $R_{\mathrm{cone}} = 0.3$ is used for both electrons and muons, rather than $R_{\mathrm{cone}} = 0.4$ for muons as in Secs. V and VI. Electron candidates that appear within the transition region $1.44 < |\eta| < 1.57$ between the barrel and endcap electromagnetic calorimeters are rejected. Jets must satisfy $p_{\mathrm{T}} > 30$ GeV and $|\eta| < 2.5$ and be separated by more than $\Delta R = 0.4$ from an electron or muon candidate. To be tagged as a b jet, the jet must satisfy the CSV-medium criteria.

Events are required to contain

(i) exactly one e^+e^- or $\mu^+\mu^-$ pair with a dilepton invariant mass $m_{\ell\ell}$ in the Z boson mass region $81 < m_{\ell\ell} < 101$ GeV;

(ii) no third electron or muon candidate, selected using the above criteria except with $p_{\mathrm{T}} > 10$ GeV;

(iii) no τ_h candidate with $p_{\mathrm{T}} > 20$ GeV;

(iv) at least two tagged b jets, where the two most b-like jets yield a dijet mass in the Higgs boson mass region $100 < m_{b\bar{b}} < 150$ GeV.

The reason to reject events with a third lepton is to avoid overlap with the three-or-more-lepton sample discussed in Sec. VIII.

Events with a $t\bar{t}$ pair represent a large potential source of background, especially if both top quarks decay to a state with a lepton. To reduce this background, we use the $M_{\mathrm{T2}}^{j\ell}$ variable [80,81], which corresponds to the minimum mass of a pair-produced parent particle compatible with the observed four-momenta in the event, where each parent is assumed to decay to a b jet, a charged lepton ℓ, and an undetected particle, and where the vector sum of the p_{T} values of the two undetected particles is assumed to equal the observed result for $E_{\mathrm{T}}^{\mathrm{miss}}$. For $t\bar{t}$ events with perfect event reconstruction, $M_{\mathrm{T2}}^{j\ell}$ has an upper bound at the top-quark mass. For signal events, $M_{\mathrm{T2}}^{j\ell}$ can be much larger. To account for imperfect reconstruction and finite detector resolution, we require $M_{\mathrm{T2}}^{j\ell} > 200$ GeV. The distribution of $M_{\mathrm{T2}}^{j\ell}$ is shown in Fig. 13.

We further require $E_{\mathrm{T}}^{\mathrm{miss}} > 60$, 80, or 100 GeV, where the lower bound on $E_{\mathrm{T}}^{\mathrm{miss}}$ depends on which choice yields the largest expected signal sensitivity for a given value of the higgsino mass.

The remaining background mostly consists of events from SM Z + jets, $t\bar{t}$, W^+W^-, $\tau^+\tau^-$, and tW single-top-quark production. These backgrounds are evaluated using data, as described below. Other remaining SM background processes are combined into an "other" category, which is evaluated using simulation and assigned an uncertainty of 50%. The "other" category includes background from ZW and ZZ boson pair production, $t\bar{t}$ processes with an associated W or Z boson, and processes with three vector bosons.

For the SM Z + jets background, significant values of $E_{\mathrm{T}}^{\mathrm{miss}}$ arise primarily because of the mismeasurement of jet p_{T}. Another source is the semileptonic decay of charm and bottom quarks. As in Ref. [82], we evaluate this background using a sample of γ + jets events, which is selected using similar criteria to those used for the nominal selection, including the same b-jet tagging requirements and restriction on $m_{b\bar{b}}$. We account for kinematic differences between the γ + jets and signal samples by reweighting the H_{T} and boson-p_{T} spectra of the former
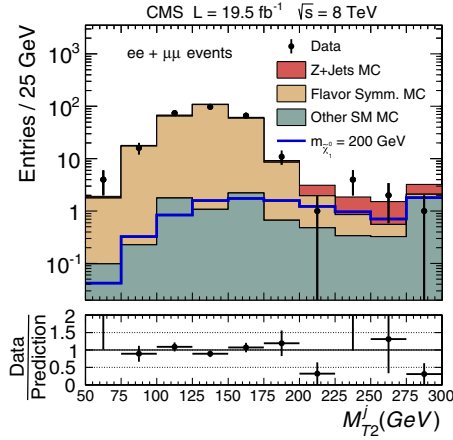
FIG. 13 (color online). Distribution of $M_{\mathrm{T2}}^{j\ell}$ for the $h(\to b\bar{b})Z(\to \ell^+\ell^-)$ analysis after all signal-region requirements are applied except for that on $M_{\mathrm{T2}}^{j\ell}$, in comparison with (stacked) SM background estimates taken from simulation. For this result, $E_{\mathrm{T}}^{\mathrm{miss}} > 60$ GeV. The (unstacked) signal results for a higgsino ($\tilde{\chi}_1^0$) mass of 200 GeV and an LSP (gravitino) mass of 1 GeV are also shown.

sample to match those of the latter, where H_{T} is the scalar sum of jet p_{T} values using jets with $p_{\mathrm{T}} > 15$ GeV. The resulting $\gamma +$ jets $E_{\mathrm{T}}^{\mathrm{miss}}$ distributions are then normalized to unit area to define templates. Two different templates are formed: one from $\gamma +$ jets events with exactly two jets, and one from the events with three or more jets. The SM $Z +$ jets background estimate is given by the sum of the two templates, each weighted by the number of events in the signal sample with the respective jet multiplicity. To account for the small level of background expected in the signal sample from SM processes other than SM $Z +$ jets production, which is mostly due to $t\bar{t}$ production, the prediction is normalized to the data yield in the $0 < E_{\mathrm{T}}^{\mathrm{miss}} < 50$ GeV region, where the contribution of SM $Z +$ jets events dominates. The impact of signal events on the estimate of the SM $Z +$ jets background is found to be negligible. The corresponding systematic uncertainty is evaluated by varying the criteria used to select $\gamma +$ jets events, by assessing the impact of $t\bar{t}$ events, and by determining the difference between the predicted and genuine SM $Z +$ jets event yields when the simulation is used to describe the $\gamma +$ jets and signal samples. The three sources of systematic uncertainty are added in quadrature to define the total systematic uncertainty.

For the $t\bar{t}$, W^+W^-, $\tau^+\tau^-$, and tW background, the rate of decay to events with exactly one electron and exactly one muon is the same as the rate of decay to events with either exactly one e^+e^- or one $\mu^+\mu^-$ pair, once the difference between the electron and muon reconstruction efficiencies is taken into account. We therefore refer to this category of events as the "flavor-symmetric" background. The flavor-symmetric background is thus evaluated by measuring the number of events in a sample of $e\mu$ events, which is
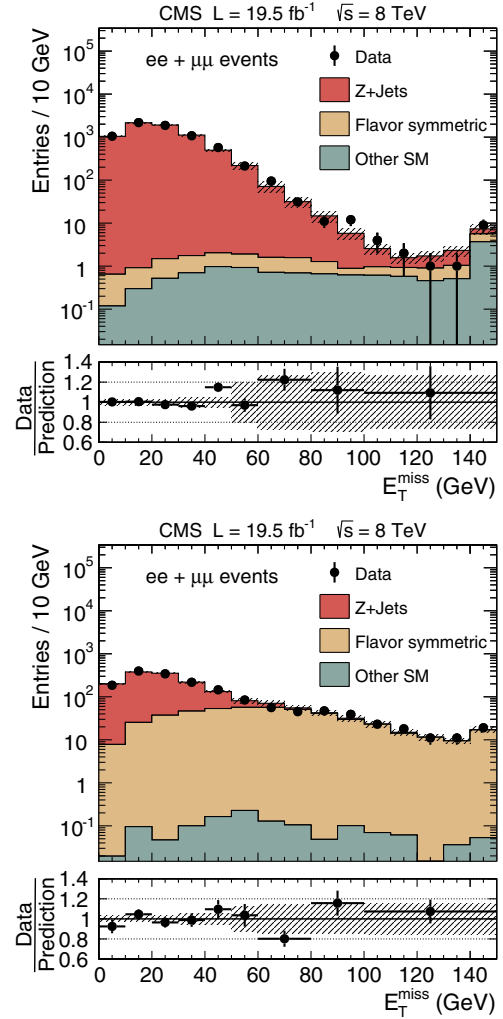

FIG. 14 (color online). Distribution of $E_{\mathrm{T}}^{\mathrm{miss}}$ in comparison with the (stacked) SM background estimates for the $h(\to b\bar{b})Z(\to \ell^+\ell^-)$ analysis, for data control samples enriched in (top) SM $Z +$ jets events, and (bottom) $t\bar{t}$ events. The hatched bands in the ratio plots (lower panels) indicate the uncertainty of the total background prediction, with statistical and systematic terms combined.

selected in the manner described above for the e^+e^- and $\mu^+\mu^-$ samples except without the requirement on the dilepton mass: instead of applying an invariant mass restriction $81 < m_{e\mu} < 101$ GeV in analogy with the mass restriction imposed on $m_{\ell\ell}$, we apply a factor, derived from simulation, that gives the probability for $m_{e\mu}$ to fall into this interval, with a systematic uncertainty defined by the difference between this factor in data and simulation. This procedure yields improved statistical precision compared to the result based on an $m_{e\mu}$ requirement [82].

The background evaluation procedures are validated using data control samples enriched in the principal background components. As an example, Fig. 14 (top) shows the $E_{\mathrm{T}}^{\mathrm{miss}}$ distribution for a control sample selected in the same manner as the standard sample except with the
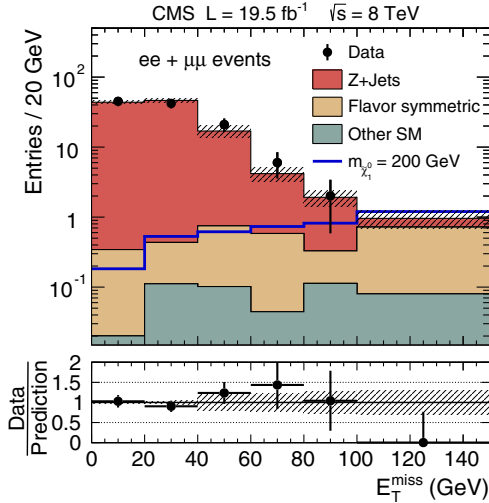
FIG. 15 (color online). Observed numbers of events as a function of E_T^{miss} for the $h(\to b\bar{b})Z(\to \ell^+\ell^-)$ analysis, in comparison with the (stacked) SM background estimates. The (unstacked) results for a higgsino ($\tilde{\chi}_1^0$) mass of 200 GeV and an LSP (gravitino) mass of 1 GeV are also shown. The hatched band in the ratio plot (lower panel) indicates the uncertainty of the total background prediction, with statistical and systematic terms combined.

requirement that there be no tagged b jet: this yields a sample dominated by SM Z + jets events. Figure 14 (bottom) shows the results for a sample selected with the nominal requirements except with the $M_{\mathrm{T2}}^{j\ell}$ requirement inverted: this yields a sample dominated by $t\bar{t}$ events. For both these control samples, the SM background estimate is seen to accurately represent the data.

The distribution of E_T^{miss} for the selected events is presented in Fig. 15 in comparison with the corresponding background prediction and with the prediction from a signal scenario. Numerical values are given in Table V.

VIII. SEARCH IN CHANNELS WITH THREE OR MORE LEPTONS OR WITH A $ZZ \to \ell^+\ell^- + 2$ JETS COMBINATION

The SUSY scenarios of interest to this study (Fig. 1) can yield events with three or more leptons if the h, Z, or W bosons decay to final states with leptons. We therefore combine the results presented here with our results on final states with three or more leptons [35] to derive unified conclusions for these scenarios. The three-or-more-lepton results provide sensitivity to the SUSY ZZ channel, i.e., to events in which the two Higgs bosons in Fig. 1 (left) are each replaced by a Z boson. In contrast, the studies presented in Secs. V–VII have little sensitivity to ZZ production. In addition, the three-or-more-lepton results provide sensitivity to the SUSY hh and hZ channels, especially for low values of the higgsino ($\tilde{\chi}_1^0$) mass.

The analysis of Ref. [35] requires events to contain at least three charged lepton candidates including at most one τ_h candidate. The events are divided into exclusive categories based on the number and flavor of the leptons, the presence or absence of an opposite-sign, same-flavor (OSSF) lepton pair, the invariant mass of the OSSF pair including its consistency with the Z boson mass, the presence or absence of a tagged b jet, the E_T^{miss} value, and the H_T value. As in Ref. [35], we order the search channels by their expected sensitivities and, for the interpretation of results (Sec. X), select channels starting with

TABLE V. Observed numbers of events and corresponding SM background estimates, in bins of missing transverse energy E_T^{miss}, for the $h(\to b\bar{b})Z(\to \ell^+\ell^-)$ analysis. The uncertainties shown for the SM background estimates are the combined statistical and systematic terms, while those shown for signal events are statistical. For bins with $E_T^{\mathrm{miss}} > 60$ GeV, signal event yields are given for four values of the higgsino ($\tilde{\chi}_1^0$) mass, with an LSP (gravitino) mass of 1 GeV.

	$E_T^{\mathrm{miss}} < 25$ GeV	$25 < E_T^{\mathrm{miss}} < 50$ GeV	$50 < E_T^{\mathrm{miss}} < 60$ GeV
Z + jets background	56.7 ± 1.9	43.3 ± 2.3	5.7 ± 1.2
Flavor symmetric background	0.4 ± 0.3	0.4 ± 0.3	0.4 ± 0.3
Other SM background	< 0.1	0.1 ± 0.1	0.1 ± 0.1
Total SM background	57.2 ± 1.9	43.8 ± 2.3	6.2 ± 1.2
Data	54	47	7
	$E_T^{\mathrm{miss}} > 60$ GeV	$E_T^{\mathrm{miss}} > 80$ GeV	$E_T^{\mathrm{miss}} > 100$ GeV
Z + jets background	5.7 ± 1.8	2.2 ± 0.9	0.6 ± 0.3
Flavor symmetric background	2.4 ± 0.9	1.8 ± 0.7	1.6 ± 0.6
Other SM background	0.3 ± 0.2	0.3 ± 0.2	0.2 ± 0.1
Total SM background	8.5 ± 2.0	4.3 ± 1.2	2.4 ± 0.7
Data	8	2	0
hZ events			
$m_{\tilde{\chi}_1^0} = 130$ GeV	5.4 ± 0.1	3.1 ± 0.1	1.7 ± 0.1
$m_{\tilde{\chi}_1^0} = 150$ GeV	5.3 ± 0.1	3.3 ± 0.1	2.0 ± 0.1
$m_{\tilde{\chi}_1^0} = 200$ GeV	4.7 ± 0.1	4.2 ± 0.1	3.3 ± 0.1
$m_{\tilde{\chi}_1^0} = 250$ GeV	3.5 ± 0.1	3.2 ± 0.1	2.8 ± 0.1

TABLE VI. The seven most sensitive search channels of the three-or-more-lepton analysis [35] for the $\tilde{\chi}_1^0(\to h\tilde{G})\tilde{\chi}_1^0(\to h\tilde{G})$ di-higgsino production scenario assuming a higgsino mass of 150 GeV and an LSP (gravitino) mass of 1 GeV. For all channels, $H_T < 200$ GeV and the number of tagged b jets is zero. The symbols N_ℓ, N_{τ_h}, and N_{OSSF} indicate the number of charged leptons, hadronically decaying τ-lepton candidates, and opposite-sign same-flavor (OSSF) lepton pairs, respectively. "Below Z" means that the invariant mass $m_{\ell\ell}$ of the OSSF pair (if present) lies below the region of the Z boson ($m_{\ell\ell} < 75$ GeV), while "Off Z" means that either $m_{\ell\ell} < 75$ GeV or $m_{\ell\ell} > 105$ GeV. The uncertainties shown for the SM background estimates are the combined statistical and systematic terms, while those shown for signal events are statistical. The channels are ordered according to the values of N_ℓ, N_{τ_h}, N_{OSSF}, and E_T^{miss}.

N_ℓ	N_{τ_h}	N_{OSSF}	$m_{\ell\ell}$ range	E_T^{miss} (GeV)	SM background	Data	hh events, $m_{\tilde{\chi}_1^0} = 150$ GeV
3	0	0	$\cdots$	0–50	51 ± 11	53	3.1 ± 0.6
3	0	0	$\cdots$	50–100	38 ± 15	35	2.7 ± 0.6
3	0	1	Below Z	50–100	130 ± 27	142	7.4 ± 1.6
3	1	0	$\cdots$	50–100	400 ± 150	406	8.0 ± 1.4
4	0	1	Off Z	50–100	0.2 ± 0.1	0	0.5 ± 0.2
4	1	1	Off Z	0–50	7.5 ± 2.0	15	0.8 ± 0.2
4	1	1	Off Z	50–100	2.1 ± 0.5	4	0.7 ± 0.2

the most sensitive one, and do not consider additional channels once the expected number of signal events, integrated over the retained channels, equals or exceeds 90% of the total expected number.

As an illustration of the information provided by the three-or-more-lepton analysis, the seven most sensitive channels for hh signal events, assuming a higgsino mass of $m_{\tilde{\chi}_1^0} = 150$ GeV and a $\tilde{\chi}_1^0 \to h\tilde{G}$ branching fraction of unity, are presented in Table VI. Similar results are obtained for other values of the higgsino mass. Table VI includes the observed numbers of events, the SM background estimates [35], and the predicted signal yields. Some excesses in the data relative to the expectations are seen for the last two channels listed in the table, for which 15 and 4 events are observed, compared to 7.5 ± 2.0 and 2.1 ± 0.5 events, respectively, that are expected. The combined local excess is 2.6 standard deviations. The excesses in these two search channels are discussed in Ref. [35], where it is demonstrated that they are consistent with a statistical fluctuation once the large number of search channels in the analysis is taken into account (look-elsewhere effect).

We also make use of our results [36] on final states with two or more jets and either a $Z \to e^+e^-$ or $Z \to \mu^+\mu^-$ decay, which provide yet more sensitivity to the SUSY ZZ channel. In the study of Ref. [36], events must contain either an e^+e^- or $\mu^+\mu^-$ pair and no other lepton, at least two jets, no tagged b jets, and large values of E_T^{miss}. The invariant mass of the lepton pair, and the dijet mass formed from the two jets with highest p_T values, are both required to be consistent with the Z boson mass. Reference [36] also contains results on the hW signal scenario of Fig. 1 (right) in decay channels that are complementary to those considered here. We make use of these results in our interpretation of the hW scenario.

IX. SYSTEMATIC UNCERTAINTIES

Systematic uncertainties for the various background estimates are presented in the respective sections above,

or, in the case of the studies mentioned in Sec. VIII, in Refs. [35,36].

Systematic uncertainties associated with the selection efficiency for signal events arise from various sources. The uncertainties related to the jet energy scale, jet energy resolution, pileup modeling, trigger efficiencies, b-jet tagging efficiency correction factors, lepton identification and isolation criteria, and the ISR modeling are evaluated by varying the respective quantities by their uncertainties, while those associated with the parton distribution functions are determined [73,83,84] using the recommendations of Refs. [85,86]. The uncertainty of the luminosity determination is 2.6% [87]. Table VII lists typical values of the uncertainties. The uncertainty listed for lepton identification and isolation includes an uncertainty of 1% per lepton to account for differences between the fast simulation and GEANT-based modeling of the detector response. In setting limits (Sec. X), correlations between systematic uncertainties across the different search channels are taken into account, and the systematic uncertainties are treated as nuisance parameters as described in Ref. [88].

TABLE VII. Typical values of the systematic uncertainty for signal efficiency, in percentage.

Source	
Jet energy scale	5–10
Jet energy resolution	2–4
Pileup modeling	4
Trigger efficiency	1–5
b-jet tagging efficiency	5–10
Lepton identification and isolation	5
ISR modeling	1
Parton distribution functions	1
Integrated luminosity	2.6

X. INTERPRETATION

In this section, we present the interpretation of our results. We set 95% confidence level upper limits on the production cross sections of the considered scenarios using a modified frequentist CL_S method based on the LHC-style test statistic [88–90]. The input to the procedure is the number of observed events, the number of expected SM background events (with uncertainties), and the number of predicted signal events in each bin of the distributions of Figs. 6, 8 (bottom), 9 (bottom), 11, and 15, as well as the relevant results from Refs. [35,36] (see Tables 2–3 of Ref. [35] and Tables 4–6 of Ref. [36]). The contributions of signal events are incorporated into the likelihood function for both signal and control regions. The cross section upper limits are compared to the predicted cross sections, which have uncertainties [86] of approximately 5%.

We first present upper limits for the GMSB higgsino NLSP model [28,34] discussed in the introduction. The limits are presented as a function of the higgsino ($\tilde{\chi}_1^0$) mass for the hh, ZZ, and hZ topologies separately and then in the two-dimensional plane of the $\tilde{\chi}_1^0 \to h\tilde{G}$ branching fraction versus $m_{\tilde{\chi}_1^0}$. We assume that the higgsino $\tilde{\chi}_1^0$ can decay only to the $h\tilde{G}$ or $Z\tilde{G}$ states. Following our discussion of the GMSB model, we present limits for the electroweak chargino-neutralino pair production process of Fig. 1 (right) as a function of the LSP ($\tilde{\chi}_1^0$) and common $\tilde{\chi}_2^0$, $\tilde{\chi}_1^\pm$ masses, taking the $\tilde{\chi}_2^0 \to h\tilde{\chi}_1^0$ and $\tilde{\chi}_1^\pm \to W^\pm \tilde{\chi}_1^0$ branching fractions each to be unity.

A. Limits on the GMSB di-higgsino NLSP model

1. The hh topology

Figure 16 shows the 95% C.L. cross section upper limits on higgsino pair production through the hh channel [Fig. 1 (left)], i.e., assuming the $\tilde{\chi}_1^0 \to h\tilde{G}$ branching fraction to be unity. The limits are derived using the combined results from the $hh \to b\bar{b}b\bar{b}$, $\gamma\gamma b\bar{b}$, $\gamma\gamma$ + leptons, and three-or-more-lepton channels, corresponding to the results presented in Secs. V, VI A, VI C, and VIII, respectively. Both the expected and observed limits are shown, where the expected limits are derived from the SM background estimates. The expected results are presented with one, two, and three standard-deviation bands of the experimental uncertainties, which account for the uncertainties of the background prediction and for the statistical uncertainties of the signal observables. The NLO + NLL theoretical cross section [38,67,68] with its one-standard-deviation uncertainty band is also shown.

The observed exclusion contour in Fig. 16 (solid line) is seen to lie above the theoretical cross section for all examined higgsino mass values. Therefore, we do not exclude higgsinos for any mass value in the hh topology scenario. It is nonetheless seen that the expected exclusion contour (short-dashed line with uncertainty bands) lies just above the theoretical higgsino pair production cross section
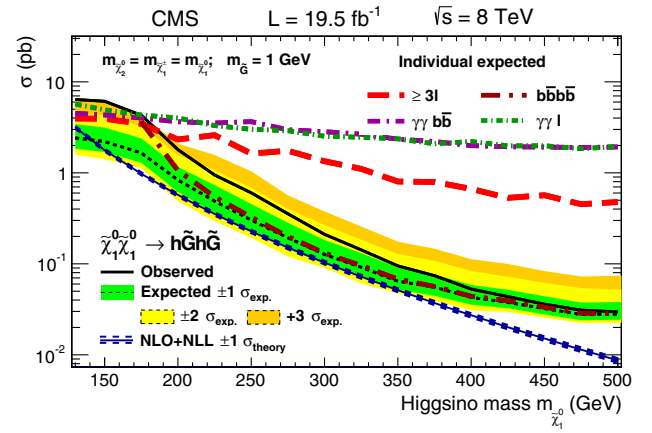

FIG. 16 (color online). Observed and expected 95% confidence level upper limits on the cross section for higgsino pair production in the hh topology as a function of the higgsino mass for the combined $b\bar{b}b\bar{b}$, $\gamma\gamma b\bar{b}$, $\gamma\gamma$ + leptons, and three-or-more-lepton channels. The dark (green), light (yellow), and medium-dark (orange) bands indicate the one-, two-, and three-standard-deviation uncertainty intervals, respectively, for the expected results. The theoretical cross section and the expected curves for the individual search channels are also shown.

for higgsino mass values $m_{\tilde{\chi}_1^0} \lesssim 360$ GeV. Most of this sensitivity is provided by the $hh \to b\bar{b}b\bar{b}$ channel, which dominates the results for $m_{\tilde{\chi}_1^0} \gtrsim 200$ GeV. For lower mass values, the $\gamma\gamma b\bar{b}$ and three-or-more-lepton channels provide the greatest sensitivity. The $hh \to b\bar{b}b\bar{b}$ channel loses sensitivity for $m_{\tilde{\chi}_1^0} \lesssim 200$ GeV because the $\mathcal{S}_{MET}$ spectrum of signal events becomes similar to the spectrum from SM events.

The observed limits in Fig. 16 are seen to deviate from the expected ones by slightly more than three standard deviations for $m_{\tilde{\chi}_1^0} \lesssim 170$ GeV. The main contribution to this excess (2.6 standard deviations, discussed in Sec. VIII) arises from the three-or-more-lepton channel, and was also reported in Ref. [35]. The electron (but not muon) component of the $\gamma\gamma$ + leptons channel contributes to the excess at the level of 2.1 standard deviations, as discussed in Sec. VI C [Fig. 11 (bottom)]. As already mentioned in Secs. VI C and VIII, we consider the excesses in the $\gamma\gamma$ + electron and three-or-more-lepton channels to be consistent with statistical fluctuations.

2. The ZZ and hZ topologies

The 95% C.L. cross section upper limits on higgsino pair production through the ZZ channel are presented in Fig. 17 (top). For these results, we assume the $\tilde{\chi}_1^0 \to Z\tilde{G}$ branching fraction to be unity. These results are derived using the two search channels that dominate the sensitivity to the ZZ topology: the three-or-more-lepton and $\ell^+\ell^- + 2$ jets channels (Sec. VIII). In the context of this scenario, higgsino masses below 380 GeV are excluded.
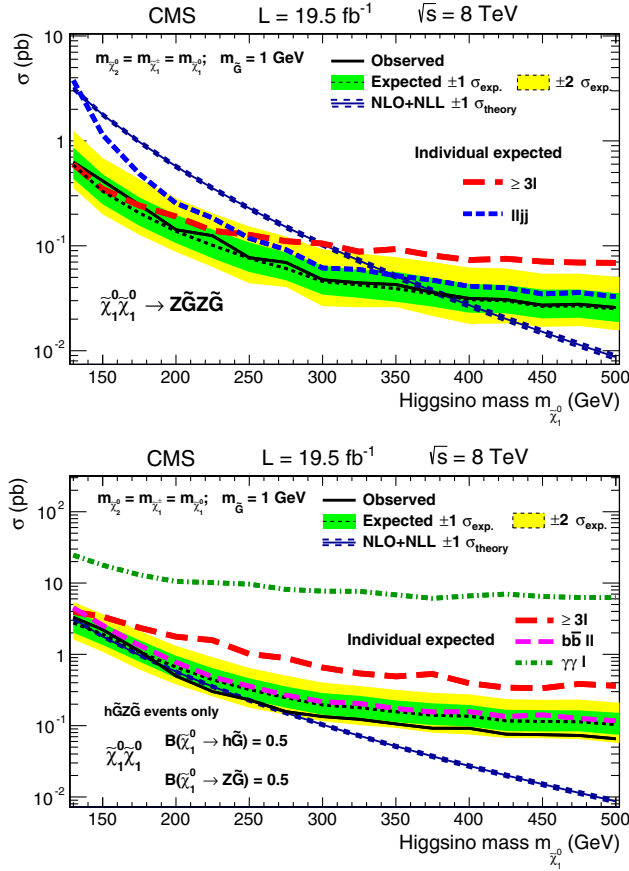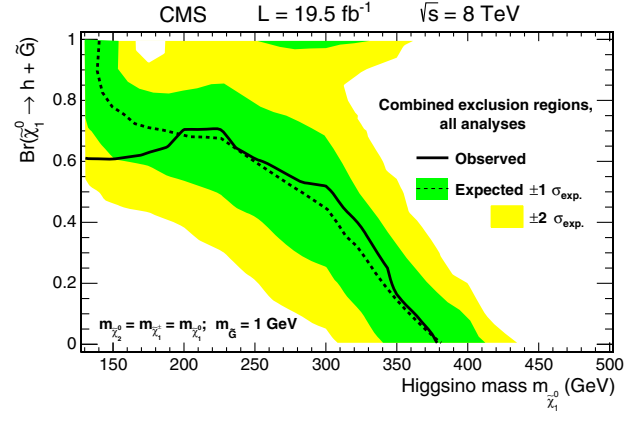
FIG. 18 (color online). Observed and expected 95% confidence level exclusion regions for higgsino pair production, with all channels combined, in the plane of the higgsino branching fraction to a Higgs boson and LSP, versus the higgsino mass. The dark (green) and light (yellow) bands indicate the one- and two-standard-deviation uncertainty intervals, respectively. The excluded regions correspond to the area below the contours.

FIG. 17 (color online). (Top) Observed and expected 95% confidence level upper limits on the cross section for higgsino pair production in the ZZ topology as a function of the higgsino mass for the combined three-or-more-lepton and $\ell^+\ell^- + 2$ jets channels. The dark (green) and light (yellow) bands indicate the one- and two-standard-deviation uncertainty intervals, respectively, for the expected results. The theoretical cross section and the expected curves for the individual search channels are also shown. (Bottom) Corresponding results for the hZ topology, assuming the $\tilde{\chi}_1^0 \to h\tilde{G}$ and $\tilde{\chi}_1^0 \to Z\tilde{G}$ branching fractions each to be 0.5, ignoring contributions from hh and ZZ events, for the individual and combined $\gamma\gamma$ + leptons, $b\bar{b}\ell^+\ell^-$, and three-or-more-lepton channels.

To illustrate the sensitivity of our analysis to the hZ topology [Fig. 1 (middle)], we assume the $\tilde{\chi}_1^0 \to h\tilde{G}$ and $\tilde{\chi}_1^0 \to Z\tilde{G}$ branching fractions each to be 0.5 and ignore contributions from the hh and ZZ channels. Figure 17 (bottom) shows 95% C.L. cross section upper limits for the hZ topology derived from the combined $\gamma\gamma$ + leptons, $b\bar{b}\ell^+\ell^-$, and three-or-more-lepton samples (Secs. VI C, VII, and VIII, respectively). The results are dominated by the $b\bar{b}\ell^+\ell^-$ channel. The main contribution of the three-or-more-lepton channel arises for higgsino mass values below around 170 GeV. The sensitivity of the $\gamma\gamma$ + leptons channel is minimal. [The $\gamma\gamma$ + 2 jets channel also contributes minimally and is not included in the combination of Fig. 17 (bottom).]

3. Exclusion region as a function of the $\tilde{\chi}_1^0$ mass and $\tilde{\chi}_1^0 \to h\tilde{G}$ branching fraction

Figure 18 presents the 95% C.L. exclusion region for the GMSB higgsino NLSP scenario in the two-dimensional plane of the $\tilde{\chi}_1^0 \to h\tilde{G}$ higgsino branching fraction versus the higgsino mass $m_{\tilde{\chi}_1^0}$. The results are based on all relevant studies discussed in this paper including those of Refs. [35,36]. The combined results exclude a significant fraction of the Fig. 18 plane. For higgsino mass values above around 200 GeV, the observed results are in agreement with the expected ones within one standard deviation of the uncertainties. For smaller higgsino mass values, the observed exclusion boundary lies below the expected one because of the excesses in data discussed in Section X A 1. Horizontal slices of Fig. 18 at branching fractions of one and zero correspond to the results presented in Figs. 16 and 17 (top) for the hh and ZZ topologies, respectively. The corresponding results for a horizontal slice at a branching fraction of 0.5 are shown in Fig. 19. It is seen that higgsino masses below around 300 GeV are excluded for this latter scenario.

To illustrate the relative importance of the different search channels for the results of Fig. 18, we present in Fig. 20 the observed and expected exclusion regions when each principal component of the analysis is in turn removed from the combination. For this purpose, the $h \to \gamma\gamma$ studies of Sec. VI are grouped together into a "$2\gamma + X$" category, and the $h(\to b\bar{b})Z(\to \ell^+\ell^-)$ and $Z(\to \ell^+\ell^-)Z(\to 2\,\text{jets})$ studies of Secs. VII and VIII into a "$2\ell + X$" category. The greatest impact is from the three-or-more-lepton and combined $b\bar{b}\ell^+\ell^-$ and $\ell^+\ell^- + 2$ jets channels, because of the stringent constraints they impose on ZZ production [Fig. 17 (top)]. A distribution showing which search
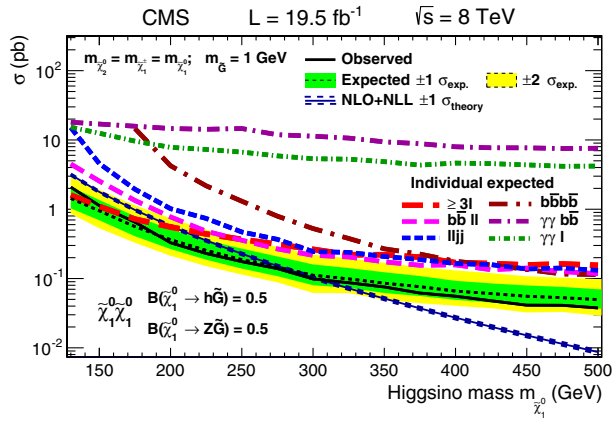
FIG. 19 (color online). Observed and expected 95% confidence level upper limits on the cross section for higgsino pair production as a function of the higgsino mass assuming the $\tilde{\chi}_1^0 \to h\tilde{G}$ and $\tilde{\chi}_1^0 \to Z\tilde{G}$ branching fractions each to be 0.5, including contributions from hh and ZZ events, for the combined $b\bar{b}b\bar{b}$, $\gamma\gamma b\bar{b}$, $\gamma\gamma$ + leptons, $b\bar{b}\ell^+\ell^-$, three-or-more-lepton, and $\ell^+\ell^-$ + 2 jets channels. The dark (green) and light (yellow) bands indicate the one- and two-standard-deviation uncertainty intervals, respectively, for the expected results. The theoretical cross section and the expected curves for the individual search channels are also shown.

channel provides the most stringent 95% C.L. cross section upper limit in the plane of the $\tilde{\chi}_1^0$ branching fraction versus the $\tilde{\chi}_1^0$ mass is presented in Fig. 21.

B. The hW topology

In Ref. [36], we present limits on the chargino-neutralino pair-production scenario of Fig. 1 (right), i.e., on a generic new-physics SUSY-like process with a Higgs boson, a W boson, and E_T^{miss}. The event signatures considered are those that yield a single electron or muon and a $b\bar{b}$ pair, a same-sign ee, $\mu\mu$, or $e\mu$ pair and no third charged lepton, and three or more charged leptons [35]. These results target the $h(\to b\bar{b})W(\to \ell\nu)$ and $h(\to ZZ, WW, \tau\tau)W(\to \ell\nu)$ channels, with ℓ an electron, muon, or leptonically decaying τ lepton. With the present work, we add the search channels with $h \to \gamma\gamma$ and either $W \to 2$ jets or $W \to \ell\nu$, corresponding to the studies of Secs. VI B and VI C.

The 95% C.L. upper bounds on the chargino-neutralino cross section based on the combination of results from Ref. [36] with the two $\gamma\gamma$ search channels considered here are shown in Fig. 22. The top plot shows the cross section limits in the LSP versus $\tilde{\chi}_2^0 = \tilde{\chi}_1^\pm$ mass plane. The bottom plot shows the limits as a function of the $\tilde{\chi}_2^0 = \tilde{\chi}_1^\pm$ mass assuming an LSP mass of $m_{\tilde{\chi}_1^0} = 1$ GeV. The single most sensitive channel is the single-lepton search from Ref. [36].

For small values of the LSP mass, we exclude chargino-neutralino pair production for $\tilde{\chi}_2^0 = \tilde{\chi}_1^\pm$ mass values up to 210 GeV, based on the theoretical prediction for the cross section minus one standard deviation of its uncertainty. This represents a modest improvement of about 5%
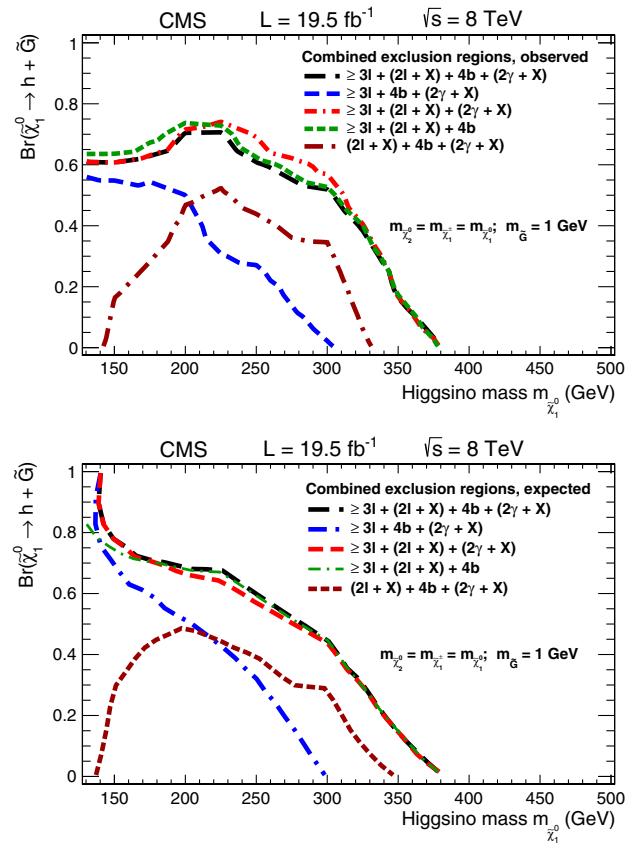
FIG. 20 (color online). (Top) Observed and (bottom) expected 95% confidence level exclusion regions for higgsino pair production in the plane of the higgsino branching fraction to a Higgs boson and the LSP, versus the higgsino mass, with each principal search channel group removed in turn from the combination. The excluded regions correspond to the area below the contours.

FIG. 21 (color online). The search channel that provides the most stringent 95% confidence level upper limit on $\tilde{\chi}_1^0$ higgsino pair production in the plane of the higgsino branching fraction to a Higgs boson and the LSP, versus the higgsino mass.
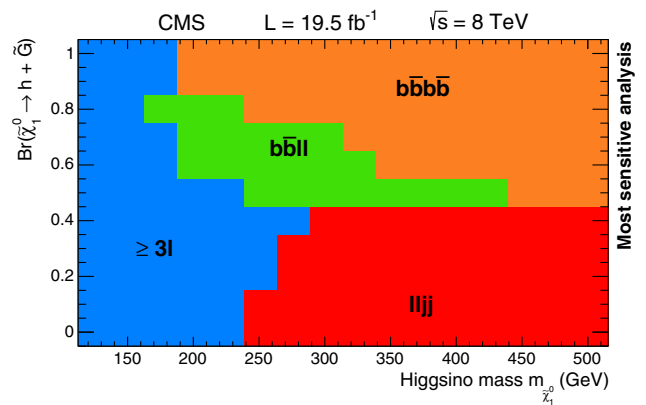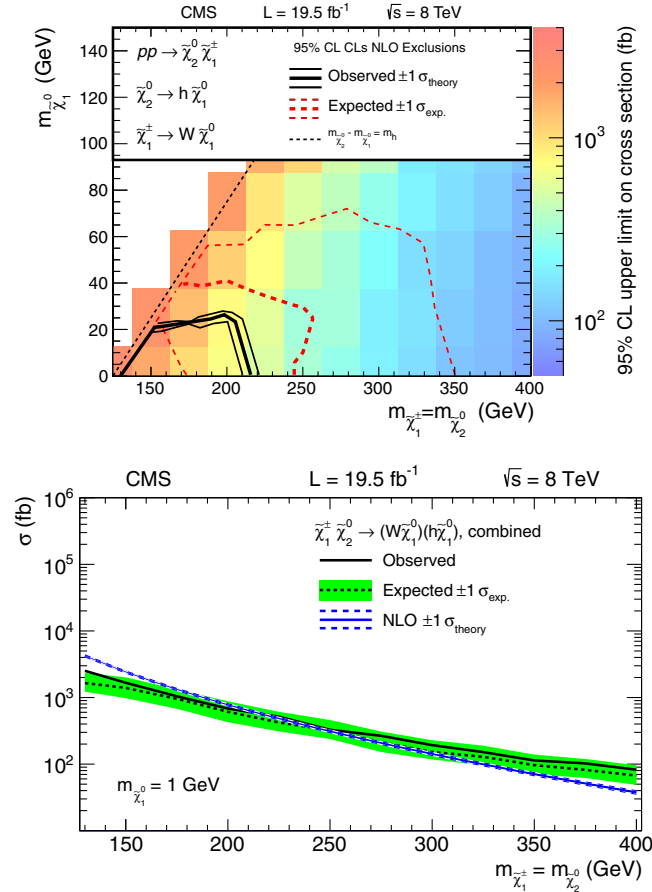
FIG. 22 (color online).   (Top) Observed and expected 95% confidence level upper limits on the cross section for electroweak chargino-neutralino $\tilde{\chi}_1^{\pm}\tilde{\chi}_2^0$ pair production (with $m_{\tilde{\chi}_1^{\pm}} = m_{\tilde{\chi}_2^0}$) as a function of the LSP and $\tilde{\chi}_2^0$ masses for the combined results on single-lepton, same-sign dilepton, and multilepton data from Ref. [36] with the diphoton data presented here. (Bottom) Corresponding results as a function of the $\tilde{\chi}_2^0$ mass for an LSP mass of 1 GeV. The dark (green) band indicates the one-standard-deviation interval. The theoretical cross section is also shown.

compared to the corresponding result in Ref. [36]. The individual diphoton cross section results assuming $m_{\tilde{\chi}_1^0} = 1$ GeV are presented in Fig. 23.

XI. SUMMARY

Searches are presented for the electroweak pair production of higgsinos ($\tilde{\chi}_1^0$) in proton-proton collisions at 8 TeV, based on the gauge-mediated-SUSY-breaking scenario of Ref. [28]. Each higgsino is presumed to decay to a Higgs boson (h) and the lightest supersymmetric particle (LSP), which escapes without detection, or else to a Z boson and an LSP, where the LSP is an almost massless gravitino $\tilde{G}$. We search for an excess, relative to the expectation from standard model processes, of events with an hh, hZ, or ZZ boson pair produced in association with a large value of either missing transverse energy E_T^{miss}, transverse mass M_T,
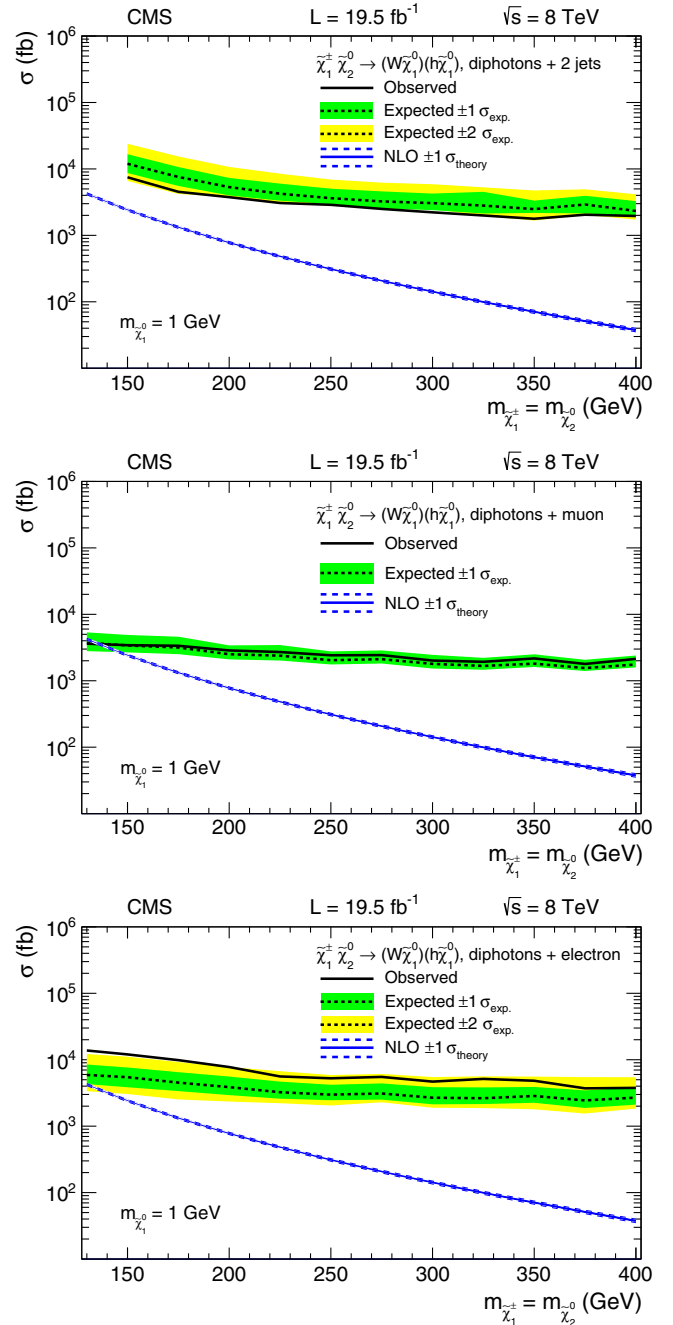
FIG. 23 (color online).   Observed and expected 95% confidence level upper limits on the cross section for chargino-neutralino $\tilde{\chi}_1^{\pm}\tilde{\chi}_2^0$ pair production (with $m_{\tilde{\chi}_1^{\pm}} = m_{\tilde{\chi}_2^0}$) as a function of the $\tilde{\chi}_2^0$ mass assuming an LSP mass of 1 GeV, for (top) the $\gamma\gamma + 2$ jets study of Sec. VI B, and (middle and bottom), the $\gamma\gamma$ + leptons studies (for the muon and electron samples, respectively) of Sec. VI C. The dark (green) and light (yellow) bands indicate the one- and two-standard-deviation uncertainty intervals, respectively. The theoretical cross section is also shown.

or the scalar sum S_T^h of the two boson transverse momenta, depending on the search channel. In addition, we perform searches for electroweak chargino-neutralino ($\tilde{\chi}_1^{\pm}\tilde{\chi}_2^0$) pair production in channels with an hW boson pair and E_T^{miss}. In

the latter case, the LSP is a massive neutralino, also denoted $\tilde{\chi}_1^0$. The assumed decay modes are $\tilde{\chi}_1^\pm \to W \tilde{\chi}_1^0$ and $\tilde{\chi}_2^0 \to h \tilde{\chi}_1^0$. The data sample, collected with the CMS detector at the LHC in 2012, corresponds to an integrated luminosity of about 19.5 fb^{-1}.

We select events with four bottom-quark jets (b jets), events with two b jets and two photons, and events with two b jets and an $\ell^+\ell^-$ pair (with ℓ an electron or muon), providing sensitivity to the $h(\to b\bar{b})h(\to b\bar{b})$, $h(\to \gamma\gamma)h(\to b\bar{b})$, and $h(\to b\bar{b})Z(\to \ell^+\ell^-)$ channels, respectively. We also select events with two photons accompanied by two light-quark jets, and events with two photons accompanied by at least one electron or muon, providing sensitivity to the $h(\to \gamma\gamma)Z/W(\to 2\,\text{jets})$ channels, and to the $h(\to \gamma\gamma)h(\to ZZ/WW/\tau\tau)$ and $h(\to \gamma\gamma)Z/W$ channels where the Z and W bosons decay leptonically. As an aid for studies of signal scenarios other than those considered in this paper Tables VIII–XII of the Appendix provide results for the signal yields at different stages of the event selection process for the studies presented herein. We incorporate results from Refs. [35] and [36] to gain sensitivity to higgsino pair production in the ZZ channel and to access complementary $\tilde{\chi}_1^\pm \tilde{\chi}_2^0$ decay modes.

The results are combined in a likelihood fit to derive 95% confidence level upper limits on the higgsino pair production cross section in the two-dimensional plane of the higgsino branching fraction to the $h\tilde{G}$ state versus the higgsino mass $m_{\tilde{\chi}_1^0}$, where $\tilde{\chi}_1^0 \to h\tilde{G}$ and $\tilde{\chi}_1^0 \to Z\tilde{G}$ are taken as the only possible higgsino decay modes. With the $\tilde{\chi}_1^0 \to Z\tilde{G}$ branching fraction set to unity, higgsinos with a mass value below 380 GeV are excluded. With the $\tilde{\chi}_1^0 \to h\tilde{G}$ branching fraction set to unity, higgsinos are not excluded for any mass value, but we obtain an expected exclusion region that lies just above the theoretical higgsino pair production cross section for higgsino mass values $m_{\tilde{\chi}_1^0} \lesssim 360$ GeV.

We also determine 95% confidence level upper limits on the cross section for electroweak chargino-neutralino $\tilde{\chi}_1^\pm \tilde{\chi}_2^0$ pair production, adding the search channels with $h \to \gamma\gamma$ and either $W \to 2$ jets or $W \to \ell\nu$ to the results presented in Ref. [36]. For small values of the LSP mass, we exclude this process for chargino mass values up to 210 GeV, where the $\tilde{\chi}_1^\pm$ and $\tilde{\chi}_2^0$ masses are taken to be equal.

ACKNOWLEDGMENTS

APPENDIX: EVENT SELECTION FLOW TABLES

In this Appendix, we present tables that illustrate the event selection process, or "flow," for the analyses presented in Secs. V–VII. For each analysis, the selection flow is illustrated for two or more signal points. These tables are intended as an aid for those wishing to replicate these analyses using signal scenarios other than those considered in the present work.

TABLE VIII. Number of signal events remaining after each stage of the event selection for the $hh \to b\bar{b}b\bar{b}$ search, with a higgsino mass of 250 GeV and an LSP (gravitino) mass of 1 GeV. The results are normalized to an integrated luminosity of 19.3 fb^{-1} using NLO + NLL calculations. The uncertainties are statistical. "$\mathcal{S}_{\mathrm{MET}}$ bin 0" corresponds to $0 < \mathcal{S}_{\mathrm{MET}} < 30$. The baseline selection accounts for the primary vertex criteria and for quality requirements applied to the $E_{\mathrm{T}}^{\mathrm{miss}}$ distribution. This search is described in Sec. V.

hh events, $m_{\tilde{\chi}_1^0} = 250$ GeV	$\mathcal{S}_{\mathrm{MET}}$ bin 0	$\mathcal{S}_{\mathrm{MET}}$ bin 1	$\mathcal{S}_{\mathrm{MET}}$ bin 2	$\mathcal{S}_{\mathrm{MET}}$ bin 3	$\mathcal{S}_{\mathrm{MET}}$ bin 4
All events	590 ± 2	264 ± 2	376 ± 2	107 ± 1	22.7 ± 0.5
Baseline selection	548 ± 2	257 ± 2	369 ± 2	106 ± 1	22.1 ± 0.5
$p_{\mathrm{T}} > 50$ GeV, leading 2 jets	470 ± 2	220 ± 1	321 ± 2	95 ± 1	20.7 ± 0.5
Number of jets = 4 or 5	288 ± 2	132 ± 1	196 ± 1	58.3 ± 0.8	12.2 ± 0.4
Lepton vetoes	280 ± 2	128 ± 1	190 ± 1	56.7 ± 0.8	11.7 ± 0.4
Isolated track veto	253 ± 2	116 ± 1	173 ± 1	51.9 ± 0.7	10.8 ± 0.3
$\Delta\phi_{\mathrm{min}}$ requirement	111 ± 1	64.3 ± 0.8	133 ± 1	42.6 ± 0.7	9.1 ± 0.3
$3b$ selection	15.3 ± 0.4	8.6 ± 0.3	19.0 ± 0.4	6.3 ± 0.3	1.3 ± 0.1
$\Delta R_{\mathrm{max}} < 2.2$	6.6 ± 0.3	3.4 ± 0.2	7.6 ± 0.3	2.5 ± 0.2	0.53 ± 0.08
Higgs boson SIG region	2.7 ± 0.2	1.3 ± 0.1	2.7 ± 0.2	0.87 ± 0.10	0.14 ± 0.04
Trigger emulation	0.41 ± 0.06	0.83 ± 0.08	2.3 ± 0.1	0.82 ± 0.09	0.13 ± 0.04
$4b$ selection	20.3 ± 0.5	12.3 ± 0.4	26.3 ± 0.5	8.4 ± 0.3	1.7 ± 0.1
$\Delta R_{\mathrm{max}} < 2.2$	9.8 ± 0.3	5.9 ± 0.2	11.6 ± 0.3	3.6 ± 0.2	0.79 ± 0.09
Higgs boson SIG region	4.7 ± 0.2	3.0 ± 0.2	5.1 ± 0.2	1.5 ± 0.1	0.30 ± 0.06
Trigger emulation	0.55 ± 0.07	1.8 ± 0.1	4.4 ± 0.2	1.4 ± 0.1	0.28 ± 0.05

TABLE IX. Number of signal events remaining after each stage of the event selection for the $hh \to b\bar{b}b\bar{b}$ search, with a higgsino mass of 400 GeV and an LSP (gravitino) mass of 1 GeV. The results are normalized to an integrated luminosity of 19.3 fb^{-1} using NLO + NLL calculations. The uncertainties are statistical. "$\mathcal{S}_{\mathrm{MET}}$ bin 0" corresponds to $0 < \mathcal{S}_{\mathrm{MET}} < 30$. The baseline selection accounts for the primary vertex criteria and for quality requirements applied to the $E_{\mathrm{T}}^{\mathrm{miss}}$ distribution. This search is described in Sec. V.

hh events, $m_{\tilde{\chi}_1^0} = 400$ GeV	$\mathcal{S}_{\mathrm{MET}}$ bin 0	$\mathcal{S}_{\mathrm{MET}}$ bin 1	$\mathcal{S}_{\mathrm{MET}}$ bin 2	$\mathcal{S}_{\mathrm{MET}}$ bin 3	$\mathcal{S}_{\mathrm{MET}}$ bin 4
All events	28.8 ± 0.3	15.9 ± 0.2	35.3 ± 0.3	31.1 ± 0.3	51.9 ± 0.4
Baseline selection	26.9 ± 0.3	15.6 ± 0.2	34.6 ± 0.3	30.5 ± 0.3	50.9 ± 0.4
$p_{\mathrm{T}} > 50$ GeV, leading 2 jets	25.3 ± 0.2	14.6 ± 0.2	32.4 ± 0.3	28.8 ± 0.3	49.3 ± 0.3
Number of jets $= 4$ or 5	15.7 ± 0.2	9.1 ± 0.1	19.8 ± 0.2	17.6 ± 0.2	30.4 ± 0.3
Lepton vetoes	15.3 ± 0.2	8.8 ± 0.1	19.3 ± 0.2	17.1 ± 0.2	29.8 ± 0.3
Isolated track veto	13.9 ± 0.2	8.0 ± 0.1	17.6 ± 0.2	15.6 ± 0.2	27.3 ± 0.3
$\Delta\phi_{\min}$ requirement	5.9 ± 0.1	4.25 ± 0.10	13.3 ± 0.2	12.9 ± 0.2	24.4 ± 0.2
$3b$ selection	0.85 ± 0.04	0.56 ± 0.04	1.90 ± 0.07	1.70 ± 0.06	3.64 ± 0.09
$\Delta R_{\max} < 2.2$	0.44 ± 0.03	0.31 ± 0.03	1.03 ± 0.05	0.91 ± 0.05	2.12 ± 0.07
Higgs boson SIG region	0.22 ± 0.02	0.13 ± 0.02	0.45 ± 0.03	0.30 ± 0.03	0.88 ± 0.05
Trigger emulation	0.029 ± 0.007	0.09 ± 0.01	0.39 ± 0.03	0.29 ± 0.03	0.83 ± 0.04
$4b$ selection	1.18 ± 0.05	0.85 ± 0.04	2.44 ± 0.08	2.57 ± 0.08	4.6 ± 0.1
$\Delta R_{\max} < 2.2$	0.77 ± 0.04	0.52 ± 0.04	1.40 ± 0.06	1.59 ± 0.06	3.02 ± 0.09
Higgs boson SIG region	0.45 ± 0.03	0.29 ± 0.03	0.77 ± 0.04	0.83 ± 0.04	1.56 ± 0.06
Trigger emulation	0.07 ± 0.01	0.20 ± 0.02	0.68 ± 0.04	0.78 ± 0.04	1.47 ± 0.06

TABLE X. Number of signal events remaining after each stage of the event selection for the $hh \to \gamma\gamma b\bar{b}$ search, described in Sec. VI A, and for the hZ and $hW \to \gamma\gamma + 2$ jets search, described in Sec. VI B. The hh and hZ scenarios assume a higgsino mass value of 130 GeV and an LSP (gravitino) mass of 1 GeV. For the hW scenario, $m_{\tilde{\chi}_1^\pm} = m_{\tilde{\chi}_2^0} = 130$ GeV and the LSP ($\tilde{\chi}_1^0$) mass is 1 GeV. The results are normalized to an integrated luminosity of 19.7 fb^{-1} using NLO + NLL calculations for the hh and hZ results and NLO calculations for the hW results. The uncertainties are statistical.

	hh events	hZ events	hW events
All events	71.5 ± 0.4	63.3 ± 0.3	118 ± 1
Trigger emulation	53.6 ± 0.4	48.3 ± 0.2	89.9 ± 0.4
Photon selection (except for η requirement)	34.0 ± 0.3	30.9 ± 0.2	57.2 ± 0.4
$120 < m_{\gamma\gamma} < 131$ GeV	31.1 ± 0.3	28.0 ± 0.2	51.9 ± 0.3
$|\eta| < 1.4442$ for photons	20.0 ± 0.2	17.9 ± 0.1	32.9 ± 0.3
Lepton vetoes	4.1 ± 0.1	16.7 ± 0.1	27.5 ± 0.2
Reject events with $95 < m_{b\bar{b}} < 155$ GeV	$\cdots$	7.7 ± 0.1	13.0 ± 0.2
$70 < m_{\mathrm{jj}} < 110$ GeV	$\cdots$	4.6 ± 0.1	7.9 ± 0.1
Exactly two b jets	4.1 ± 0.1	$\cdots$	$\cdots$
$95 < m_{b\bar{b}} < 155$ GeV	3.5 ± 0.1	$\cdots$	$\cdots$

TABLE XI.   Number of signal events remaining after each stage of the event selection for the *hh* and *hW* → $\gamma\gamma$ + leptons searches. The *hh* scenario assumes a higgsino mass value of 130 GeV and an LSP (gravitino) mass of 1 GeV. For the *hW* scenario, $m_{\tilde{\chi}_1^\pm} = m_{\tilde{\chi}_2^0} = 130$ GeV and the LSP ($\tilde{\chi}_1^0$) mass is 1 GeV. The results are normalized to an integrated luminosity of 19.5 fb^{-1} using NLO + NLL calculations for the *hh* results and NLO calculations for the *hW* results. The uncertainties are statistical. The baseline selection accounts for the primary vertex criteria and for quality requirements applied to the E_T^{miss} distribution. This search is described in Sec. VI C.

	hh events		*hW* events	
	$\gamma\gamma$ + muon	$\gamma\gamma$ + electron	$\gamma\gamma$ + muon	$\gamma\gamma$ + electron
All events	90.3 ± 0.6	90.3 ± 0.6	261 ± 1	261 ± 1
Baseline selection	90.3 ± 0.6	90.3 ± 0.6	261 ± 1	261 ± 1
Trigger emulation	70.7 ± 0.5	70.7 ± 0.5	200 ± 1	200 ± 1
Photon selection	27.4 ± 0.3	27.4 ± 0.3	77.8 ± 0.6	77.8 ± 0.6
Lepton selection	3.3 ± 0.1	3.5 ± 0.1	6.8 ± 0.2	7.2 ± 0.2
At most one *b* jet	3.3 ± 0.1	3.5 ± 0.1	6.8 ± 0.2	7.2 ± 0.2
$\Delta R(\gamma, \text{lepton}) > 0.3$	3.3 ± 0.1	3.5 ± 0.1	6.8 ± 0.2	7.1 ± 0.2
Reject events with $86 < m_{e\gamma} < 96$ GeV	3.3 ± 0.1	2.5 ± 0.1	6.8 ± 0.2	4.8 ± 0.1
$120 < m_{\gamma\gamma} < 131$ GeV	3.1 ± 0.1	2.3 ± 0.1	6.4 ± 0.2	4.5 ± 0.1

TABLE XII.   Number of signal events remaining after each stage of the event selection for the *hZ* search with $h \to b\bar{b}$ and $Z \to \ell^+\ell^-$, with higgsino mass values of 130 and 200 GeV and an LSP (gravitino) mass of 1 GeV. The results are normalized to an integrated luminosity of 19.5 fb^{-1} using NLO + NLL calculations. The uncertainties are statistical. The baseline selection accounts for the primary vertex criteria and for quality requirements applied to the E_T^{miss} distribution. This search is described in Sec. VII.

hZ events	$m_{\tilde{\chi}_1^0} = 130$ GeV			$m_{\tilde{\chi}_1^0} = 200$ GeV		
	ee	$\mu\mu$	$ee + \mu\mu$	*ee*	$\mu\mu$	$ee + \mu\mu$
Baseline selection	579 ± 2	576 ± 2	1154 ± 2	100 ± 1	102 ± 1	202 ± 1
Trigger emulation	548 ± 1	494 ± 1	1042 ± 2	95.5 ± 0.6	87.2 ± 0.5	183 ± 1
Lepton ID and isolation	262 ± 1	315 ± 1	577 ± 1	50.0 ± 0.4	60.9 ± 0.5	111 ± 1
2 leptons ($p_T > 20$ GeV)	238 ± 1	287 ± 1	525 ± 1	47.2 ± 0.4	57.3 ± 0.4	105 ± 1
$81 < m_{\ell\ell} < 101$ GeV	231 ± 1	277 ± 1	507 ± 1	45.7 ± 0.4	55.3 ± 0.4	101 ± 1
Third-lepton veto	230 ± 1	276 ± 1	505 ± 1	45.5 ± 0.4	55.1 ± 0.4	101 ± 1
Hadronic τ-lepton veto	226 ± 1	271 ± 1	496 ± 1	44.8 ± 0.4	54.3 ± 0.4	99.1 ± 0.5
≥ 2 jets	148 ± 1	176 ± 1	323 ± 1	31.0 ± 0.3	37.5 ± 0.3	68.5 ± 0.4
≥ 2 *b* jets	44.1 ± 0.4	51.1 ± 0.4	95.2 ± 0.6	9.2 ± 0.2	11.1 ± 0.2	20.3 ± 0.3
$100 < m_{b\bar{b}} < 150$ GeV	34.6 ± 0.3	40.0 ± 0.3	74.6 ± 0.5	7.2 ± 0.2	8.7 ± 0.2	15.9 ± 0.3
$M_{T2}^{j\ell} > 200$ GeV	7.6 ± 0.1	8.4 ± 0.1	16.0 ± 0.1	3.0 ± 0.1	3.3 ± 0.1	6.3 ± 0.1
$E_T^{miss} > 60$ GeV	2.6 ± 0.1	2.8 ± 0.1	5.4 ± 0.1	2.2 ± 0.1	2.5 ± 0.1	4.7 ± 0.1
$E_T^{miss} > 80$ GeV	1.5 ± 0.1	1.6 ± 0.1	3.1 ± 0.1	2.0 ± 0.1	2.2 ± 0.1	4.2 ± 0.1
$E_T^{miss} > 100$ GeV	0.8 ± 0.1	0.9 ± 0.1	1.7 ± 0.1	1.6 ± 0.1	1.7 ± 0.1	3.3 ± 0.1

[1] P. Ramond, Phys. Rev. D **3**, 2415 (1971).
[2] Y. A. Golfand and E. P. Likhtman, Pis'ma Zh. Eksp. Teor. Fiz. **13**, 452 (1971) [JETP Lett. **13**, 323 (1971)].
[3] A. Neveu and J. H. Schwarz, Nucl. Phys. **B31**, 86 (1971).
[4] D. V. Volkov and V. P. Akulov, Pis'ma Zh. Eksp. Teor. Fiz. **16**, 621 (1972) [JETP Lett. **16**, 438 (1972)].
[5] J. Wess and B. Zumino, Phys. Lett. **49B**, 52 (1974).
[6] J. Wess and B. Zumino, Nucl. Phys. **B70**, 39 (1974).
[7] P. Fayet, Nucl. Phys. **B90**, 104 (1975).
[8] H. P. Nilles, Phys. Rep. **110**, 1 (1984).
[9] H. E. Haber and G. L. Kane, Phys. Rep. **117**, 75 (1985).
[10] G. R. Farrar and P. Fayet, Phys. Lett. **76B**, 575 (1978).
[11] ATLAS Collaboration, J. High Energy Phys. 10 (2013) 130.
[12] ATLAS Collaboration, J. High Energy Phys. 10 (2013) 189.
[13] ATLAS Collaboration, J. High Energy Phys. 04 (2014) 169.
[14] ATLAS Collaboration, J. High Energy Phys. 06 (2014) 124.
[15] ATLAS Collaboration, J. High Energy Phys. 05 (2014) 071.
[16] ATLAS Collaboration, Phys. Rev. D **90**, 052001 (2014).
[17] CMS Collaboration, Phys. Lett. B **725**, 243 (2013).
[18] CMS Collaboration, Eur. Phys. J. C **73**, 2677 (2013).

[19] CMS Collaboration, Phys. Lett. B **733**, 328 (2014).
[20] CMS Collaboration, J. High Energy Phys. 01 (2014) 163.
[21] CMS Collaboration, J. High Energy Phys. 06 (2014) 055.
[22] CMS Collaboration, Phys. Lett. B **736**, 371 (2014).
[23] ATLAS Collaboration, Phys. Lett. B **716**, 1 (2012).
[24] CMS Collaboration, J. High Energy Phys. 06 (2013) 081.
[25] CMS Collaboration, Phys. Lett. B **716**, 30 (2012).
[26] G. C. Branco, P. M. Ferreira, L. Lavoura, M. N. Rebelo, M. Sher, and J. P. Silva, Phys. Rep. **516**, 1 (2012).
[27] S. P. Martin, Adv. Ser. Dir. High Energy Phys. **21**, 1 (2010).
[28] K. T. Matchev and S. D. Thomas, Phys. Rev. D **62**, 077702 (2000).
[29] M. Asano, H. D. Kim, R. Kitano, and Y. Shimizu, J. High Energy Phys. 12 (2010) 019.
[30] Y. Kats, P. Meade, M. Reece, and D. Shih, J. High Energy Phys. 02 (2012) 115.
[31] H. Baer, V. Barger, A. Lessa, W. Sreethawong, and X. Tata, Phys. Rev. D **85**, 055022 (2012).
[32] P. Byakti and D. Ghosh, Phys. Rev. D **86**, 095027 (2012).
[33] K. Howe and P. Saraswat, J. High Energy Phys. 10 (2012) 065.
[34] J. T. Ruderman and D. Shih, J. High Energy Phys. 08 (2012) 159.
[35] CMS Collaboration, Phys. Rev. D **90**, 032006 (2014).
[36] CMS Collaboration, Eur. Phys. J. C **74**, 3036 (2014).
[37] G. F. Giudice and R. Rattazzi, Phys. Rep. **322**, 419 (1999).
[38] W. Beenakker, M. Klasen, M. Krämer, T. Plehn, M. Spira, and P. M. Zerwas, Phys. Rev. Lett. **83**, 3780 (1999); **100**, 029901(E) (2008).
[39] CMS Collaboration, JINST **3**, S08004 (2008).
[40] CMS Collaboration, CMS Report No. CMS-PAS-PFT-09-001, 2009, http://cdsweb.cern.ch/record/1194487.
[41] CMS Collaboration, CMS Report No. CMS-PAS-PFT-10-001, 2010, http://cdsweb.cern.ch/record/1247373.
[42] CMS Collaboration, JINST **7**, P01001 (2012).
[43] CMS Collaboration, CMS Report No. CMS-PAS-JME-13-005, 2013, http://cds.cern.ch/record/1581583.
[44] M. Cacciari, G. P. Salam, and G. Soyez, J. High Energy Phys. 04 (2008) 063.
[45] M. Cacciari, G. P. Salam, and G. Soyez, Eur. Phys. J. C **72**, 1896 (2012).
[46] CMS Collaboration, CMS Report No. CMS-PAS-JME-10-003, 2010, http://cdsweb.cern.ch/record/1279362.
[47] M. Cacciari and G. P. Salam, Phys. Lett. B **659**, 119 (2008).
[48] CMS Collaboration, JINST **6**, P11002 (2011).
[49] CMS Collaboration, JINST **6**, P09001 (2011).
[50] CMS Collaboration, JINST **8**, P04013 (2013).
[51] CMS Collaboration, CMS Report No. CMS-PAS-BTV-13-001, 2013, http://cds.cern.ch/record/1581306.
[52] J. Alwall, R. Frederix, S. Frixione, V. Hirschi, F. Maltoni, O. Mattelaer, H.-S. Shao, T. Stelzer, P. Torielli, and M. Zaro, J. High Energy Phys. 07 (2014) 079.
[53] S. Frixione, P. Nason, and C. Oleari, J. High Energy Phys. 11 (2007) 070.
[54] S. Alioli, P. Nason, C. Oleari, and E. Re, J. High Energy Phys. 09 (2009) 111; 10 (2010) 11(E).
[55] G. Luisoni, P. Nason, C. Oleari, and F. Tramontano, J. High Energy Phys. 10 (2013) 083.
[56] T. Sjöstrand, S. Mrenna, and P. Skands, J. High Energy Phys. 05 (2006) 026.
[57] S. Frixione and B. R. Webber, J. High Energy Phys. 06 (2002) 029.
[58] S. Frixione, P. Nason, and B. R. Webber, J. High Energy Phys. 08 (2003) 007.
[59] M. Czakon, P. Fiedler, and A. Mitov, Phys. Rev. Lett. **110**, 252004 (2013).
[60] J. M. Campbell and R. K. Ellis, J. High Energy Phys. 07 (2012) 052.
[61] M. V. Garzelli, A. Kardos, C. G. Papadopoulos, and Z. Trocsanyi, J. High Energy Phys. 11 (2012) 056.
[62] J. M. Campbell, R. K. Ellis, and C. Williams, J. High Energy Phys. 07 (2011) 018.
[63] R. Gavin, Y. Li, F. Petriello, and S. Quackenbush, Comput. Phys. Commun. **184**, 209 (2013).
[64] S. Agostinelli et al. (GEANT4 Collaboration), Nucl. Instrum. Methods Phys. Res., Sect. A **506**, 250 (2003).
[65] CMS Collaboration, Phys. Rev. D **89**, 092007 (2014).
[66] CMS Collaboration, J. Phys. Conf. Ser. **331**, 032049 (2011).
[67] B. Fuks, M. Klasen, D. R. Lamprea, and M. Rothering, J. High Energy Phys. 10 (2012) 081.
[68] B. Fuks, M. Klasen, D. R. Lamprea, and M. Rothering, Eur. Phys. J. C **73**, 2480 (2013).
[69] M. Krämer, A. Kulesza, R. van der Leeuw, M. Mangano, S. Padhi, T. Plehn, and X. Portell, arXiv:1206.2892.
[70] P. Meade and M. Reece, arXiv:hep-ph/0703031.
[71] ALEPH, DELPHI, L3, OPAL, and SLD Collaborations, Phys. Rep. **427**, 257 (2006).
[72] M. Carena, G. Nardini, M. Quiros, and C. E. M. Wagner, J. High Energy Phys. 02 (2013) 001.
[73] J. Pumplin, D. R. Stump, J. Huston, H.-L. Lai, P. Nadolsky, and W.-K. Tung, J. High Energy Phys. 07 (2002) 012.
[74] P. M. Nadolsky, H.-L. Lai, Q.-H. Cao, J. Huston, J. Pumplin, D. Stump, W.-K. Tung, and C.-P. Yuan, Phys. Rev. D **78**, 013004 (2008).
[75] S. Heinemeyer et al., CERN Report No. CERN-2013-004, 2013, http://dx.doi.org/10.5170/CERN-2013-004.
[76] CMS Collaboration, CMS Report No. CMS-PAS-EGM-10-005, 2010, http://cds.cern.ch/record/1279143.
[77] CMS Collaboration, JINST **8**, P09009 (2013).
[78] CMS Collaboration, CMS Report No. CMS-DP-2013-010, 2013, http://cds.cern.ch/record/1279143.
[79] E. Gross and O. Vitells, Eur. Phys. J. C **70**, 525 (2010).
[80] C. G. Lester and D. J. Summers, Phys. Lett. B **463**, 99 (1999).
[81] A. Barr, C. G. Lester, and P. Stephens, J. Phys. G **29**, 2343 (2003).
[82] CMS Collaboration, Phys. Lett. B **716**, 260 (2012).
[83] A. D. Martin, W. J. Stirling, R. S. Thorne, and G. Watt, Eur. Phys. J. C **63**, 189 (2009).
[84] R. D. Ball, V. Bertone, F. Cerutti, L. Del Debbio, S. Forte, A. Guffanti, J. I. Latorre, J. Rojo, and M. Ubiali, Nucl. Phys. **B849**, 296 (2011).
[85] S. Alekhin et al., arXiv:1101.0536.

[86] M. Botje, J. Butterworth, A. Cooper-Sarkar, A. de Roeck, J. Feltesse, S. Forte, A. Glazov, J. Huston, R. McNulty, and T. Sjöstrand, arXiv:1101.0538.

[87] CMS Collaboration, CMS Report No. CMS-PAS-LUM-13-001, 2013, http://cds.cern.ch/record/1598864.

[88] ATLAS and CMS Collaborations, CMS Report No. CMS-NOTE-2011-005, http://cdsweb.cern.ch/record/1379837, ATLAS Report No. ATL-PHYS-PUB-2011-11, 2011.

[89] A. L. Read, J. Phys. G **28**, 2693 (2002).

[90] T. Junk, Nucl. Instrum. Methods Phys. Res., Sect. A **434**, 435 (1999).

V. Khachatryan,[1] A. M. Sirunyan,[1] A. Tumasyan,[1] W. Adam,[2] T. Bergauer,[2] M. Dragicevic,[2] J. Erö,[2] C. Fabjan,[2,b]
M. Friedl,[2] R. Frühwirth,[2,b] V. M. Ghete,[2] C. Hartl,[2] N. Hörmann,[2] J. Hrubec,[2] M. Jeitler,[2,b] W. Kiesenhofer,[2] V. Knünz,[2]
M. Krammer,[2,b] I. Krätschmer,[2] D. Liko,[2] I. Mikulec,[2] D. Rabady,[2,c] B. Rahbaran,[2] H. Rohringer,[2] R. Schöfbeck,[2]
J. Strauss,[2] A. Taurok,[2] W. Treberer-Treberspurg,[2] W. Waltenberger,[2] C.-E. Wulz,[2,b] V. Mossolov,[3] N. Shumeiko,[3]
J. Suarez Gonzalez,[3] S. Alderweireldt,[4] M. Bansal,[4] S. Bansal,[4] T. Cornelis,[4] E. A. De Wolf,[4] X. Janssen,[4] A. Knutsson,[4]
S. Luyckx,[4] S. Ochesanu,[4] R. Rougny,[4] M. Van De Klundert,[4] H. Van Haevermaet,[4] P. Van Mechelen,[4] N. Van Remortel,[4]
A. Van Spilbeeck,[4] F. Blekman,[5] S. Blyweert,[5] J. D'Hondt,[5] N. Daci,[5] N. Heracleous,[5] J. Keaveney,[5] S. Lowette,[5] M. Maes,[5]
A. Olbrechts,[5] Q. Python,[5] D. Strom,[5] S. Tavernier,[5] W. Van Doninck,[5] P. Van Mulders,[5] G. P. Van Onsem,[5] I. Villella,[5]
C. Caillol,[6] B. Clerbaux,[6] G. De Lentdecker,[6] D. Dobur,[6] L. Favart,[6] A. P. R. Gay,[6] A. Grebenyuk,[6] A. Léonard,[6]
A. Mohammadi,[6] L. Perniè,[6,c] T. Reis,[6] T. Seva,[6] L. Thomas,[6] C. Vander Velde,[6] P. Vanlaer,[6] J. Wang,[6] F. Zenoni,[6] V. Adler,[7]
K. Beernaert,[7] L. Benucci,[7] A. Cimmino,[7] S. Costantini,[7] S. Crucy,[7] S. Dildick,[7] A. Fagot,[7] G. Garcia,[7] J. Mccartin,[7]
A. A. Ocampo Rios,[7] D. Ryckbosch,[7] S. Salva Diblen,[7] M. Sigamani,[7] N. Strobbe,[7] F. Thyssen,[7] M. Tytgat,[7] E. Yazgan,[7]
N. Zaganidis,[7] S. Basegmez,[8] C. Beluffi,[8,d] G. Bruno,[8] R. Castello,[8] A. Caudron,[8] L. Ceard,[8] G. G. Da Silveira,[8] C. Delaere,[8]
T. du Pree,[8] D. Favart,[8] L. Forthomme,[8] A. Giammanco,[8,e] J. Hollar,[8] A. Jafari,[8] P. Jez,[8] M. Komm,[8] V. Lemaitre,[8]
C. Nuttens,[8] D. Pagano,[8] L. Perrini,[8] A. Pin,[8] K. Piotrzkowski,[8] A. Popov,[8,f] L. Quertenmont,[8] M. Selvaggi,[8]
M. Vidal Marono,[8] J. M. Vizan Garcia,[8] N. Beliy,[9] T. Caebergs,[9] E. Daubie,[9] G. H. Hammad,[9] W. L. Aldá Júnior,[10]
G. A. Alves,[10] L. Brito,[10] M. Correa Martins Junior,[10] T. Dos Reis Martins,[10] C. Mora Herrera,[10] M. E. Pol,[10] W. Carvalho,[11]
J. Chinellato,[11,g] A. Custódio,[11] E. M. Da Costa,[11] D. De Jesus Damiao,[11] C. De Oliveira Martins,[11] S. Fonseca De Souza,[11]
H. Malbouisson,[11] D. Matos Figueiredo,[11] L. Mundim,[11] H. Nogima,[11] W. L. Prado Da Silva,[11] J. Santaolalla,[11]
A. Santoro,[11] A. Sznajder,[11] E. J. Tonelli Manganote,[11,g] A. Vilela Pereira,[11] C. A. Bernardes,[12b] S. Dogra,[12a]
T. R. Fernandez Perez Tomei,[12a] E. M. Gregores,[12b] P. G. Mercadante,[12b] S. F. Novaes,[12a] Sandra S. Padula,[12a]
A. Aleksandrov,[13] V. Genchev,[13,c] P. Iaydjiev,[13] A. Marinov,[13] S. Piperov,[13] M. Rodozov,[13] S. Stoykova,[13] G. Sultanov,[13]
V. Tcholakov,[13] M. Vutova,[13] A. Dimitrov,[14] I. Glushkov,[14] R. Hadjiiska,[14] V. Kozhuharov,[14] L. Litov,[14] B. Pavlov,[14]
P. Petkov,[14] J. G. Bian,[15] G. M. Chen,[15] H. S. Chen,[15] M. Chen,[15] R. Du,[15] C. H. Jiang,[15] R. Plestina,[15,h] J. Tao,[15] Z. Wang,[15]
C. Asawatangtrakuldee,[16] Y. Ban,[16] Q. Li,[16] S. Liu,[16] Y. Mao,[16] S. J. Qian,[16] D. Wang,[16] W. Zou,[16] C. Avila,[17]
L. F. Chaparro Sierra,[17] C. Florez,[17] J. P. Gomez,[17] B. Gomez Moreno,[17] J. C. Sanabria,[17] N. Godinovic,[18] D. Lelas,[18]
D. Polic,[18] I. Puljak,[18] Z. Antunovic,[19] M. Kovac,[19] V. Brigljevic,[20] K. Kadija,[20] J. Luetic,[20] D. Mekterovic,[20] L. Sudic,[20]
A. Attikis,[21] G. Mavromanolakis,[21] J. Mousa,[21] C. Nicolaou,[21] F. Ptochos,[21] P. A. Razis,[21] M. Bodlak,[22] M. Finger,[22]
M. Finger Jr.,[22,i] Y. Assran,[23,j] A. Ellithi Kamel,[23,k] M. A. Mahmoud,[23,l] A. Radi,[23,m,n] M. Kadastik,[24] M. Murumaa,[24]
M. Raidal,[24] A. Tiko,[24] P. Eerola,[25] G. Fedi,[25] M. Voutilainen,[25] J. Härkönen,[26] V. Karimäki,[26] R. Kinnunen,[26]
M. J. Kortelainen,[26] T. Lampén,[26] K. Lassila-Perini,[26] S. Lehti,[26] T. Lindén,[26] P. Luukka,[26] T. Mäenpää,[26] T. Peltola,[26]
E. Tuominen,[26] J. Tuominiemi,[26] E. Tuovinen,[26] L. Wendland,[26] J. Talvitie,[27] T. Tuuva,[27] M. Besancon,[28] F. Couderc,[28]
M. Dejardin,[28] D. Denegri,[28] B. Fabbro,[28] J. L. Faure,[28] C. Favaro,[28] F. Ferri,[28] S. Ganjour,[28] A. Givernaud,[28] P. Gras,[28]
G. Hamel de Monchenault,[28] P. Jarry,[28] E. Locci,[28] J. Malcles,[28] J. Rander,[28] A. Rosowsky,[28] M. Titov,[28] S. Baffioni,[29]
F. Beaudette,[29] P. Busson,[29] C. Charlot,[29] T. Dahms,[29] M. Dalchenko,[29] L. Dobrzynski,[29] N. Filipovic,[29] A. Florent,[29]
R. Granier de Cassagnac,[29] L. Mastrolorenzo,[29] P. Miné,[29] C. Mironov,[29] I. N. Naranjo,[29] M. Nguyen,[29] C. Ochando,[29]
P. Paganini,[29] S. Regnard,[29] R. Salerno,[29] J. B. Sauvan,[29] Y. Sirois,[29] C. Veelken,[29] Y. Yilmaz,[29] A. Zabi,[29] J.-L. Agram,[30,o]
J. Andrea,[30] A. Aubin,[30] D. Bloch,[30] J.-M. Brom,[30] E. C. Chabert,[30] C. Collard,[30] E. Conte,[30,o] J.-C. Fontaine,[30,o] D. Gelé,[30]
U. Goerlach,[30] C. Goetzmann,[30] A.-C. Le Bihan,[30] P. Van Hove,[30] S. Gadrat,[31] S. Beauceron,[32] N. Beaupere,[32]
G. Boudoul,[32,c] E. Bouvier,[32] S. Brochet,[32] C. A. Carrillo Montoya,[32] J. Chasserat,[32] R. Chierici,[32] D. Contardo,[32,c]
P. Depasse,[32] H. El Mamouni,[32] J. Fan,[32] J. Fay,[32] S. Gascon,[32] M. Gouzevitch,[32] B. Ille,[32] T. Kurca,[32] M. Lethuillier,[32]

L. Mirabito,[32] S. Perries,[32] J. D. Ruiz Alvarez,[32] D. Sabes,[32] L. Sgandurra,[32] V. Sordini,[32] M. Vander Donckt,[32] P. Verdier,[32] S. Viret,[32] H. Xiao,[32] Z. Tsamalaidze,[33,i] C. Autermann,[34] S. Beranek,[34] M. Bontenackels,[34] M. Edelhoff,[34] L. Feld,[34] O. Hindrichs,[34] K. Klein,[34] A. Ostapchuk,[34] A. Perieanu,[34] F. Raupach,[34] J. Sammet,[34] S. Schael,[34] H. Weber,[34] B. Wittmer,[34] V. Zhukov,[34,f] M. Ata,[35] M. Brodski,[35] E. Dietz-Laursonn,[35] D. Duchardt,[35] M. Erdmann,[35] R. Fischer,[35] A. Güth,[35] T. Hebbeker,[35] C. Heidemann,[35] K. Hoepfner,[35] D. Klingebiel,[35] S. Knutzen,[35] P. Kreuzer,[35] M. Merschmeyer,[35] A. Meyer,[35] P. Millet,[35] M. Olschewski,[35] K. Padeken,[35] P. Papacz,[35] H. Reithler,[35] S. A. Schmitz,[35] L. Sonnenschein,[35] D. Teyssier,[35] S. Thüer,[35] M. Weber,[35] V. Cherepanov,[36] Y. Erdogan,[36] G. Flügge,[36] H. Geenen,[36] M. Geisler,[36] W. Haj Ahmad,[36] A. Heister,[36] F. Hoehle,[36] B. Kargoll,[36] T. Kress,[36] Y. Kuessel,[36] A. Künsken,[36] J. Lingemann,[36,c] A. Nowack,[36] I. M. Nugent,[36] L. Perchalla,[36] O. Pooth,[36] A. Stahl,[36] I. Asin,[37] N. Bartosik,[37] J. Behr,[37] W. Behrenhoff,[37] U. Behrens,[37] A. J. Bell,[37] M. Bergholz,[37,p] A. Bethani,[37] K. Borras,[37] A. Burgmeier,[37] A. Cakir,[37] L. Calligaris,[37] A. Campbell,[37] S. Choudhury,[37] F. Costanza,[37] C. Diez Pardos,[37] S. Dooling,[37] T. Dorland,[37] G. Eckerlin,[37] D. Eckstein,[37] T. Eichhorn,[37] G. Flucke,[37] J. Garay Garcia,[37] A. Geiser,[37] P. Gunnellini,[37] J. Hauk,[37] M. Hempel,[37,p] D. Horton,[37] H. Jung,[37] A. Kalogeropoulos,[37] M. Kasemann,[37] P. Katsas,[37] J. Kieseler,[37] C. Kleinwort,[37] D. Krücker,[37] W. Lange,[37] J. Leonard,[37] K. Lipka,[37] A. Lobanov,[37] W. Lohmann,[37,p] B. Lutz,[37] R. Mankel,[37] I. Marfin,[37,p] I.-A. Melzer-Pellmann,[37] A. B. Meyer,[37] G. Mittag,[37] J. Mnich,[37] A. Mussgiller,[37] S. Naumann-Emme,[37] A. Nayak,[37] O. Novgorodova,[37] E. Ntomari,[37] H. Perrey,[37] D. Pitzl,[37] R. Placakyte,[37] A. Raspereza,[37] P. M. Ribeiro Cipriano,[37] B. Roland,[37] E. Ron,[37] M. Ö. Sahin,[37] J. Salfeld-Nebgen,[37] P. Saxena,[37] R. Schmidt,[37,p] T. Schoerner-Sadenius,[37] M. Schröder,[37] C. Seitz,[37] S. Spannagel,[37] A. D. R. Vargas Trevino,[37] R. Walsh,[37] C. Wissing,[37] M. Aldaya Martin,[38] V. Blobel,[38] M. Centis Vignali,[38] A. R. Draeger,[38] J. Erfle,[38] E. Garutti,[38] K. Goebel,[38] M. Görner,[38] J. Haller,[38] M. Hoffmann,[38] R. S. Höing,[38] H. Kirschenmann,[38] R. Klanner,[38] R. Kogler,[38] J. Lange,[38] T. Lapsien,[38] T. Lenz,[38] I. Marchesini,[38] J. Ott,[38] T. Peiffer,[38] N. Pietsch,[38] J. Poehlsen,[38] T. Poehlsen,[38] D. Rathjens,[38] C. Sander,[38] H. Schettler,[38] P. Schleper,[38] E. Schlieckau,[38] A. Schmidt,[38] M. Seidel,[38] V. Sola,[38] H. Stadie,[38] G. Steinbrück,[38] D. Troendle,[38] E. Usai,[38] L. Vanelderen,[38] A. Vanhoefer,[38] C. Barth,[39] C. Baus,[39] J. Berger,[39] C. Böser,[39] E. Butz,[39] T. Chwalek,[39] W. De Boer,[39] A. Descroix,[39] A. Dierlamm,[39] M. Feindt,[39] F. Frensch,[39] M. Giffels,[39] F. Hartmann,[39,c] T. Hauth,[39,c] U. Husemann,[39] I. Katkov,[39,f] A. Kornmayer,[39,c] E. Kuznetsova,[39] P. Lobelle Pardo,[39] M. U. Mozer,[39] Th. Müller,[39] A. Nürnberg,[39] G. Quast,[39] K. Rabbertz,[39] F. Ratnikov,[39] S. Röcker,[39] H. J. Simonis,[39] F. M. Stober,[39] R. Ulrich,[39] J. Wagner-Kuhr,[39] S. Wayand,[39] T. Weiler,[39] R. Wolf,[39] G. Anagnostou,[40] G. Daskalakis,[40] T. Geralis,[40] V. A. Giakoumopoulou,[40] A. Kyriakis,[40] D. Loukas,[40] A. Markou,[40] C. Markou,[40] A. Psallidas,[40] I. Topsis-Giotis,[40] S. Kesisoglou,[41] A. Panagiotou,[41] N. Saoulidou,[41] E. Stiliaris,[41] X. Aslanoglou,[42] I. Evangelou,[42] G. Flouris,[42] C. Foudas,[42] P. Kokkas,[42] N. Manthos,[42] I. Papadopoulos,[42] E. Paradas,[42] G. Bencze,[43] C. Hajdu,[43] P. Hidas,[43] D. Horvath,[43,q] F. Sikler,[43] V. Veszpremi,[43] G. Vesztergombi,[43,r] A. J. Zsigmond,[43] N. Beni,[44] S. Czellar,[44] J. Karancsi,[44,s] J. Molnar,[44] J. Palinkas,[44] Z. Szillasi,[44] P. Raics,[45] Z. L. Trocsanyi,[45] B. Ujvari,[45] S. K. Swain,[46] S. B. Beri,[47] V. Bhatnagar,[47] R. Gupta,[47] U. Bhawandeep,[47] A. K. Kalsi,[47] M. Kaur,[47] R. Kumar,[47] M. Mittal,[47] N. Nishu,[47] J. B. Singh,[47] Ashok Kumar,[48] Arun Kumar,[48] S. Ahuja,[48] A. Bhardwaj,[48] B. C. Choudhary,[48] A. Kumar,[48] S. Malhotra,[48] M. Naimuddin,[48] K. Ranjan,[48] V. Sharma,[48] S. Banerjee,[49] S. Bhattacharya,[49] K. Chatterjee,[49] S. Dutta,[49] B. Gomber,[49] Sa. Jain,[49] Sh. Jain,[49] R. Khurana,[49] A. Modak,[49] S. Mukherjee,[49] D. Roy,[49] S. Sarkar,[49] M. Sharan,[49] A. Abdulsalam,[50] D. Dutta,[50] S. Kailas,[50] V. Kumar,[50] A. K. Mohanty,[50,c] L. M. Pant,[50] P. Shukla,[50] A. Topkar,[50] T. Aziz,[51] S. Banerjee,[51] S. Bhowmik,[51,t] R. M. Chatterjee,[51] R. K. Dewanjee,[51] S. Dugad,[51] S. Ganguly,[51] S. Ghosh,[51] M. Guchait,[51] A. Gurtu,[51,u] G. Kole,[51] S. Kumar,[51] M. Maity,[51,t] G. Majumder,[51] K. Mazumdar,[51] G. B. Mohanty,[51] B. Parida,[51] K. Sudhakar,[51] N. Wickramage,[51,v] H. Bakhshiansohi,[52] H. Behnamian,[52] S. M. Etesami,[52,w] A. Fahim,[52,x] R. Goldouzian,[52] M. Khakzad,[52] M. Mohammadi Najafabadi,[52] M. Naseri,[52] S. Paktinat Mehdiabadi,[52] F. Rezaei Hosseinabadi,[52] B. Safarzadeh,[52,y] M. Zeinali,[52] M. Felcini,[53] M. Grunewald,[53] M. Abbrescia,[54a,54b] L. Barbone,[54a,54b] C. Calabria,[54a,54b] S. S. Chhibra,[54a,54b] A. Colaleo,[54a] D. Creanza,[54a,54c] N. De Filippis,[54a,54c] M. De Palma,[54a,54b] L. Fiore,[54a] G. Iaselli,[54a,54c] G. Maggi,[54a,54c] M. Maggi,[54a] S. My,[54a,54c] S. Nuzzo,[54a,54b] A. Pompili,[54a,54b] G. Pugliese,[54a,54c] R. Radogna,[54a,54b,c] G. Selvaggi,[54a,54b] L. Silvestris,[54a,c] G. Singh,[54a,54b] R. Venditti,[54a,54b] G. Zito,[54a] G. Abbiendi,[55a] A. C. Benvenuti,[55a] D. Bonacorsi,[55a,55b] S. Braibant-Giacomelli,[55a,55b] L. Brigliadori,[55a,55b] R. Campanini,[55a,55b] P. Capiluppi,[55a,55b] A. Castro,[55a,55b] F. R. Cavallo,[55a] G. Codispoti,[55a,55b] M. Cuffiani,[55a,55b] G. M. Dallavalle,[55a] F. Fabbri,[55a] A. Fanfani,[55a,55b] D. Fasanella,[55a,55b] P. Giacomelli,[55a] C. Grandi,[55a] L. Guiducci,[55a,55b] S. Marcellini,[55a] G. Masetti,[55a] A. Montanari,[55a] F. L. Navarria,[55a,55b] A. Perrotta,[55a] F. Primavera,[55a,55b] A. M. Rossi,[55a,55b] T. Rovelli,[55a,55b] G. P. Siroli,[55a,55b] N. Tosi,[55a,55b] R. Travaglini,[55a,55b] S. Albergo,[56a,56b] G. Cappello,[56a] M. Chiorboli,[56a,56b] S. Costa,[56a,56b] F. Giordano,[56a,56c,c] R. Potenza,[56a,56b] A. Tricomi,[56a,56b]

C. Tuve,[56a,56b] G. Barbagli,[57a] V. Ciulli,[57a,57b] C. Civinini,[57a] R. D'Alessandro,[57a,57b] E. Focardi,[57a,57b] E. Gallo,[57a] S. Gonzi,[57a,57b] V. Gori,[57a,57b,c] P. Lenzi,[57a,57b] M. Meschini,[57a] S. Paoletti,[57a] G. Sguazzoni,[57a] A. Tropiano,[57a,57b] L. Benussi,[58] S. Bianco,[58] F. Fabbri,[58] D. Piccolo,[58] R. Ferretti,[59a,59b] F. Ferro,[59a] M. Lo Vetere,[59a,59b] E. Robutti,[59a] S. Tosi,[59a,59b] M. E. Dinardo,[60a,60b] S. Fiorendi,[60a,60b,c] S. Gennai,[60a,c] R. Gerosa,[60a,c] A. Ghezzi,[60a,60b] P. Govoni,[60a,60b] M. T. Lucchini,[60a,60b,c] S. Malvezzi,[60a] R. A. Manzoni,[60a,60b] A. Martelli,[60a,60b] B. Marzocchi,[60a] D. Menasce,[60a] L. Moroni,[60a] M. Paganoni,[60a,60b] D. Pedrini,[60a] S. Ragazzi,[60a,60b] N. Redaelli,[60a] T. Tabarelli de Fatis,[60a,60b] S. Buontempo,[61a] N. Cavallo,[61a,61c] S. Di Guida,[61a,61d,c] F. Fabozzi,[61a,61c] A. O. M. Iorio,[61a,61b] L. Lista,[61a] S. Meola,[61a,61d,c] M. Merola,[61a] P. Paolucci,[61a,c] P. Azzi,[62a] N. Bacchetta,[62a] D. Bisello,[62a,62b] A. Branca,[62a,62b] R. Carlin,[62a,62b] P. Checchia,[62a] M. Dall'Osso,[62a,62b] T. Dorigo,[62a] M. Galanti,[62a,62b] F. Gasparini,[62a,62b] U. Gasparini,[62a,62b] P. Giubilato,[62a,62b] F. Gonella,[62a] A. Gozzelino,[62a] K. Kanishchev,[62a,62c] S. Lacaprara,[62a] M. Margoni,[62a,62b] A. T. Meneguzzo,[62a,62b] J. Pazzini,[62a,62b] N. Pozzobon,[62a,62b] P. Ronchese,[62a,62b] F. Simonetto,[62a,62b] E. Torassa,[62a] M. Tosi,[62a,62b] P. Zotto,[62a,62b] A. Zucchetta,[62a,62b] G. Zumerle,[62a,62b] M. Gabusi,[63a,63b] S. P. Ratti,[63a,63b] V. Re,[63a] C. Riccardi,[63a,63b] P. Salvini,[63a] P. Vitulo,[63a,63b] M. Biasini,[64a,64b] G. M. Bilei,[64a] D. Ciangottini,[64a,64b] L. Fanò,[64a,64b] P. Lariccia,[64a,64b] G. Mantovani,[64a,64b] M. Menichelli,[64a] F. Romeo,[64a,64b] A. Saha,[64a] A. Santocchia,[64a,64b] A. Spiezia,[64a,64b,c] K. Androsov,[65a,z] P. Azzurri,[65a] G. Bagliesi,[65a] J. Bernardini,[65a] T. Boccali,[65a] G. Broccolo,[65a,65c] R. Castaldi,[65a] M. A. Ciocci,[65a,z] R. Dell'Orso,[65a] S. Donato,[65a,65c] F. Fiori,[65a,65c] L. Foà,[65a,65c] A. Giassi,[65a] M. T. Grippo,[65a,z] F. Ligabue,[65a,65c] T. Lomtadze,[65a] L. Martini,[65a,65b] A. Messineo,[65a,65b] C. S. Moon,[65a,aa] F. Palla,[65a,c] A. Rizzi,[65a,65b] A. Savoy-Navarro,[65a,bb] A. T. Serban,[65a] P. Spagnolo,[65a] P. Squillacioti,[65a,z] R. Tenchini,[65a] G. Tonelli,[65a,65b] A. Venturi,[65a] P. G. Verdini,[65a] C. Vernieri,[65a,65c,c] L. Barone,[66a,66b] F. Cavallari,[66a] G. D'imperio,[66a,66b] D. Del Re,[66a,66b] M. Diemoz,[66a] M. Grassi,[66a,66b] C. Jorda,[66a] E. Longo,[66a,66b] F. Margaroli,[66a,66b] P. Meridiani,[66a] F. Micheli,[66a,66b,c] S. Nourbakhsh,[66a,66b] G. Organtini,[66a,66b] R. Paramatti,[66a] S. Rahatlou,[66a,66b] C. Rovelli,[66a] F. Santanastasio,[66a,66b] L. Soffi,[66a,66b,c] P. Traczyk,[66a,66b] N. Amapane,[67a,67b] R. Arcidiacono,[67a,67c] S. Argiro,[67a,67b,c] M. Arneodo,[67a,67c] R. Bellan,[67a,67b] C. Biino,[67a] N. Cartiglia,[67a] S. Casasso,[67a,67b,c] M. Costa,[67a,67b] A. Degano,[67a,67b] N. Demaria,[67a] L. Finco,[67a,67b] C. Mariotti,[67a] S. Maselli,[67a] E. Migliore,[67a,67b] V. Monaco,[67a,67b] M. Musich,[67a] M. M. Obertino,[67a,67c,c] G. Ortona,[67a,67b] L. Pacher,[67a,67b] N. Pastrone,[67a] M. Pelliccioni,[67a] G. L. Pinna Angioni,[67a,67b] A. Potenza,[67a,67b] A. Romero,[67a,67b] M. Ruspa,[67a,67c] R. Sacchi,[67a,67b] A. Solano,[67a,67b] A. Staiano,[67a] U. Tamponi,[67a] S. Belforte,[68a] V. Candelise,[68a,68b] M. Casarsa,[68a] F. Cossutti,[68a] G. Della Ricca,[68a,68b] B. Gobbo,[68a] C. La Licata,[68a,68b] M. Marone,[68a,68b] A. Schizzi,[68a,68b,c] T. Umer,[68a,68b] A. Zanetti,[68a] S. Chang,[69] A. Kropivnitskaya,[69] S. K. Nam,[69] D. H. Kim,[70] G. N. Kim,[70] M. S. Kim,[70] D. J. Kong,[70] S. Lee,[70] Y. D. Oh,[70] H. Park,[70] A. Sakharov,[70] D. C. Son,[70] T. J. Kim,[71] J. Y. Kim,[72] S. Song,[72] S. Choi,[73] D. Gyun,[73] B. Hong,[73] M. Jo,[73] H. Kim,[73] Y. Kim,[73] B. Lee,[73] K. S. Lee,[73] S. K. Park,[73] Y. Roh,[73] M. Choi,[74] J. H. Kim,[74] I. C. Park,[74] G. Ryu,[74] M. S. Ryu,[74] Y. Choi,[75] Y. K. Choi,[75] J. Goh,[75] D. Kim,[75] E. Kwon,[75] J. Lee,[75] H. Seo,[75] I. Yu,[75] A. Juodagalvis,[76] J. R. Komaragiri,[77] M. A. B. Md Ali,[77] H. Castilla-Valdez,[78] E. De La Cruz-Burelo,[78] I. Heredia-de La Cruz,[78,cc] A. Hernandez-Almada,[78] R. Lopez-Fernandez,[78] A. Sanchez-Hernandez,[78] S. Carrillo Moreno,[79] F. Vazquez Valencia,[79] I. Pedraza,[80] H. A. Salazar Ibarguen,[80] E. Casimiro Linares,[81] A. Morelos Pineda,[81] D. Krofcheck,[82] P. H. Butler,[83] S. Reucroft,[83] A. Ahmad,[84] M. Ahmad,[84] Q. Hassan,[84] H. R. Hoorani,[84] S. Khalid,[84] W. A. Khan,[84] T. Khurshid,[84] M. A. Shah,[84] M. Shoaib,[84] H. Bialkowska,[85] M. Bluj,[85] B. Boimska,[85] T. Frueboes,[85] M. Górski,[85] M. Kazana,[85] K. Nawrocki,[85] K. Romanowska-Rybinska,[85] M. Szleper,[85] P. Zalewski,[85] G. Brona,[86] K. Bunkowski,[86] M. Cwiok,[86] W. Dominik,[86] K. Doroba,[86] A. Kalinowski,[86] M. Konecki,[86] J. Krolikowski,[86] M. Misiura,[86] M. Olszewski,[86] W. Wolszczak,[86] P. Bargassa,[87] C. Beirão Da Cruz E Silva,[87] P. Faccioli,[87] P. G. Ferreira Parracho,[87] M. Gallinaro,[87] L. Lloret Iglesias,[87] F. Nguyen,[87] J. Rodrigues Antunes,[87] J. Seixas,[87] J. Varela,[87] P. Vischia,[87] S. Afanasiev,[88] P. Bunin,[88] M. Gavrilenko,[88] I. Golutvin,[88] I. Gorbunov,[88] A. Kamenev,[88] V. Karjavin,[88] V. Konoplyanikov,[88] A. Lanev,[88] A. Malakhov,[88] V. Matveev,[88,dd] P. Moisenz,[88] V. Palichik,[88] V. Perelygin,[88] S. Shmatov,[88] N. Skatchkov,[88] V. Smirnov,[88] A. Zarubin,[88] V. Golovtsov,[89] Y. Ivanov,[89] V. Kim,[89,ee] P. Levchenko,[89] V. Murzin,[89] V. Oreshkin,[89] I. Smirnov,[89] V. Sulimov,[89] L. Uvarov,[89] S. Vavilov,[89] A. Vorobyev,[89] An. Vorobyev,[89] Yu. Andreev,[90] A. Dermenev,[90] S. Gninenko,[90] N. Golubev,[90] M. Kirsanov,[90] N. Krasnikov,[90] A. Pashenkov,[90] D. Tlisov,[90] A. Toropin,[90] V. Epshteyn,[91] V. Gavrilov,[91] N. Lychkovskaya,[91] V. Popov,[91] G. Safronov,[91] S. Semenov,[91] A. Spiridonov,[91] V. Stolin,[91] E. Vlasov,[91] A. Zhokin,[91] V. Andreev,[92] M. Azarkin,[92] I. Dremin,[92] M. Kirakosyan,[92] A. Leonidov,[92] G. Mesyats,[92] S. V. Rusakov,[92] A. Vinogradov,[92] A. Belyaev,[93] E. Boos,[93] M. Dubinin,[93,ff] L. Dudko,[93] A. Ershov,[93] A. Gribushin,[93] V. Klyukhin,[93] O. Kodolova,[93] I. Lokhtin,[93] S. Obraztsov,[93] S. Petrushanko,[93] V. Savrin,[93] A. Snigirev,[93] I. Azhgirey,[94] I. Bayshev,[94] S. Bitioukov,[94] V. Kachanov,[94] A. Kalinin,[94]

D. Konstantinov,[94] V. Krychkine,[94] V. Petrov,[94] R. Ryutin,[94] A. Sobol,[94] L. Tourtchanovitch,[94] S. Troshin,[94] N. Tyurin,[94] A. Uzunian,[94] A. Volkov,[94] P. Adzic,[95,gg] M. Ekmedzic,[95] J. Milosevic,[95] V. Rekovic,[95] J. Alcaraz Maestre,[96] C. Battilana,[96] E. Calvo,[96] M. Cerrada,[96] M. Chamizo Llatas,[96] N. Colino,[96] B. De La Cruz,[96] A. Delgado Peris,[96] D. Domínguez Vázquez,[96] A. Escalante Del Valle,[96] C. Fernandez Bedoya,[96] J. P. Fernández Ramos,[96] J. Flix,[96] M. C. Fouz,[96] P. Garcia-Abia,[96] O. Gonzalez Lopez,[96] S. Goy Lopez,[96] J. M. Hernandez,[96] M. I. Josa,[96] E. Navarro De Martino,[96] A. Pérez-Calero Yzquierdo,[96] J. Puerta Pelayo,[96] A. Quintario Olmeda,[96] I. Redondo,[96] L. Romero,[96] M. S. Soares,[96] C. Albajar,[97] J. F. de Trocóniz,[97] M. Missiroli,[97] D. Moran,[97] H. Brun,[98] J. Cuevas,[98] J. Fernandez Menendez,[98] S. Folgueras,[98] I. Gonzalez Caballero,[98] J. A. Brochero Cifuentes,[99] I. J. Cabrillo,[99] A. Calderon,[99] J. Duarte Campderros,[99] M. Fernandez,[99] G. Gomez,[99] A. Graziano,[99] A. Lopez Virto,[99] J. Marco,[99] R. Marco,[99] C. Martinez Rivero,[99] F. Matorras,[99] F. J. Munoz Sanchez,[99] J. Piedra Gomez,[99] T. Rodrigo,[99] A. Y. Rodríguez-Marrero,[99] A. Ruiz-Jimeno,[99] L. Scodellaro,[99] I. Vila,[99] R. Vilar Cortabitarte,[99] D. Abbaneo,[100] E. Auffray,[100] G. Auzinger,[100] M. Bachtis,[100] P. Baillon,[100] A. H. Ball,[100] D. Barney,[100] A. Benaglia,[100] J. Bendavid,[100] L. Benhabib,[100] J. F. Benitez,[100] C. Bernet,[100,h] G. Bianchi,[100] P. Bloch,[100] A. Bocci,[100] A. Bonato,[100] O. Bondu,[100] C. Botta,[100] H. Breuker,[100] T. Camporesi,[100] G. Cerminara,[100] S. Colafranceschi,[100,hh] M. D'Alfonso,[100] D. d'Enterria,[100] A. Dabrowski,[100] A. David,[100] F. De Guio,[100] A. De Roeck,[100] S. De Visscher,[100] E. Di Marco,[100] M. Dobson,[100] M. Dordevic,[100] N. Dupont-Sagorin,[100] A. Elliott-Peisert,[100] J. Eugster,[100] G. Franzoni,[100] W. Funk,[100] D. Gigi,[100] K. Gill,[100] D. Giordano,[100] M. Girone,[100] F. Glege,[100] R. Guida,[100] S. Gundacker,[100] M. Guthoff,[100] J. Hammer,[100] M. Hansen,[100] P. Harris,[100] J. Hegeman,[100] V. Innocente,[100] P. Janot,[100] K. Kousouris,[100] K. Krajczar,[100] P. Lecoq,[100] C. Lourenço,[100] N. Magini,[100] L. Malgeri,[100] M. Mannelli,[100] J. Marrouche,[100] L. Masetti,[100] F. Meijers,[100] S. Mersi,[100] E. Meschi,[100] F. Moortgat,[100] S. Morovic,[100] M. Mulders,[100] P. Musella,[100] L. Orsini,[100] L. Pape,[100] E. Perez,[100] L. Perrozzi,[100] A. Petrilli,[100] G. Petrucciani,[100] A. Pfeiffer,[100] M. Pierini,[100] M. Pimiä,[100] D. Piparo,[100] M. Plagge,[100] A. Racz,[100] G. Rolandi,[100,ii] M. Rovere,[100] H. Sakulin,[100] C. Schäfer,[100] C. Schwick,[100] A. Sharma,[100] P. Siegrist,[100] P. Silva,[100] M. Simon,[100] P. Sphicas,[100,jj] D. Spiga,[100] J. Steggemann,[100] B. Stieger,[100] M. Stoye,[100] Y. Takahashi,[100] D. Treille,[100] A. Tsirou,[100] G. I. Veres,[100,r] J. R. Vlimant,[100] N. Wardle,[100] H. K. Wöhri,[100] H. Wollny,[100] W. D. Zeuner,[100] W. Bertl,[101] K. Deiters,[101] W. Erdmann,[101] R. Horisberger,[101] Q. Ingram,[101] H. C. Kaestli,[101] D. Kotlinski,[101] U. Langenegger,[101] D. Renker,[101] T. Rohe,[101] F. Bachmair,[102] L. Bäni,[102] L. Bianchini,[102] M. A. Buchmann,[102] B. Casal,[102] N. Chanon,[102] G. Dissertori,[102] M. Dittmar,[102] M. Donegà,[102] M. Dünser,[102] P. Eller,[102] C. Grab,[102] D. Hits,[102] J. Hoss,[102] W. Lustermann,[102] B. Mangano,[102] A. C. Marini,[102] P. Martinez Ruiz del Arbol,[102] M. Masciovecchio,[102] D. Meister,[102] N. Mohr,[102] C. Nägeli,[102,kk] F. Nessi-Tedaldi,[102] F. Pandolfi,[102] F. Pauss,[102] M. Peruzzi,[102] M. Quittnat,[102] L. Rebane,[102] M. Rossini,[102] A. Starodumov,[102,ll] M. Takahashi,[102] K. Theofilatos,[102] R. Wallny,[102] H. A. Weber,[102] C. Amsler,[103,mm] M. F. Canelli,[103] V. Chiochia,[103] A. De Cosa,[103] A. Hinzmann,[103] T. Hreus,[103] B. Kilminster,[103] C. Lange,[103] B. Millan Mejias,[103] J. Ngadiuba,[103] P. Robmann,[103] F. J. Ronga,[103] S. Taroni,[103] M. Verzetti,[103] Y. Yang,[103] M. Cardaci,[104] K. H. Chen,[104] C. Ferro,[104] C. M. Kuo,[104] W. Lin,[104] Y. J. Lu,[104] R. Volpe,[104] S. S. Yu,[104] P. Chang,[105] Y. H. Chang,[105] Y. W. Chang,[105] Y. Chao,[105] K. F. Chen,[105] P. H. Chen,[105] C. Dietz,[105] U. Grundler,[105] W.-S. Hou,[105] K. Y. Kao,[105] Y. J. Lei,[105] Y. F. Liu,[105] R.-S. Lu,[105] D. Majumder,[105] E. Petrakou,[105] Y. M. Tzeng,[105] R. Wilken,[105] B. Asavapibhop,[106] N. Srimanobhas,[106] N. Suwonjandee,[106] A. Adiguzel,[107] M. N. Bakirci,[107,nn] S. Cerci,[107,oo] C. Dozen,[107] I. Dumanoglu,[107] E. Eskut,[107] S. Girgis,[107] G. Gokbulut,[107] E. Gurpinar,[107] I. Hos,[107] E. E. Kangal,[107] A. Kayis Topaksu,[107] G. Onengut,[107,pp] K. Ozdemir,[107] S. Ozturk,[107,nn] A. Polatoz,[107] D. Sunar Cerci,[107,oo] B. Tali,[107,oo] H. Topakli,[107,nn] M. Vergili,[107] I. V. Akin,[108] B. Bilin,[108] S. Bilmis,[108] H. Gamsizkan,[108,qq] G. Karapinar,[108,rr] K. Ocalan,[108,ss] S. Sekmen,[108] U. E. Surat,[108] M. Yalvac,[108] M. Zeyrek,[108] E. Gülmez,[109] B. Isildak,[109,tt] M. Kaya,[109,uu] O. Kaya,[109,vv] K. Cankocak,[110] F. I. Vardarlı,[110] L. Levchuk,[111] P. Sorokin,[111] J. J. Brooke,[112] E. Clement,[112] D. Cussans,[112] H. Flacher,[112] R. Frazier,[112] J. Goldstein,[112] M. Grimes,[112] G. P. Heath,[112] H. F. Heath,[112] J. Jacob,[112] L. Kreczko,[112] C. Lucas,[112] Z. Meng,[112] D. M. Newbold,[112,ww] S. Paramesvaran,[112] A. Poll,[112] S. Senkin,[112] V. J. Smith,[112] T. Williams,[112] K. W. Bell,[113] A. Belyaev,[113,xx] C. Brew,[113] R. M. Brown,[113] D. J. A. Cockerill,[113] J. A. Coughlan,[113] K. Harder,[113] S. Harper,[113] E. Olaiya,[113] D. Petyt,[113] C. H. Shepherd-Themistocleous,[113] A. Thea,[113] I. R. Tomalin,[113] W. J. Womersley,[113] S. D. Worm,[113] M. Baber,[114] R. Bainbridge,[114] O. Buchmuller,[114] D. Burton,[114] D. Colling,[114] N. Cripps,[114] M. Cutajar,[114] P. Dauncey,[114] G. Davies,[114] M. Della Negra,[114] P. Dunne,[114] W. Ferguson,[114] J. Fulcher,[114] D. Futyan,[114] A. Gilbert,[114] G. Hall,[114] G. Iles,[114] M. Jarvis,[114] G. Karapostoli,[114] M. Kenzie,[114] R. Lane,[114] R. Lucas,[114,ww] L. Lyons,[114] A.-M. Magnan,[114] S. Malik,[114] B. Mathias,[114] J. Nash,[114] A. Nikitenko,[114,ll] J. Pela,[114] M. Pesaresi,[114] K. Petridis,[114] D. M. Raymond,[114] S. Rogerson,[114] A. Rose,[114]

C. Seez,[114] P. Sharp,[114,a] A. Tapper,[114] M. Vazquez Acosta,[114] T. Virdee,[114] S. C. Zenz,[114] J. E. Cole,[115] P. R. Hobson,[115] A. Khan,[115] P. Kyberd,[115] D. Leggat,[115] D. Leslie,[115] W. Martin,[115] I. D. Reid,[115] P. Symonds,[115] L. Teodorescu,[115] M. Turner,[115] J. Dittmann,[116] K. Hatakeyama,[116] A. Kasmi,[116] H. Liu,[116] T. Scarborough,[116] O. Charaf,[117] S. I. Cooper,[117] C. Henderson,[117] P. Rumerio,[117] A. Avetisyan,[118] T. Bose,[118] C. Fantasia,[118] P. Lawson,[118] C. Richardson,[118] J. Rohlf,[118] J. St. John,[118] L. Sulak,[118] J. Alimena,[119] E. Berry,[119] S. Bhattacharya,[119] G. Christopher,[119] D. Cutts,[119] Z. Demiragli,[119] N. Dhingra,[119] A. Ferapontov,[119] A. Garabedian,[119] U. Heintz,[119] G. Kukartsev,[119] E. Laird,[119] G. Landsberg,[119] M. Luk,[119] M. Narain,[119] M. Segala,[119] T. Sinthuprasith,[119] T. Speer,[119] J. Swanson,[119] R. Breedon,[120] G. Breto,[120] M. Calderon De La Barca Sanchez,[120] S. Chauhan,[120] M. Chertok,[120] J. Conway,[120] R. Conway,[120] P. T. Cox,[120] R. Erbacher,[120] M. Gardner,[120] W. Ko,[120] R. Lander,[120] T. Miceli,[120] M. Mulhearn,[120] D. Pellett,[120] J. Pilot,[120] F. Ricci-Tam,[120] M. Searle,[120] S. Shalhout,[120] J. Smith,[120] M. Squires,[120] D. Stolp,[120] M. Tripathi,[120] S. Wilbur,[120] R. Yohay,[120] R. Cousins,[121] P. Everaerts,[121] C. Farrell,[121] J. Hauser,[121] M. Ignatenko,[121] G. Rakness,[121] E. Takasugi,[121] V. Valuev,[121] M. Weber,[121] K. Burt,[122] R. Clare,[122] J. Ellison,[122] J. W. Gary,[122] G. Hanson,[122] J. Heilman,[122] M. Ivova Rikova,[122] P. Jandir,[122] E. Kennedy,[122] F. Lacroix,[122] O. R. Long,[122] A. Luthra,[122] M. Malberti,[122] H. Nguyen,[122] M. Olmedo Negrete,[122] A. Shrinivas,[122] S. Sumowidagdo,[122] S. Wimpenny,[122] W. Andrews,[123] J. G. Branson,[123] G. B. Cerati,[123] S. Cittolin,[123] R. T. D'Agnolo,[123] D. Evans,[123] A. Holzner,[123] R. Kelley,[123] D. Klein,[123] M. Lebourgeois,[123] J. Letts,[123] I. Macneill,[123] D. Olivito,[123] S. Padhi,[123] C. Palmer,[123] M. Pieri,[123] M. Sani,[123] V. Sharma,[123] S. Simon,[123] E. Sudano,[123] M. Tadel,[123] Y. Tu,[123] A. Vartak,[123] C. Welke,[123] F. Würthwein,[123] A. Yagil,[123] D. Barge,[124] J. Bradmiller-Feld,[124] C. Campagnari,[124] T. Danielson,[124] A. Dishaw,[124] K. Flowers,[124] M. Franco Sevilla,[124] P. Geffert,[124] C. George,[124] F. Golf,[124] L. Gouskos,[124] J. Gran,[124] J. Incandela,[124] C. Justus,[124] N. Mccoll,[124] J. Richman,[124] D. Stuart,[124] W. To,[124] C. West,[124] J. Yoo,[124] A. Apresyan,[125] A. Bornheim,[125] J. Bunn,[125] Y. Chen,[125] J. Duarte,[125] A. Mott,[125] H. B. Newman,[125] C. Pena,[125] C. Rogan,[125] M. Spiropulu,[125] V. Timciuc,[125] R. Wilkinson,[125] S. Xie,[125] R. Y. Zhu,[125] V. Azzolini,[126] A. Calamba,[126] B. Carlson,[126] T. Ferguson,[126] Y. Iiyama,[126] M. Paulini,[126] J. Russ,[126] H. Vogel,[126] I. Vorobiev,[126] J. P. Cumalat,[127] W. T. Ford,[127] A. Gaz,[127] E. Luiggi Lopez,[127] U. Nauenberg,[127] J. G. Smith,[127] K. Stenson,[127] K. A. Ulmer,[127] S. R. Wagner,[127] J. Alexander,[128] A. Chatterjee,[128] J. Chu,[128] S. Dittmer,[128] N. Eggert,[128] N. Mirman,[128] G. Nicolas Kaufman,[128] J. R. Patterson,[128] A. Ryd,[128] E. Salvati,[128] L. Skinnari,[128] W. Sun,[128] W. D. Teo,[128] J. Thom,[128] J. Thompson,[128] J. Tucker,[128] Y. Weng,[128] L. Winstrom,[128] P. Wittich,[128] D. Winn,[129] S. Abdullin,[130] M. Albrow,[130] J. Anderson,[130] G. Apollinari,[130] L. A. T. Bauerdick,[130] A. Beretvas,[130] J. Berryhill,[130] P. C. Bhat,[130] G. Bolla,[130] K. Burkett,[130] J. N. Butler,[130] H. W. K. Cheung,[130] F. Chlebana,[130] S. Cihangir,[130] V. D. Elvira,[130] I. Fisk,[130] J. Freeman,[130] Y. Gao,[130] E. Gottschalk,[130] L. Gray,[130] D. Green,[130] S. Grünendahl,[130] O. Gutsche,[130] J. Hanlon,[130] D. Hare,[130] R. M. Harris,[130] J. Hirschauer,[130] B. Hooberman,[130] S. Jindariani,[130] M. Johnson,[130] U. Joshi,[130] K. Kaadze,[130] B. Klima,[130] B. Kreis,[130] S. Kwan,[130] J. Linacre,[130] D. Lincoln,[130] R. Lipton,[130] T. Liu,[130] J. Lykken,[130] K. Maeshima,[130] J. M. Marraffino,[130] V. I. Martinez Outschoorn,[130] S. Maruyama,[130] D. Mason,[130] P. McBride,[130] P. Merkel,[130] K. Mishra,[130] S. Mrenna,[130] Y. Musienko,[130,dd] S. Nahn,[130] C. Newman-Holmes,[130] V. O'Dell,[130] O. Prokofyev,[130] E. Sexton-Kennedy,[130] S. Sharma,[130] A. Soha,[130] W. J. Spalding,[130] L. Spiegel,[130] L. Taylor,[130] S. Tkaczyk,[130] N. V. Tran,[130] L. Uplegger,[130] E. W. Vaandering,[130] R. Vidal,[130] A. Whitbeck,[130] J. Whitmore,[130] F. Yang,[130] D. Acosta,[131] P. Avery,[131] P. Bortignon,[131] D. Bourilkov,[131] M. Carver,[131] T. Cheng,[131] D. Curry,[131] S. Das,[131] M. De Gruttola,[131] G. P. Di Giovanni,[131] R. D. Field,[131] M. Fisher,[131] I. K. Furic,[131] J. Hugon,[131] J. Konigsberg,[131] A. Korytov,[131] T. Kypreos,[131] J. F. Low,[131] K. Matchev,[131] P. Milenovic,[131,yy] G. Mitselmakher,[131] L. Muniz,[131] A. Rinkevicius,[131] L. Shchutska,[131] M. Snowball,[131] D. Sperka,[131] J. Yelton,[131] M. Zakaria,[131] S. Hewamanage,[132] S. Linn,[132] P. Markowitz,[132] G. Martinez,[132] J. L. Rodriguez,[132] T. Adams,[133] A. Askew,[133] J. Bochenek,[133] B. Diamond,[133] J. Haas,[133] S. Hagopian,[133] V. Hagopian,[133] K. F. Johnson,[133] H. Prosper,[133] V. Veeraraghavan,[133] M. Weinberg,[133] M. M. Baarmand,[134] M. Hohlmann,[134] H. Kalakhety,[134] F. Yumiceva,[134] M. R. Adams,[135] L. Apanasevich,[135] V. E. Bazterra,[135] D. Berry,[135] R. R. Betts,[135] I. Bucinskaite,[135] R. Cavanaugh,[135] O. Evdokimov,[135] L. Gauthier,[135] C. E. Gerber,[135] D. J. Hofman,[135] S. Khalatyan,[135] P. Kurt,[135] D. H. Moon,[135] C. O'Brien,[135] C. Silkworth,[135] P. Turner,[135] N. Varelas,[135] E. A. Albayrak,[136,zz] B. Bilki,[136,aaa] W. Clarida,[136] K. Dilsiz,[136] F. Duru,[136] M. Haytmyradov,[136] J.-P. Merlo,[136] H. Mermerkaya,[136,bbb] A. Mestvirishvili,[136] A. Moeller,[136] J. Nachtman,[136] H. Ogul,[136] Y. Onel,[136] F. Ozok,[136,zz] A. Penzo,[136] R. Rahmat,[136] S. Sen,[136] P. Tan,[136] E. Tiras,[136] J. Wetzel,[136] T. Yetkin,[136,ccc] K. Yi,[136] B. A. Barnett,[137] B. Blumenfeld,[137] S. Bolognesi,[137] D. Fehling,[137] A. V. Gritsan,[137] P. Maksimovic,[137] C. Martin,[137] M. Swartz,[137] P. Baringer,[138] A. Bean,[138] G. Benelli,[138] C. Bruner,[138] R. P. Kenny III,[138] M. Malek,[138] M. Murray,[138] D. Noonan,[138] S. Sanders,[138] J. Sekaric,[138] R. Stringer,[138] Q. Wang,[138] J. S. Wood,[138] A. F. Barfuss,[139]

I. Chakaberia,[139] A. Ivanov,[139] S. Khalil,[139] M. Makouski,[139] Y. Maravin,[139] L. K. Saini,[139] S. Shrestha,[139] N. Skhirtladze,[139] I. Svintradze,[139] J. Gronberg,[140] D. Lange,[140] F. Rebassoo,[140] D. Wright,[140] A. Baden,[141] A. Belloni,[141] B. Calvert,[141] S. C. Eno,[141] J. A. Gomez,[141] N. J. Hadley,[141] R. G. Kellogg,[141] T. Kolberg,[141] Y. Lu,[141] M. Marionneau,[141] A. C. Mignerey,[141] K. Pedro,[141] A. Skuja,[141] M. B. Tonjes,[141] S. C. Tonwar,[141] A. Apyan,[142] R. Barbieri,[142] G. Bauer,[142] W. Busza,[142] I. A. Cali,[142] M. Chan,[142] L. Di Matteo,[142] V. Dutta,[142] G. Gomez Ceballos,[142] M. Goncharov,[142] D. Gulhan,[142] M. Klute,[142] Y. S. Lai,[142] Y.-J. Lee,[142] A. Levin,[142] P. D. Luckey,[142] T. Ma,[142] C. Paus,[142] D. Ralph,[142] C. Roland,[142] G. Roland,[142] G. S. F. Stephans,[142] F. Stöckli,[142] K. Sumorok,[142] D. Velicanu,[142] J. Veverka,[142] B. Wyslouch,[142] M. Yang,[142] M. Zanetti,[142] V. Zhukova,[142] B. Dahmes,[143] A. Gude,[143] S. C. Kao,[143] K. Klapoetke,[143] Y. Kubota,[143] J. Mans,[143] N. Pastika,[143] R. Rusack,[143] A. Singovsky,[143] N. Tambe,[143] J. Turkewitz,[143] J. G. Acosta,[144] S. Oliveros,[144] E. Avdeeva,[145] K. Bloom,[145] S. Bose,[145] D. R. Claes,[145] A. Dominguez,[145] R. Gonzalez Suarez,[145] J. Keller,[145] D. Knowlton,[145] I. Kravchenko,[145] J. Lazo-Flores,[145] S. Malik,[145] F. Meier,[145] G. R. Snow,[145] M. Zvada,[145] J. Dolen,[146] A. Godshalk,[146] I. Iashvili,[146] A. Kharchilava,[146] A. Kumar,[146] S. Rappoccio,[146] G. Alverson,[147] E. Barberis,[147] D. Baumgartel,[147] M. Chasco,[147] J. Haley,[147] A. Massironi,[147] D. M. Morse,[147] D. Nash,[147] T. Orimoto,[147] D. Trocino,[147] R.-J. Wang,[147] D. Wood,[147] J. Zhang,[147] K. A. Hahn,[148] A. Kubik,[148] N. Mucia,[148] N. Odell,[148] B. Pollack,[148] A. Pozdnyakov,[148] M. Schmitt,[148] S. Stoynev,[148] K. Sung,[148] M. Velasco,[148] S. Won,[148] A. Brinkerhoff,[149] K. M. Chan,[149] A. Drozdetskiy,[149] M. Hildreth,[149] C. Jessop,[149] D. J. Karmgard,[149] N. Kellams,[149] K. Lannon,[149] W. Luo,[149] S. Lynch,[149] N. Marinelli,[149] T. Pearson,[149] M. Planer,[149] R. Ruchti,[149] N. Valls,[149] M. Wayne,[149] M. Wolf,[149] A. Woodard,[149] L. Antonelli,[150] J. Brinson,[150] B. Bylsma,[150] L. S. Durkin,[150] S. Flowers,[150] C. Hill,[150] R. Hughes,[150] K. Kotov,[150] T. Y. Ling,[150] D. Puigh,[150] M. Rodenburg,[150] G. Smith,[150] B. L. Winer,[150] H. Wolfe,[150] H. W. Wulsin,[150] O. Driga,[151] P. Elmer,[151] P. Hebda,[151] A. Hunt,[151] S. A. Koay,[151] P. Lujan,[151] D. Marlow,[151] T. Medvedeva,[151] M. Mooney,[151] J. Olsen,[151] P. Piroué,[151] X. Quan,[151] H. Saka,[151] D. Stickland,[151,c] C. Tully,[151] J. S. Werner,[151] A. Zuranski,[151] E. Brownson,[152] H. Mendez,[152] J. E. Ramirez Vargas,[152] V. E. Barnes,[153] D. Benedetti,[153] D. Bortoletto,[153] M. De Mattia,[153] L. Gutay,[153] Z. Hu,[153] M. K. Jha,[153] M. Jones,[153] K. Jung,[153] M. Kress,[153] N. Leonardo,[153] D. Lopes Pegna,[153] V. Maroussov,[153] D. H. Miller,[153] N. Neumeister,[153] B. C. Radburn-Smith,[153] X. Shi,[153] I. Shipsey,[153] D. Silvers,[153] A. Svyatkovskiy,[153] F. Wang,[153] W. Xie,[153] L. Xu,[153] H. D. Yoo,[153] J. Zablocki,[153] Y. Zheng,[153] N. Parashar,[154] J. Stupak,[154] A. Adair,[155] B. Akgun,[155] K. M. Ecklund,[155] F. J. M. Geurts,[155] W. Li,[155] B. Michlin,[155] B. P. Padley,[155] R. Redjimi,[155] J. Roberts,[155] J. Zabel,[155] B. Betchart,[156] A. Bodek,[156] R. Covarelli,[156] P. de Barbaro,[156] R. Demina,[156] Y. Eshaq,[156] T. Ferbel,[156] A. Garcia-Bellido,[156] P. Goldenzweig,[156] J. Han,[156] A. Harel,[156] A. Khukhunaishvili,[156] G. Petrillo,[156] D. Vishnevskiy,[156] R. Ciesielski,[157] L. Demortier,[157] K. Goulianos,[157] G. Lungu,[157] C. Mesropian,[157] S. Arora,[158] A. Barker,[158] J. P. Chou,[158] C. Contreras-Campana,[158] E. Contreras-Campana,[158] N. Craig,[158] D. Duggan,[158] J. Evans,[158] D. Ferencek,[158] Y. Gershtein,[158] R. Gray,[158] E. Halkiadakis,[158] D. Hidas,[158] S. Kaplan,[158] A. Lath,[158] S. Panwalkar,[158] M. Park,[158] R. Patel,[158] S. Salur,[158] S. Schnetzer,[158] S. Somalwar,[158] R. Stone,[158] S. Thomas,[158] P. Thomassen,[158] M. Walker,[158] P. Zywicki,[158] K. Rose,[159] S. Spanier,[159] A. York,[159] O. Bouhali,[160,ddd] A. Castaneda Hernandez,[160] R. Eusebi,[160] W. Flanagan,[160] J. Gilmore,[160] T. Kamon,[160,eee] V. Khotilovich,[160] V. Krutelyov,[160] R. Montalvo,[160] I. Osipenkov,[160] Y. Pakhotin,[160] A. Perloff,[160] J. Roe,[160] A. Rose,[160] A. Safonov,[160] T. Sakuma,[160] I. Suarez,[160] A. Tatarinov,[160] N. Akchurin,[161] C. Cowden,[161] J. Damgov,[161] C. Dragoiu,[161] P. R. Dudero,[161] J. Faulkner,[161] K. Kovitanggoon,[161] S. Kunori,[161] S. W. Lee,[161] T. Libeiro,[161] I. Volobouev,[161] E. Appelt,[162] A. G. Delannoy,[162] S. Greene,[162] A. Gurrola,[162] W. Johns,[162] C. Maguire,[162] Y. Mao,[162] A. Melo,[162] M. Sharma,[162] P. Sheldon,[162] B. Snook,[162] S. Tuo,[162] J. Velkovska,[162] M. W. Arenton,[163] S. Boutle,[163] B. Cox,[163] B. Francis,[163] J. Goodell,[163] R. Hirosky,[163] A. Ledovskoy,[163] H. Li,[163] C. Lin,[163] C. Neu,[163] J. Wood,[163] C. Clarke,[164] R. Harr,[164] P. E. Karchin,[164] C. Kottachchi Kankanamge Don,[164] P. Lamichhane,[164] J. Sturdy,[164] D. A. Belknap,[165] D. Carlsmith,[165] M. Cepeda,[165] S. Dasu,[165] L. Dodd,[165] S. Duric,[165] E. Friis,[165] R. Hall-Wilton,[165] M. Herndon,[165] A. Hervé,[165] P. Klabbers,[165] A. Lanaro,[165] C. Lazaridis,[165] A. Levine,[165] R. Loveless,[165] A. Mohapatra,[165] I. Ojalvo,[165] T. Perry,[165] G. A. Pierro,[165] G. Polese,[165] I. Ross,[165] T. Sarangi,[165] A. Savin,[165] W. H. Smith,[165] D. Taylor,[165] P. Verwilligen,[165] C. Vuosalo[165] and N. Woods[165]

(CMS Collaboration)

[1]Yerevan Physics Institute, Yerevan, Armenia
[2]Institut für Hochenergiephysik der OeAW, Wien, Austria
[3]National Centre for Particle and High Energy Physics, Minsk, Belarus

[4]*Universiteit Antwerpen, Antwerpen, Belgium*
[5]*Vrije Universiteit Brussel, Brussel, Belgium*
[6]*Université Libre de Bruxelles, Bruxelles, Belgium*
[7]*Ghent University, Ghent, Belgium*
[8]*Université Catholique de Louvain, Louvain-la-Neuve, Belgium*
[9]*Université de Mons, Mons, Belgium*
[10]*Centro Brasileiro de Pesquisas Fisicas, Rio de Janeiro, Brazil*
[11]*Universidade do Estado do Rio de Janeiro, Rio de Janeiro, Brazil*
[12a]*Universidade Estadual Paulista, São Paulo, Brazil*
[12b]*Universidade Federal do ABC, São Paulo, Brazil*
[13]*Institute for Nuclear Research and Nuclear Energy, Sofia, Bulgaria*
[14]*University of Sofia, Sofia, Bulgaria*
[15]*Institute of High Energy Physics, Beijing, China*
[16]*State Key Laboratory of Nuclear Physics and Technology, Peking University, Beijing, China*
[17]*Universidad de Los Andes, Bogota, Colombia*
[18]*University of Split, Faculty of Electrical Engineering, Mechanical Engineering and Naval Architecture,
Split, Croatia*
[19]*University of Split, Faculty of Science, Split, Croatia*
[20]*Institute Rudjer Boskovic, Zagreb, Croatia*
[21]*University of Cyprus, Nicosia, Cyprus*
[22]*Charles University, Prague, Czech Republic*
[23]*Academy of Scientific Research and Technology of the Arab Republic of Egypt,
Egyptian Network of High Energy Physics, Cairo, Egypt*
[24]*National Institute of Chemical Physics and Biophysics, Tallinn, Estonia*
[25]*Department of Physics, University of Helsinki, Helsinki, Finland*
[26]*Helsinki Institute of Physics, Helsinki, Finland*
[27]*Lappeenranta University of Technology, Lappeenranta, Finland*
[28]*DSM/IRFU, CEA/Saclay, Gif-sur-Yvette, France*
[29]*Laboratoire Leprince-Ringuet, Ecole Polytechnique, IN2P3-CNRS, Palaiseau, France*
[30]*Institut Pluridisciplinaire Hubert Curien, Université de Strasbourg,
Université de Haute Alsace Mulhouse, CNRS/IN2P3, Strasbourg, France*
[31]*Centre de Calcul de l'Institut National de Physique Nucleaire et de Physique des Particules,
CNRS/IN2P3, Villeurbanne, France*
[32]*Université de Lyon, Université Claude Bernard Lyon 1, CNRS-IN2P3,
Institut de Physique Nucléaire de Lyon, Villeurbanne, France*
[33]*Institute of High Energy Physics and Informatization, Tbilisi State University, Tbilisi, Georgia*
[34]*RWTH Aachen University, I. Physikalisches Institut, Aachen, Germany*
[35]*RWTH Aachen University, III. Physikalisches Institut A, Aachen, Germany*
[36]*RWTH Aachen University, III. Physikalisches Institut B, Aachen, Germany*
[37]*Deutsches Elektronen-Synchrotron, Hamburg, Germany*
[38]*University of Hamburg, Hamburg, Germany*
[39]*Institut für Experimentelle Kernphysik, Karlsruhe, Germany*
[40]*Institute of Nuclear and Particle Physics (INPP), NCSR Demokritos, Aghia Paraskevi, Greece*
[41]*University of Athens, Athens, Greece*
[42]*University of Ioánnina, Ioánnina, Greece*
[43]*Wigner Research Centre for Physics, Budapest, Hungary*
[44]*Institute of Nuclear Research ATOMKI, Debrecen, Hungary*
[45]*University of Debrecen, Debrecen, Hungary*
[46]*National Institute of Science Education and Research, Bhubaneswar, India*
[47]*Panjab University, Chandigarh, India*
[48]*University of Delhi, Delhi, India*
[49]*Saha Institute of Nuclear Physics, Kolkata, India*
[50]*Bhabha Atomic Research Centre, Mumbai, India*
[51]*Tata Institute of Fundamental Research, Mumbai, India*
[52]*Institute for Research in Fundamental Sciences (IPM), Tehran, Iran*
[53]*University College Dublin, Dublin, Ireland*
[54a]*INFN Sezione di Bari, Bari, Italy*
[54b]*Università di Bari, Bari, Italy*
[54c]*Politecnico di Bari, Bari, Italy*
[55a]*INFN Sezione di Bologna, Bologna, Italy*

[55b]*Università di Bologna, Bologna, Italy*
[56a]*INFN Sezione di Catania, Catania, Italy*
[56b]*Università di Catania, Catania, Italy*
[56c]*CSFNSM, Catania, Italy*
[57a]*INFN Sezione di Firenze, Firenze, Italy*
[57b]*Università di Firenze, Firenze, Italy*
[58]*INFN Laboratori Nazionali di Frascati, Frascati, Italy*
[59a]*INFN Sezione di Genova, Genova, Italy*
[59b]*Università di Genova, Genova, Italy*
[60a]*INFN Sezione di Milano-Bicocca, Milano, Italy*
[60b]*Università di Milano-Bicocca, Milano, Italy*
[61a]*INFN Sezione di Napoli, Napoli, Italy*
[61b]*Università di Napoli 'Federico II', Napoli, Italy*
[61c]*Università della Basilicata (Potenza), Napoli, Italy*
[61d]*Università G. Marconi (Roma), Napoli, Italy*
[62a]*INFN Sezione di Padova, Padova, Italy*
[62b]*Università di Padova, Padova, Italy*
[62c]*Università di Trento (Trento), Padova, Italy*
[63a]*INFN Sezione di Pavia, Pavia, Italy*
[63b]*Università di Pavia, Pavia, Italy*
[64a]*INFN Sezione di Perugia, Perugia, Italy*
[64b]*Università di Perugia, Perugia, Italy*
[65a]*INFN Sezione di Pisa, Pisa, Italy*
[65b]*Università di Pisa, Pisa, Italy*
[65c]*Scuola Normale Superiore di Pisa, Pisa, Italy*
[66a]*INFN Sezione di Roma, Roma, Italy*
[66b]*Università di Roma, Roma, Italy*
[67a]*INFN Sezione di Torino, Torino, Italy*
[67b]*Università di Torino, Torino, Italy*
[67c]*Università del Piemonte Orientale (Novara), Torino, Italy*
[68a]*INFN Sezione di Trieste, Trieste, Italy*
[68b]*Università di Trieste, Trieste, Italy*
[69]*Kangwon National University, Chunchon, Korea*
[70]*Kyungpook National University, Daegu, Korea*
[71]*Chonbuk National University, Jeonju, Korea*
[72]*Chonnam National University, Institute for Universe and Elementary Particles, Kwangju, Korea*
[73]*Korea University, Seoul, Korea*
[74]*University of Seoul, Seoul, Korea*
[75]*Sungkyunkwan University, Suwon, Korea*
[76]*Vilnius University, Vilnius, Lithuania*
[77]*National Centre for Particle Physics, Universiti Malaya, Kuala Lumpur, Malaysia*
[78]*Centro de Investigacion y de Estudios Avanzados del IPN, Mexico City, Mexico*
[79]*Universidad Iberoamericana, Mexico City, Mexico*
[80]*Benemerita Universidad Autonoma de Puebla, Puebla, Mexico*
[81]*Universidad Autónoma de San Luis Potosí, San Luis Potosí, Mexico*
[82]*University of Auckland, Auckland, New Zealand*
[83]*University of Canterbury, Christchurch, New Zealand*
[84]*National Centre for Physics, Quaid-I-Azam University, Islamabad, Pakistan*
[85]*National Centre for Nuclear Research, Swierk, Poland*
[86]*Institute of Experimental Physics, Faculty of Physics, University of Warsaw, Warsaw, Poland*
[87]*Laboratório de Instrumentação e Física Experimental de Partículas, Lisboa, Portugal*
[88]*Joint Institute for Nuclear Research, Dubna, Russia*
[89]*Petersburg Nuclear Physics Institute, Gatchina (St. Petersburg), Russia*
[90]*Institute for Nuclear Research, Moscow, Russia*
[91]*Institute for Theoretical and Experimental Physics, Moscow, Russia*
[92]*P.N. Lebedev Physical Institute, Moscow, Russia*
[93]*Skobeltsyn Institute of Nuclear Physics, Lomonosov Moscow State University, Moscow, Russia*
[94]*State Research Center of Russian Federation, Institute for High Energy Physics, Protvino, Russia*
[95]*University of Belgrade, Faculty of Physics and Vinca Institute of Nuclear Sciences, Belgrade, Serbia*
[96]*Centro de Investigaciones Energéticas Medioambientales y Tecnológicas (CIEMAT), Madrid, Spain*

[97]*Universidad Autónoma de Madrid, Madrid, Spain*

[98]*Universidad de Oviedo, Oviedo, Spain*

[99]*Instituto de Física de Cantabria (IFCA), CSIC-Universidad de Cantabria, Santander, Spain*

[100]*CERN, European Organization for Nuclear Research, Geneva, Switzerland*

[101]*Paul Scherrer Institut, Villigen, Switzerland*

[102]*Institute for Particle Physics, ETH Zurich, Zurich, Switzerland*

[103]*Universität Zürich, Zurich, Switzerland*

[104]*National Central University, Chung-Li, Taiwan*

[105]*National Taiwan University (NTU), Taipei, Taiwan*

[106]*Chulalongkorn University, Faculty of Science, Department of Physics, Bangkok, Thailand*

[107]*Cukurova University, Adana, Turkey*

[108]*Middle East Technical University, Physics Department, Ankara, Turkey*

[109]*Bogazici University, Istanbul, Turkey*

[110]*Istanbul Technical University, Istanbul, Turkey*

[111]*National Scientific Center, Kharkov Institute of Physics and Technology, Kharkov, Ukraine*

[112]*University of Bristol, Bristol, United Kingdom*

[113]*Rutherford Appleton Laboratory, Didcot, United Kingdom*

[114]*Imperial College, London, United Kingdom*

[115]*Brunel University, Uxbridge, United Kingdom*

[116]*Baylor University, Waco, Texas 76798, USA*

[117]*The University of Alabama, Tuscaloosa, Alabama 35487, USA*

[118]*Boston University, Boston, Massachusetts 02215, USA*

[119]*Brown University, Providence, Rhode Island 02912, USA*

[120]*University of California, Davis, Davis, California 95616, USA*

[121]*University of California, Los Angeles, California 90095, USA*

[122]*University of California, Riverside, Riverside, California 92521, USA*

[123]*University of California, San Diego, La Jolla, California 92093, USA*

[124]*University of California, Santa Barbara, Santa Barbara, California 93106, USA*

[125]*California Institute of Technology, Pasadena, California 91125, USA*

[126]*Carnegie Mellon University, Pittsburgh, Pennsylvania 15213, USA*

[127]*University of Colorado at Boulder, Boulder, Colorado 80309, USA*

[128]*Cornell University, Ithaca, New York 14853, USA*

[129]*Fairfield University, Fairfield, Connecticut 06430, USA*

[130]*Fermi National Accelerator Laboratory, Batavia, Illinois 60510, USA*

[131]*University of Florida, Gainesville, Florida 32611, USA*

[132]*Florida International University, Miami, Florida 33199, USA*

[133]*Florida State University, Tallahassee, Florida 32306, USA*

[134]*Florida Institute of Technology, Melbourne, Florida 32901, USA*

[135]*University of Illinois at Chicago (UIC), Chicago, Illinois 60637, USA*

[136]*The University of Iowa, Iowa City, Iowa 52242, USA*

[137]*Johns Hopkins University, Baltimore, Maryland 21218, USA*

[138]*The University of Kansas, Lawrence, Kansas 66045, USA*

[139]*Kansas State University, Manhattan, Kansas 66506, USA*

[140]*Lawrence Livermore National Laboratory, Livermore, California 94551, USA*

[141]*University of Maryland, College Park, Maryland 20742, USA*

[142]*Massachusetts Institute of Technology, Cambridge, Massachusetts 02139, USA*

[143]*University of Minnesota, Minneapolis, Minnesota 55455, USA*

[144]*University of Mississippi, Oxford, Mississippi 38677, USA*

[145]*University of Nebraska-Lincoln, Lincoln, Nebraska 68588, USA*

[146]*State University of New York at Buffalo, Buffalo, New York 14260, USA*

[147]*Northeastern University, Boston, Massachusetts 02115, USA*

[148]*Northwestern University, Evanston, Illinois 60208, USA*

[149]*University of Notre Dame, Notre Dame, Indiana 46556, USA*

[150]*The Ohio State University, Columbus, Ohio 43210, USA*

[151]*Princeton University, Princeton, New Jersey 08544, USA*

[152]*University of Puerto Rico, Mayaguez, PR 00681, USA*

[153]*Purdue University, West Lafayette, Indiana 47907, USA*

[154]*Purdue University Calumet, Hammond, Indiana 46323, USA*

[155]*Rice University, Houston, Texas 77005, USA*

[156]*University of Rochester, Rochester, New York 14627, USA*

[157]The Rockefeller University, New York, New York 10021, USA

[158]Rutgers, The State University of New Jersey, Piscataway, New Jersey 08855, USA

[159]University of Tennessee, Knoxville, Tennessee 37996, USA

[160]Texas A&M University, College Station, Texas 77843, USA

[161]Texas Tech University, Lubbock, Texas 79409, USA

[162]Vanderbilt University, Nashville, Tennessee 37235, USA

[163]University of Virginia, Charlottesville, Virginia 22904, USA

[164]Wayne State University, Detroit, Michigan 48201, USA

[165]University of Wisconsin, Madison, Wisconsin 53706, USA

[a]Deceased.

[b]Also at Vienna University of Technology, Vienna, Austria.

[c]Also at CERN, European Organization for Nuclear Research, Geneva, Switzerland.

[d]Also at Institut Pluridisciplinaire Hubert Curien, Université de Strasbourg, Université de Haute Alsace Mulhouse, CNRS/IN2P3, Strasbourg, France.

[e]Also at National Institute of Chemical Physics and Biophysics, Tallinn, Estonia.

[f]Also at Skobeltsyn Institute of Nuclear Physics, Lomonosov Moscow State University, Moscow, Russia.

[g]Also at Universidade Estadual de Campinas, Campinas, Brazil.

[h]Also at Laboratoire Leprince-Ringuet, Ecole Polytechnique, IN2P3-CNRS, Palaiseau, France.

[i]Also at Joint Institute for Nuclear Research, Dubna, Russia.

[j]Also at Suez University, Suez, Egypt.

[k]Also at Cairo University, Cairo, Egypt.

[l]Also at Fayoum University, El-Fayoum, Egypt.

[m]Also at British University in Egypt, Cairo, Egypt.

[n]Also at Ain Shams University, Cairo, Egypt.

[o]Also at Université de Haute Alsace, Mulhouse, France.

[p]Also at Brandenburg University of Technology, Cottbus, Germany.

[q]Also at Institute of Nuclear Research ATOMKI, Debrecen, Hungary.

[r]Also at Eötvös Loránd University, Budapest, Hungary.

[s]Also at University of Debrecen, Debrecen, Hungary.

[t]Also at University of Visva-Bharati, Santiniketan, India.

[u]Also at King Abdulaziz University, Jeddah, Saudi Arabia.

[v]Also at University of Ruhuna, Matara, Sri Lanka.

[w]Also at Isfahan University of Technology, Isfahan, Iran.

[x]Also at Sharif University of Technology, Tehran, Iran.

[y]Also at Plasma Physics Research Center, Science and Research Branch, Islamic Azad University, Tehran, Iran.

[z]Also at Università degli Studi di Siena, Siena, Italy.

[aa]Also at Centre National de la Recherche Scientifique (CNRS)—IN2P3, Paris, France.

[bb]Also at Purdue University, West Lafayette, USA.

[cc]Also at Universidad Michoacana de San Nicolas de Hidalgo, Morelia, Mexico.

[dd]Also at Institute for Nuclear Research, Moscow, Russia.

[ee]Also at St. Petersburg State Polytechnical University, St. Petersburg, Russia.

[ff]Also at California Institute of Technology, Pasadena, USA.

[gg]Also at Faculty of Physics, University of Belgrade, Belgrade, Serbia.

[hh]Also at Facoltà Ingegneria, Università di Roma, Roma, Italy.

[ii]Also at Scuola Normale e Sezione dell'INFN, Pisa, Italy.

[jj]Also at University of Athens, Athens, Greece.

[kk]Also at Paul Scherrer Institut, Villigen, Switzerland.

[ll]Also at Institute for Theoretical and Experimental Physics, Moscow, Russia.

[mm]Also at Albert Einstein Center for Fundamental Physics, Bern, Switzerland.

[nn]Also at Gaziosmanpasa University, Tokat, Turkey.

[oo]Also at Adiyaman University, Adiyaman, Turkey.

[pp]Also at Cag University, Mersin, Turkey.

[qq]Also at Anadolu University, Eskisehir, Turkey.

[rr]Also at Izmir Institute of Technology, Izmir, Turkey.

[ss]Also at Necmettin Erbakan University, Konya, Turkey.

[tt]Also at Ozyegin University, Istanbul, Turkey.

[uu]Also at Marmara University, Istanbul, Turkey.

[vv]Also at Kafkas University, Kars, Turkey.

[ww]Also at Rutherford Appleton Laboratory, Didcot, United Kingdom.

[xx]Also at School of Physics and Astronomy, University of Southampton, Southampton, United Kingdom.

[yy]Also at University of Belgrade, Faculty of Physics and Vinca Institute of Nuclear Sciences, Belgrade, Serbia.

[zz]Also at Mimar Sinan University, Istanbul, Istanbul, Turkey.

[aaa]Also at Argonne National Laboratory, Argonne, USA.

[bbb]Also at Erzincan University, Erzincan, Turkey.

[ccc]Also at Yildiz Technical University, Istanbul, Turkey.

[ddd]Also at Texas A&M University at Qatar, Doha, Qatar.

[eee]Also at Kyungpook National University, Daegu, Korea.